

AD-A087 285

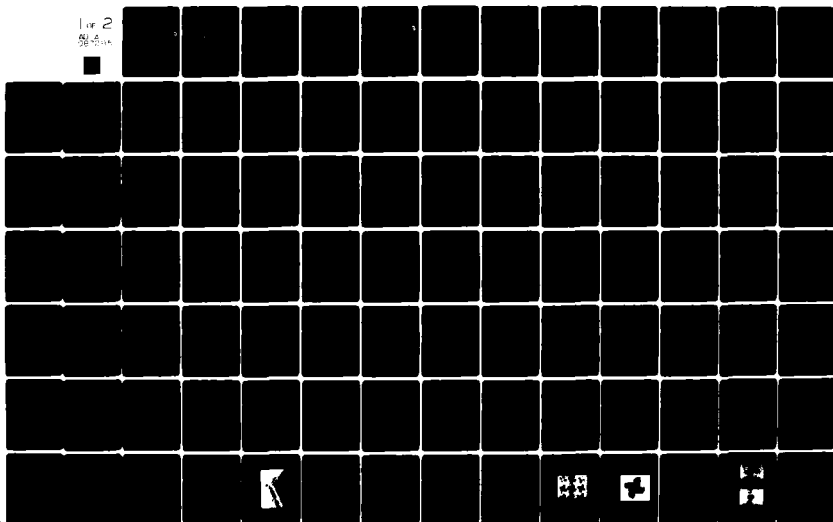
TEXAS TECH UNIV LUBBOCK OPTICAL SYSTEMS LAB F/G 14/5  
SPACE-VARIANT PROCESSING USING PHASE CODES AND FOURIER-PLANE SA--ETC(U)  
JUN 80 R KASTURI AFOSR-79-0076  
SCIENTIFIC-1

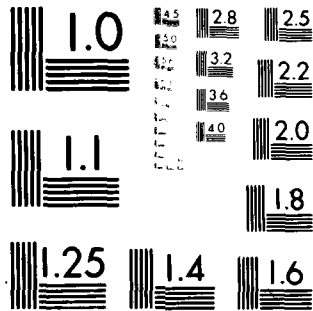
AFOSR-TR-80-0557

NL

UNCLASSIFIED

1 of 2  
AD-A087 285





MICROCOPY RESOLUTION TEST CHART  
NATIONAL BUREAU OF STANDARDS-1963-A

AFOSR-TR- 80-0557

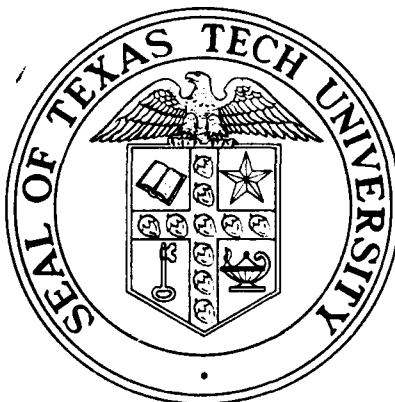
Scientific Report  
AFOSR-79-0076-1

LEVEL 12

# Space-Variant Processing Using Phase Codes and Fourier-Plane Sampling Techniques.

by

Rangachar Kasturi



DTIC  
ELECTE  
JUL 30 1980  
C D

June 1, 1980

THIS DOCUMENT IS BEST QUALITY PRACTICABLE.  
THE COPY FURNISHED TO DDC CONTAINED A  
SIGNIFICANT NUMBER OF PAGES WHICH DO NOT  
REPRODUCE LEGIBLY.

Optical Systems Laboratory  
DEPARTMENT OF ELECTRICAL ENGINEERING  
TEXAS TECH UNIVERSITY

Lubbock, Texas 79409

DDC FILE COPY

80 7 28 004

Approved for public release;  
distribution unlimited.

## **DISCLAIMER NOTICE**

**THIS DOCUMENT IS BEST QUALITY  
PRACTICABLE. THE COPY FURNISHED  
TO DTIC CONTAINED A SIGNIFICANT  
NUMBER OF PAGES WHICH DO NOT  
REPRODUCE LEGIBLY.**

REPORT DOCUMENTATION PAGE		READ INSTRUCTIONS BEFORE COMPLETING FORM
1. REPORT NUMBER <b>AFOSR-TR- 80-0557</b>	2. GOVT ACCESSION NO. <b>AD-A087285</b>	3. RECIPIENT'S CATALOG NUMBER
4. TITLE (and Subtitle) <b>SPACE-VARIANT PROCESSING USING PHASE CODES AND FOURIER-PLANE SAMPLING TECHNIQUES</b>		5. TYPE OF REPORT & PERIOD COVERED <b>Interim</b>
7. AUTHOR(s) <b>/1 Rangachar/Kasturi</b>		6. PERFORMING ORG. REPORT NUMBER <b>AFOSR-79-0076-1</b>
9. PERFORMING ORGANIZATION NAME AND ADDRESS <b>Texas Tech University Department of Electrical Engineering Lubbock, Texas 79409</b>		8. CONTRACT OR GRANT NUMBER(s) <b>AFOSR-79-0076</b>
11. CONTROLLING OFFICE NAME AND ADDRESS <b>AFOSR/NE Building 410 Bolling AFB, DC 20332</b>		10. PROGRAM ELEMENT, PROJECT, TASK AREA & WORK UNIT NUMBERS <b>61102F 2305/B1</b>
14. MONITORING AGENCY NAME & ADDRESS (if different from Controlling Office)		12. REPORT DATE <b>June 1, 1980</b>
		13. NUMBER OF PAGES <b>156</b>
		15. SECURITY CLASS. (of this report) <b>UNCLASSIFIED</b>
		15a. DECLASSIFICATION/DOWNGRADING SCHEDULE
16. DISTRIBUTION STATEMENT (of this Report)  <b>Approved for Public Release; Distribution Unlimited</b>		
17. DISTRIBUTION STATEMENT (of the abstract entered in Block 20, if different from Report)		
18. SUPPLEMENTARY NOTES		
19. KEY WORDS (Continue on reverse side if necessary and identify by block number) <b>Multiplex Holography Space-Variant Optical Processing Hologram Optical Elements Optical Computing Diffusers</b>		
20. ABSTRACT (Continue on reverse side if necessary and identify by block number) <b>This report discusses alternative approaches to using multiplex holography in representing space-variant optical systems. The first part of the report presents the results of extensive computer simulations used in evaluating the effectiveness of Gold codes in encoding the multiple reference beams required in a sampled input/multiple reference beam realization of a space-variant system. The second part considers a totally different approach which samples the input plane and the transfer function plane. This latter approach eliminates crosstalk</b>		

UNCLASSIFIED

SECURITY CLASSIFICATION OF THIS PAGE (When Data Entered)

entirely, but requires multiple copies of the sampled input function during the playback step. The results of preliminary experiments conducted to evaluate this alternative approach for representing space-variant systems holographically are presented, including experiments verifying the coherent addition of the multiplexed holograms on playback using computer-multiplexed holograms.

(1) SPACE-VARIANT PROCESSING USING PHASE CODES AND  
FOURIER-PLANE SAMPLING TECHNIQUES, (12)

(11) Rangachar/Kasturi

June 1, 1980

Scientific Report No. 1 on

(15) Grant AFOSR-79-0076

DTIC  
ECTE  
JUL 30 1980 D

"Space-Variant Optical Systems"

Principal Investigator: Dr. John F. Walkup, Assoc. Prof.

Optical Systems Laboratory

Department of Electrical Engineering

Texas Tech University

Lubbock, Texas 79409

(18) AFOSR

(19) TR-80-0557

The views and conclusions contained in this document are those of author, and should not be interpreted as necessarily representing the official policies or endorsements, either expressed or implied, of the Air Force Office of Scientific Research or the U. S. Government.

AIR FORCE OFFICE OF SCIENTIFIC RESEARCH (AFSC)  
NOTICE OF TRANSMISSION TO DDC  
This technology has been reviewed and is  
approved for release under E.O. 12812 (7b).  
Distribution is unlimited.  
A. D. Bland  
Technical Information Officer

410-11

52





## TABLE OF CONTENTS

	Page
ABSTRACT. . . . .	iii
LIST OF FIGURES . . . . .	vi
LIST OF TABLES. . . . .	x
CHAPTER 1. INTRODUCTION. . . . .	1
1.1. Sampling Theorem for Space-Variant Systems .	2
1.2. Representation of Space-Variant Systems Using Phase Coded Reference-Beams. . . . .	4
1.3. Representation of Space-Variant Systems Using a Sampled Input/Sampled Transfer Function Approach. . . . .	8
CHAPTER 2. PHASE CODED REFERENCE BEAM APPROACH . . . . .	10
2.1. Generation of Gold Codes . . . . .	10
2.1.1 Example of Generation of a Set of 511 Bit Gold Codes. . . . .	12
2.2. Evaluation of Gold Codes as Phase Diffusers in Multiplex Holography. . . . .	17
2.2.1 Results of Evaluation of Gold Codes as Perfect Phase Diffusers. . . . .	20
2.2.2 Results of Evaluation of Gold Codes as Amplitude Masks and Non Perfect Phase Masks . . . . .	37
2.2.3 Results of Evaluation of Gold Codes Illuminated by Spherical Wavefront. .	39
CHAPTER 3. SAMPLED INPUT/SAMPLED TRANSFER FUNCTION APPROACH. . . . .	50
3.1. Space Division Multiplexing of Transfer Functions. . . . .	50
3.2. An Optical Recording and Playback Scheme . .	52
3.3. One-Dimensional Computer Simulations . . . .	58
3.4. Schemes for the Generation of Multiples of the Input Function . . . . .	63
3.4.1 Multiple Image Transparencies . . . .	63
3.4.2 Multiple Imaging Using Beam Splitters	65
3.4.3 Multiple Imaging Using Phase Holo- grams . . . . .	65
3.4.4 Use of Fiber Optic Elements . . . . .	65
3.4.5 Use of Liquid Crystal Devices . . . .	65

# Table of Contents continued

	Page
CHAPTER 4. EXPERIMENTAL RESULTS USING COMPUTER MULTI- PLEXED HOLOGRAMS. . . . .	68
4.1. Computer Generation and Playback of the Multiplexed Hologram . . . . .	68
4.2. Experimental Results Using Disjoint Impulse Responses. . . . .	76
4.3. Experimental Results Using Overlapping Im- pulse Responses. . . . .	83
4.4. Multiplication of Impulse Responses by a Phase Function . . . . .	89
4.5. Computer Multiplexing Using Low Pass Filtered Transfer Functions . . . . .	94
CHAPTER 5. CONCLUSIONS . . . . .	104
REFERENCES. . . . .	107
APPENDIX A. . . . .	109
APPENDIX B. . . . .	116
APPENDIX C. . . . .	120
APPENDIX D. . . . .	125
APPENDIX E. . . . .	130
APPENDIX F. . . . .	135
APPENDIX G. . . . .	141

## LIST OF FIGURES

Figure	Page
1-1. Recording scheme for the holographic representation of a space-variant system. . . . .	5
1-2. Playback scheme for the holographic representation of a space-variant system. . . . .	6
2-1. Autocorrelation and crosscorrelations of 42 central bits of 127 bit Gold codes. . . . .	22
2-2. Simulation of multiplex holography using 42 central bits of 127 bit Gold codes. (Disjoint impulse responses). . . . .	24
2-3. Simulation of multiplex holography using 42 central bits of 127 bit Gold codes (overlapping impulse responses). . . . .	25
2-4. Simulation of multiplex holography using 42 central bits of 127 bit Gold codes. (Delta like impulse responses). . . . .	26
2-5. Autocorrelation and crosscorrelations of 127 bit Gold codes. . . . .	28
2-6. Simulation of multiplex holography using 127 bit Gold codes (disjoint impulse responses) . . . . .	29
2-7. Simulation of multiplex holography using 127 bit Gold codes (overlapping impulse responses). . . . .	30
2-8. Simulation of multiplex holography using 127 bit Gold codes (Delta like impulse responses) . . . . .	31
2-9. Autocorrelation and crosscorrelations of 511 bit Gold codes. . . . .	33
2-10. Simulation of multiplex holography using 511 bit Gold codes. (Disjoint impulse responses) . . . . .	34
2-11. Simulation of multiplex holography using 511 bit Gold codes (overlapping impulse responses). . . . .	35
2-12. Simulation of multiplex holography using 511 bit Gold codes (Delta like impulse responses) . . . . .	36

# List of Figures continued

Figure	Page
2-13. Autocorrelation and crosscorrelations of 127 bit Gold codes used as binary amplitude masks. . . .	38
2-14. Simulation of multiplex holography using 127 bit amplitude masks (Disjoint impulse responses) . .	40
2-15. Simulation of multiplex holography using 127 bit amplitude masks (overlapping impulse responses). 41	
2-16. Simulation of multiplex holography using 127 bit amplitude masks (Delta like impulse responses) .	42
2-17. Autocorrelation and crosscorrelations of 127 bit Gold codes used as non perfect phase masks . . .	43
2-18. Calculation of phase-angle at an element due to spherical wavefront. . . . .	45
2-19. Autocorrelation and crosscorrelations of 42 central bits of 127 bit Gold codes illuminated by a spherical wave of radius R and width of mask W . . . . .	47
3-1. Typical line-spread function . . . . .	51
3-2. Typical arrangement of samples of transfer functions on hologram, when $N = 3$ and $M = 4$ . . . .	51
3-3. Scheme for optically recording the multiplex hologram . . . . .	54
3-4. Scheme for the playback of multiplexed hologram.	55
3-5. Impulse responses and their Fourier transforms used in the simulations. . . . .	60
3-6. Composite hologram and the resultant output. . .	61
3-7. Sampled transfer functions and the corresponding outputs. . . . .	62
3-8. Typical input function $f(\xi)$ and the corresponding sampled multiple input function when $N = 3$ and $M = 4$ . . . . .	64
3-9. Use of optical fibers to generate multiple images of the input function . . . . .	66

# List of Figures continued

Figure	Page
4-1. Scheme for computer multiplexing the transfer functions. . . . .	70
4-2. Resolving the component values of transfer function along 3 vectors . . . . .	72
4-3. Typical cell representing the magnitude and phase using 3 vector method. . . . .	72
4-4. Optical system for playback. . . . .	73
4-5. Photograph of the Optical System used for the playback of computer multiplexed holograms . . .	74
4-6. Four disjoint impulse responses used in experiment 1 and their sum . . . . .	77
4-7. Computer multiplexed hologram using impulse responses of Fig. 4-6. . . . .	78
4-8. Output of the Optical System when the hologram of Fig. 4-7 is played back . . . . .	79
4-9. Enlarged output of the Optical System when the hologram of Fig. 4-7 is played using a binary mask to pass only one of the multiple images . .	80
4-10. Computer-simulated output when all the impulse responses of Fig. 4-6 are played back. . . . .	81
4-11. Output of the Optical System when only one of the impulse responses of Fig. 4-6 is played back . . . . .	82
4-12. Output of the Optical System when one of the impulse responses of Fig. 4-6 is played back using a binary mask to pass only one of the multiple images. . . . .	82
4-13. Four overlapping impulse responses used in experiment 2 and their sum . . . . .	84
4-14. Computer multiplexed hologram using impulse responses of Fig. 4-13 . . . . .	85
4-15. Output of the Optical System when the hologram of Fig. 4-14 is played back. . . . .	86

# List of Figures continued

Figure	Page
4-16. Computer simulated output when all the impulse responses of Fig. 4-13 are played back. . . . .	87
4-17. Output of the Optical System when only one of the impulse responses of Fig. 4-13 is played back .	88
4-18. Phase mask used to multiply the impulse responses . . . . .	90
4-19. Composite hologram when the impulse responses of Fig. 4-6 are multiplied by the phase mask of Fig. 4-18 . . . . .	91
4-20. Output of the Optical System when the hologram of Fig. 4-19 is played back . . . . .	92
4-21. Computer simulated output when all the impulse responses of Fig. 4-6 premultiplied by the phase mask of Fig. 4-18 are played back . . . .	93
4-22. Composite hologram when the impulse responses of Fig. 4-13 are multiplied by the phase mask of Fig. 4-18. . . . .	95
4-23. Output of the Optical System when the hologram of Fig. 4-22 is played back . . . . .	96
4-24. Computer simulated output when all the impulse responses of Fig. 4-13 premultiplied by the phase function of Fig. 4-18 are played back . .	97
4-25. Generation of composite transfer function array using low pass filtering technique. . . . .	99
4-26. Four impulse responses used in "Low Pass Filter" multiplexing scheme . . . . .	101
4-27. Composite hologram generated using low pass filtering technique . . . . .	102
4-28. Computer simulated output when all the impulse responses of Fig. 4-26 are played back. . . . .	103

## LIST OF TABLES

	Page
Table 2-1. Primitive Polynomials of Order 9. . . . .	14
Table 2-2. Set of nine 127 bit Gold codes. . . . .	18

## CHAPTER 1

### INTRODUCTION

A method for holographically representing any band-limited space-variant system using a sampling technique has been described [1,2]. This method requires the sequential multiplexing of a number of holograms of the system transfer functions in a single recording medium. As a result of this multiplexing, many crosstalk terms are generated upon playback in addition to the required system response terms. Several crosstalk suppressing techniques, using properties such as extinction angle effects of volume holograms [3], and the correlation properties of phase codes when used in the reference beam paths [4,5] have been suggested for implementing this scheme. Experimental results using ground-glass diffusers and binary amplitude-coded diffusers have also been reported [6]. Analytical studies to model the characteristics of various diffusers have been carried out [7]. Use of randomly generated binary amplitude diffusers with computer multiplexed holograms has also been studied [8]. Preliminary studies on diffusers based on the known correlation properties of the Gold codes used in spread spectrum communication systems have been carried out [9].

The work presented in this report consists mainly of two parts. In Chapter 2 results of extensive computer simulations to study the auto and cross-correlation properties of Gold codes of various lengths under different conditions,



along with the computer simulated outputs when these codes are used as phase diffusers in multiplex holography are presented. In Chapters 3 and 4 an alternate method of multiplexing the transfer functions using a sampling technique, along with preliminary experimental results using computer multiplexed holograms, is presented.

### 1.1. Sampling Theorem for Space-Variant Systems [1]

The output  $g(x)$  of a linear system due to an input  $f(\xi)$  is given by the superposition integral

$$\begin{aligned} g(x) &= S[f(\xi)] \\ &= \int_{-\infty}^{\infty} f(\xi) h(x-\xi, \xi) d\xi \end{aligned} \quad (1-1)$$

where  $S[\cdot]$  is the linear system operator. The system line-spread function  $h(x-\xi, \xi)$  is the system response to an input Dirac delta, [10]

$$h(x-\xi, \xi) = S[\delta(x-\xi)] \quad (1-2)$$

Now, Fourier transforming the Eqn. (1-1) we obtain

$$\begin{aligned} G(f_x) &= F_x(g(x)) \\ &= \int_{-\infty}^{\infty} f(\xi) F_x[h(x, \xi)] \exp(-j2\pi f_x \xi) d\xi \\ &= F_{\xi} F_x[f(\xi) h(x, \xi)] \Big|_{v=f_x} \end{aligned} \quad (1-3)$$

Where  $v$  and  $f_x$  are the frequency variables associated with  $\xi$  and  $x$  respectively.

Defining the system's spatial transfer function as

$$H_x(f_x, \xi) \triangleq F_x[h(x, \xi)], \quad (1-4)$$

Equation (1-3) may be rewritten as

$$G(f_x) = F_{\xi}[f(\xi)H_x(f_x, \xi)] \Big|_{v=f_x} \quad (1-5)$$

If  $f(\xi)$  and  $h(x, \xi)$  are band-limited in  $v$  and have respective band widths of  $2w_f$  and  $2w_v$ , then the total band width of their product is given by

$$2w = 2w_f + 2w_v. \quad (1-6)$$

Then applying the Whittaker-Shannon sampling theorem [11] to Eqn. (1-5) we obtain

$$G(f_x) = \frac{1}{2w} \sum_n f(\xi_n) H_x(f_x, \xi_n) \exp(-j2\pi f_x \xi_n) \text{Rect}\left(\frac{f_x}{2w}\right), \quad (1-7)$$

where  $\xi_n = \frac{n}{2w}$  and

$$\text{Rect}(x) \triangleq \begin{cases} 1, & |x| \leq 1/2, \\ 0, & |x| > 1/2. \end{cases} \quad (1-8)$$

Equivalently,

$$g(x) = \sum_n f(\xi_n) h(x - \xi_n, \xi_n) * \text{Sinc}(2wx), \quad (1-9)$$

where

$$\text{Sinc}(f_x) = F[\text{Rect}(x)].$$

Thus when the input function  $f(\xi)$  and the line spread function  $h(x, \xi)$  are band limited, the output  $g(x)$  of the system can be computed exactly by sampling the product of the

functions  $f(\xi)$  and  $h(x, \xi)$  at intervals of  $1/2w$  and passing the sum of these sampled products through a suitable low pass filter.

Although Eqn. (1-9) implies a countably infinite number of samples of the product of the spatially-varying system response  $h(x-\xi, \xi)$  and the input function  $f(\xi)$ , in practice, if  $f(\xi)$  is essentially zero outside the interval  $|\xi| \leq a$  and if the spectrum of  $f(\xi)h(x, \xi)$  is essentially zero outside of the interval  $|v| \leq w$ , then the required number of samples for a good approximation is given by the space-band width product

$$N = 4wa. \quad (1-10)$$

Two possible schemes for implementing this sampled system representation will be discussed in the following sections.

## 1.2. Representation of Space-Variant Systems Using Phase Coded Reference-Beams

A scheme for coherently representing a space-variant system using the sampling technique described in Section 1.1 is shown in Figures (1-1) and (1-2), [4]. During the recording step the space variant system is sequentially sampled in the input plane at  $N$  points denoted by  $i_1$  through  $i_N$  to generate the spread functions  $h_1$  through  $h_N$ . The corresponding reference beam diffuser functions are denoted as  $r_1$  through  $r_N$ . After Fourier transformation by lenses  $L_1$  and  $L_2$  the amplitude transmittance  $t$  of the

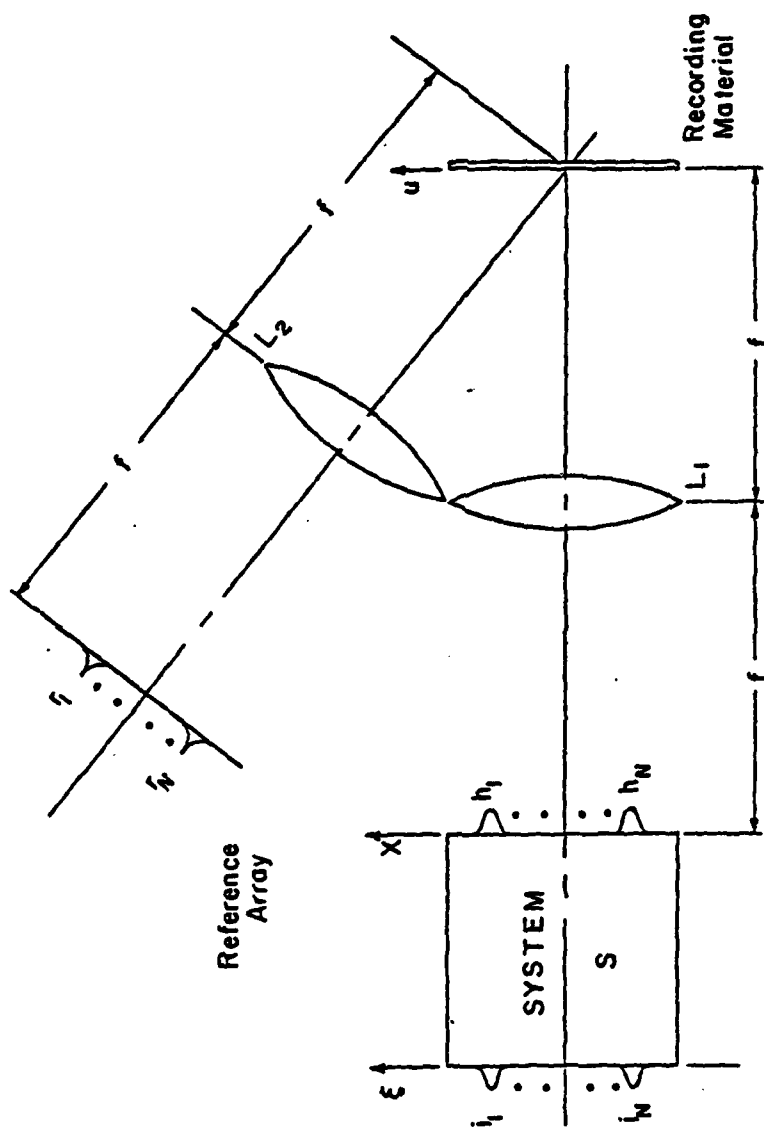


Figure 1-1. Recording scheme for the holographic representation of space-variant system  $S$ .

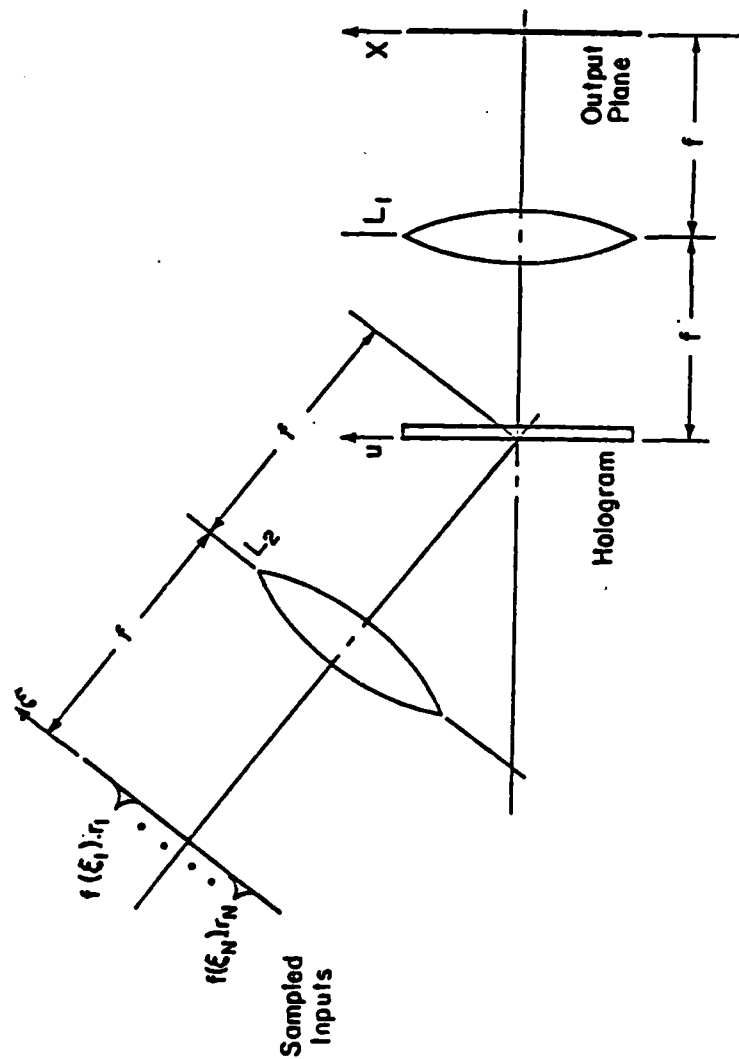


Figure 1-2. Playback scheme for the holographic representation of space-variant system.

hologram is given by

$$t = \sum_{i=1}^N |H_i + R_i|^2, \quad (1-11)$$

where  $H_i$  and  $R_i$  are the Fourier transforms of the functions  $h_i$  and  $r_i$  respectively.

During playback the input function  $f(\xi)$  is spatially sampled at the sample locations of the original reference array to produce the sampled inputs  $S_1 r_i$  through  $S_N r_N$  where  $S_i$  is the sampled value of the input function at the  $i^{\text{th}}$  location. Then the reconstructed wavefront to the right of the hologram is given by

$$\begin{aligned} G'(u) &= \left( \sum_{j=1}^N S_j R_j \right) \left( \sum_{i=1}^N |H_i + R_i|^2 \right) \\ &= \sum_{i=1}^N S_i R_i |H_i + R_i|^2 + \sum_{i=1}^N \sum_{\substack{j=1 \\ i \neq j}}^N S_j R_j |H_i + R_i|^2 \end{aligned} \quad (1-12)$$

The term  $R_i |H_i + R_i|^2$  may be expanded as

$$R_i |H_i + R_i|^2 = R_i R_i^* H_i + R_i H_i H_i^* + R_i R_i H_i^* + R_i R_i R_i^*, \quad (1-13)$$

where  $*$  represents the complex conjugate operator.

Out of these components only the term  $R_i R_i^* H_i$  is diffracted by the hologram in the direction of the output plane as a result of the offset in the reference beam path. Hence the output after Fourier transformation by lens  $L_2$  is

given by

$$g'(x) = \sum_{i=1}^N S_i h_i * (r_i \star r_i) + \sum_{i=1}^N \sum_{\substack{j=1 \\ i \neq j}}^N S_j h_j * (r_i \star r_j), \quad (1-14)$$

where  $\star$  denotes Correlation and  $*$  denotes Convolution.

The desired output  $g(x)$  is

$$g(x) = \sum_{i=1}^N S_i h_i. \quad (1-15)$$

Thus for perfect reconstruction of the output  $g(x)$  the diffusers in the reference beam path should have the following characteristics.

$$\begin{aligned} r_i(x) \star r_i(x) &= \delta(x) \text{ for all } i, \\ r_i(x) \star r_j(x) &= 0 \text{ for all } i \text{ and } j, i \neq j \end{aligned} \quad (1-16)$$

This implies that we need a set of codes for the fabrication of diffusers having delta like autocorrelations and zero cross-correlations. However such a set of ideal codes does not exist. In Chapter 2 the properties of a family of diffuser function derived from a set of codes known as Gold Codes and previously used in spread spectrum communication systems are studied through a series of computer simulations.

### 1.3 Representation of Space-Variant Systems Using a Sampled Input/Sampled Transfer Function Approach

The sampling theorem of Section 1.1 requires the multiplexing of a number of system transfer functions on a single

hologram, with the capability of independent access to each of the transfer functions. In Section 1.2 a method for achieving this independent access requirement by using diffrusers in the reference beam paths was discussed. However when the system line spread function  $h(x, \xi)$  is space limited in  $x$ , an alternate approach in which the transfer functions are sampled in the frequency plane to multiplex a number of transfer functions on a single recording medium may be employed. This is in addition to the sampling in the input plane as required by the sampling theorem of Section 1.1. This technique is described in detail in Chapter 3. Preliminary experimental results using this method are presented in Chapter 4.



## CHAPTER 2

### PHASE CODED REFERENCE BEAM APPROACH

In section 1.2 a previously developed scheme for representing a space-variant system using phase coded reference beams was presented. It was also shown [Eqn. (1-16)] that for ideal playback of the system responses the codes used in the multiplexing step should have delta-like auto-correlations and zero cross-correlations. In this chapter the properties of a set of codes known as the Gold codes are evaluated for use as phase diffusers to multiplex a number of transfer functions in a single recording medium. In section 2.1 a method for generating a set of Gold codes is described. In section 2.2 the correlation properties of the Gold codes of various lengths are evaluated through a series of computer programs. The output of a system using the Gold codes for multiplexing the transfer functions of a space-variant system are also simulated on the computer.

#### 2.1 Generation of Gold Codes

An analytical technique for constructing a large family of codes having uniformly low cross-correlations has been described by Gold [12]. The following steps describe the technique for generating a set of the Gold codes. The method is illustrated by an example at the end of this section.

1. Find the order of the primitive polynomial required by using the equation

$$L = 2^n - 1 \quad (2-1)$$

where  $n$  is the order of the polynomial and  $L$  is the length of the code. The primitive polynomials for each degree have been tabulated [13].

2. Select a pair of preferred polynomials  $f_1(x)$  and  $f_2(x)$  that result in sequences with low cross-correlations. (This step is explained in detail while describing the method with an example.)
3. Find the product of the polynomials obtained in the previous step to obtain

$$f'(x) = f_1(x) f_2(x) \quad (2-2)$$

4. Convert the coefficients of the powers of  $x$  in the polynomials  $f'(x)$  to modulo 2 to obtain  $f(x)$ .
5. Enter these coefficients as connections of a  $2n$  stage shift register. Here 0 denotes no connection and 1 denotes the presence of a connection.
6. Select a  $2n$  bit binary seed as input to the shift register. The output of the shift register is a sequence of period  $L$  and represents a Gold code.
7. To generate another member in the set select a seed that is not a  $2n$  bit segment of the codes already generated. Repeating this step a total of  $(2^n + 1)$  sequences each of length  $(2^n - 1)$  may be generated.

It has been shown that the cross-correlations  $cc(\tau)$  between any pair of these sequences obey the inequality

$$|cc(\tau)| \leq \begin{cases} 2^{\frac{n+1}{2}} + 1 & \text{for } n \text{ odd,} \\ 2^{\frac{n+2}{2}} + 1 & \text{for } n \text{ even and } n \neq 0 \bmod 4, \end{cases} \quad (2-3)$$

where the cross-correlation  $cc(\tau)$  between two codes is defined as

$$cc(\tau) = (\text{number of agreements} - \text{number of disagreements}), \quad (2-4)$$

when two codes with a displacement of  $\tau$  between each other are compared. The autocorrelation  $Ac(\tau)$  for  $\tau \neq 0$  also obeys the inequality of Eqn. (2-3) and when  $\tau = 0$  is equal to the length of the sequence.

$$Ac(0) = 2^n - 1 \quad (2-5)$$

Carter [14] has described a method for generating a family of codes for  $n = 0 \bmod 4$ , i.e., for  $n = 4, 8, 12, 16$  etc.

2.1.1 Example of Generation of a Set of 511 Bit Gold Codes: The method just described for generating a family of Gold codes is illustrated here by an example. In this example a set of codes, each with a length equal to 511 bits, is generated. The computer program used for this example along with a set of 9 codes of 511 bits each generated by the program are

given in Appendix A. The following calculations correspond to the steps described earlier for the generation of the codes.

1. The order of the primitive polynomial  $n$ , is obtained from Eqn. (2-1) as

$$511 = 2^n - 1$$

$$\therefore n = 9.$$

A table of the primitive polynomials of order 9 is given in Table (2-1) [13].

In this table the polynomials are listed in octal notation. For example,

1021 corresponds to 001,000,010,001 and represents the polynomial  $1 \cdot x^9 + 0 \cdot x^8 + 0 \cdot x^7 + 0 \cdot x^6 + 0 \cdot x^5 + 1 \cdot x^4 + 0 \cdot x^3 + 0 \cdot x^2 + 0 \cdot x^1 + 1$  i.e.,  $1 + x^4 + x^9$ .

The interpretation of the numbers in the first column is as follows.

Let  $\alpha$  be the root of the polynomial 1021. Then the number 17 in the first column of polynomial 1333 represents that  $\alpha^{17}, \alpha^{17 \cdot 2^1}, \alpha^{17 \cdot 2^2}, \alpha^{17 \cdot 2^3}, \alpha^{17 \cdot 2^4}, \alpha^{(17 \cdot 2^5 - 511)}, \alpha^{(17 \cdot 2^6 - 511)}, \alpha^{(17 \cdot 2^7 - 511)}$ , and  $\alpha^{(17 \cdot 2^8 - 511)}$  are the roots of the polynomial 1333. Here the powers of  $\alpha$  are taken as modulo 511.

1	1021	23	1751	53	1225
3	1131	25	1743	55	1275
5	1461	27	1617	73	0013
7	1231	29	1553	75	1773
9	1423	35	1401	77	1511
11	1055	37	1157	83	1425
13	1167	39	1715	85	1267
15	1541	41	1563		
17	1333	43	1713		
19	1605	45	1175		
21	1027	51	1725		

Table 2-1. Primitive Polynomials of Order 9.

2. Now we need to select a pair of polynomials with low cross correlations. The first polynomial is chosen to be 1021. Thus

$$f_1(x) = 1 + x^4 + x^9.$$

Now the second polynomial  $f_2(x)$  must be chosen such that it has the roots  $\alpha^{\frac{n+1}{2}+1}$ .

i.e., the roots of  $f_2(x)$  must be  $\alpha^{33}$ . Now we refer to the 1<sup>st</sup> column in the Table (2-1) to find the number 33. But 33 is not listed in the table. However 33 may be written as 544 modulo 511 and  $544 = 17 \cdot 2^5$ . Thus the required polynomial  $f_2(x)$  is the one which has an entry 17 in the first column. The corresponding polynomial is 1333 in octal representation. Thus,

$$f_2(x) = 1 + x + x^3 + x^4 + x^6 + x^7 + x^9.$$

3. The product of  $f_1(x)$  and  $f_2(x)$  gives

$$\begin{aligned} f'(x) &= f_1(x) \cdot f_2(x) \\ &= 1 + x + x^3 + 2x^4 + x^5 + x^6 + 2x^7 + x^8 \\ &\quad + 2x^9 + 2x^{10} + x^{11} + x^{12} + 2x^{13} + x^{15} \\ &\quad + x^{16} + x^{18}. \end{aligned}$$

4. When the coefficient of powers of  $x$  in  $f'(x)$  is taken as modulo 2 we obtain

$$f(x) = 1 + x + x^3 + x^5 + x^6 + x^8 + x^{11} + x^{12} + x^{15} \\ + x^{16} + x^{18} .$$

5. The coefficients of the powers of  $x$  in the above polynomial are entered as the shift register connections to the computer program given in Appendix A. Thus the shift register connections read through a data card in the program are 101100110010110101 starting from the highest power of  $x$  and ignoring the constant 1.

6. The computer program selects the seed for the first code as 000 000 000 000 000 001 and generates the first code in the set. This seed is then incremented by 1 and the new seed is checked to verify whether it is a segment of the code already generated. If so the seed is rejected and a new seed is obtained by incrementing the value again by 1. When a seed which is not a segment of the previously generated code is found then the program computes the next member in the set of codes. The program is written to generate a maximum of 25 sequences out of the possible 513 sequences that exist for this order of the polynomial.

The auto-correlation and the cross-correlations of these 511 bit codes are given by the Eqns. (2-3) and (2-5).

$$Ac(0) = 511, \\ |Ac(\tau)| \leq 33 \text{ for } \tau \neq 0 \\ \text{and } |cc(\tau)| \leq 33.$$

A program similar to the one just described for generating 127 bit Gold codes is given in reference [15]. A set of nine codes each of length 127 bits generated by this program is given in Table (2-2). In this table the binary elements in the code are entered as 0's and 2's. In the next section the correlation properties of these codes are evaluated through a number of computer programs.

## 2.2 Evaluation of Gold Codes as Phase Diffusers in Multiplex Holography

In this section the results of evaluation of auto and cross-correlation properties of Gold codes of different lengths are presented. Also the computer simulated outputs of a space-variant processor implementing the Gold codes as phase diffusers for multiplexing a number of transfer functions in a single hologram are given. The computations are carried out for Gold codes of lengths 127 and 511 bits under the following different conditions: The Gold codes used as (a) an ideal phase diffuser with  $180^\circ$  phase difference between the elements, (b) an amplitude diffuser with transmittance values of 0's and 1's, (c) a non-perfect phase diffuser with phase difference between the elements not equal to  $180^\circ$  and (d) an ideal phase diffuser illuminated by a spherical wave front instead of a plane wave front.

The auto correlation of a function  $r_1$  may be calculated using the relation



02020022002202002200220200220200220202202222200202  
 022200022022020000002000220002002002002002022  
 20202002022202220220020200020

02022200222200000002022202022200222202002020222  
 22220020022202220002002200222200022200202020  
 20200022202222020000000222222

0200222200220022000200200200000022200020220020  
 202020020002002000002220202200200222202022000  
 0022200202020202022222200000

220202220020022020000020020000022220002220200  
 00220202220202022222022202022200202202002022  
 0200022202220202000202020202020

20220022000002022220020020220200000220020020  
 0220202220222200222220222202200022020222002  
 20222020202022202020202020202

22022222220202220020200002020022202220002022  
 0022222220020202022022202202020202020202020220  
 002220220020022202020202020202

2220200222000020020222220202202002000000222200  
 0000020200002220222200222002002220220202020  
 002000202202002220000002222222

00020002202020220222202200200002022002222020  
 220202222002220000220220222000222200220200  
 20200220200202200000202002002

22202000002220200220220022200200202220020200020  
 202222202020222220200202022020202202022002200  
 2022002000002020220000202222

Table 2-2. Set of nine 127 bit Gold codes.

$$R_{11} \triangleq r_1 \star r_1 = F\{R_1 \cdot R_1^*\} , \quad (2-6)$$

where  $\star$  represents correlation and  $*$  represents the conjugate operator and  $r_1$ ,  $R_1$  are the Fourier transform pairs defined as

$$R_1 \triangleq F\{r_1\} . \quad (2-7)$$

Similarly the cross-correlation between the functions  $r_1$  and  $r_2$  may be obtained from the relation

$$R_{12} \triangleq r_1 \star r_2 = F\{R_1 \cdot R_2^*\} , \quad (2-8)$$

$$\text{where } R_2 \triangleq F\{r_2\} \quad (2-9)$$

If the functions  $r_1$  and  $r_2$  have spatial widths of  $w_1$  and  $w_2$  respectively then the functions  $R_{11}$  and  $R_{12}$  have spatial widths of  $w_{11}$  and  $w_{12}$  given by

$$\begin{aligned} w_{11} &\triangleq \text{width of } R_{11} = 2w_1 \text{ and} \\ w_{12} &\triangleq \text{width of } R_{12} = w_1 + w_2 \end{aligned} \quad \left. \vphantom{\begin{aligned} w_{11} \\ w_{12} \end{aligned}} \right\} \quad (2-10)$$

Thus in computer simulations sufficient allowance must be made to accommodate the larger size of the output.

Similarly the output of a space variant processor implementing the phase coded reference beam technique for multiplexing may be simulated by computing the terms in the Eqn. (1-14). Again if the impulse response  $h_1$  has a

spatial width of  $W_h$ , the width of the term  $h_1 * r_1 * r_2$  is given by

$$W_o \triangleq \text{width of the term } h_1 * r_1 * r_2 = W_h + W_1 + W_2 \quad (2-11)$$

Thus in the simulation of multiplex holography using Eqn. (1-14) the size of the output array must be made sufficiently large as given by the above equation.

### 2.2.1 Results of Evaluation of Gold Codes as Perfect Phase

Diffusers: A program for the calculation of the autocorrelation and the cross-correlations of a set of nine 127 bit Gold codes is given in Appendix B. Another program to simulate the output of a processor using these codes as phase diffusers for multiplexing is given in Appendix C. In these programs the size of the output array is taken to be 128 elements. Thus in order to satisfy the Eqn. (2-11) the widths of the codes  $r_1$  and  $r_2$  and the width of the impulse responses are all made equal to 42 bits. Thus in these programs only the central 42 bits out of the 127 bit codes are used in the computations. (Although it was possible to use 64 bits in the program SPACEVAR of Appendix B, only 42 central bits are used so that the results of the two programs may be compared.) The program SPACEVAR computes the autocorrelation of the central 42 bits of a 127 bit code and the cross-correlations of these 42 bits with the central

42 bits of the remaining codes in a set of 9 codes, using the Eqns. (2-6) and (2-8). The magnitudes of the outputs are normalized with reference to the peak of the auto-correlation. The outputs are plotted to a width of 2.56 inches and a height of 2.5 inches. The resulting plot is shown in Fig. (2-1).

Figure (2-1)a is the plot of auto correlation of mask 1 and the Figs. (2-1)b through i are the cross-correlations of mask 1 with the masks 2 through 9. Note that the cross correlations have comparable large magnitudes and hence we may expect poor reconstruction of the impulse responses when these codes are used for multiplexing the system transfer functions. The program MPXHOLE of Appendix C simulates the output of a system when two transfer functions are multiplexed using the Gold codes as phase diffusers. The program reads two impulse responses representing a space-variant system and multiplexes their transfer functions on a single composite array using a different Gold code as phase encoder for each of the responses. Thus a composite transfer function hologram is generated. This hologram includes only the terms that result in an output in the output plane as explained in Section 1.2. The output of the processor when the composite hologram is accessed by a reference beam encoded by a duplicate of the code used for recording is simulated by this program. The program also simulates the

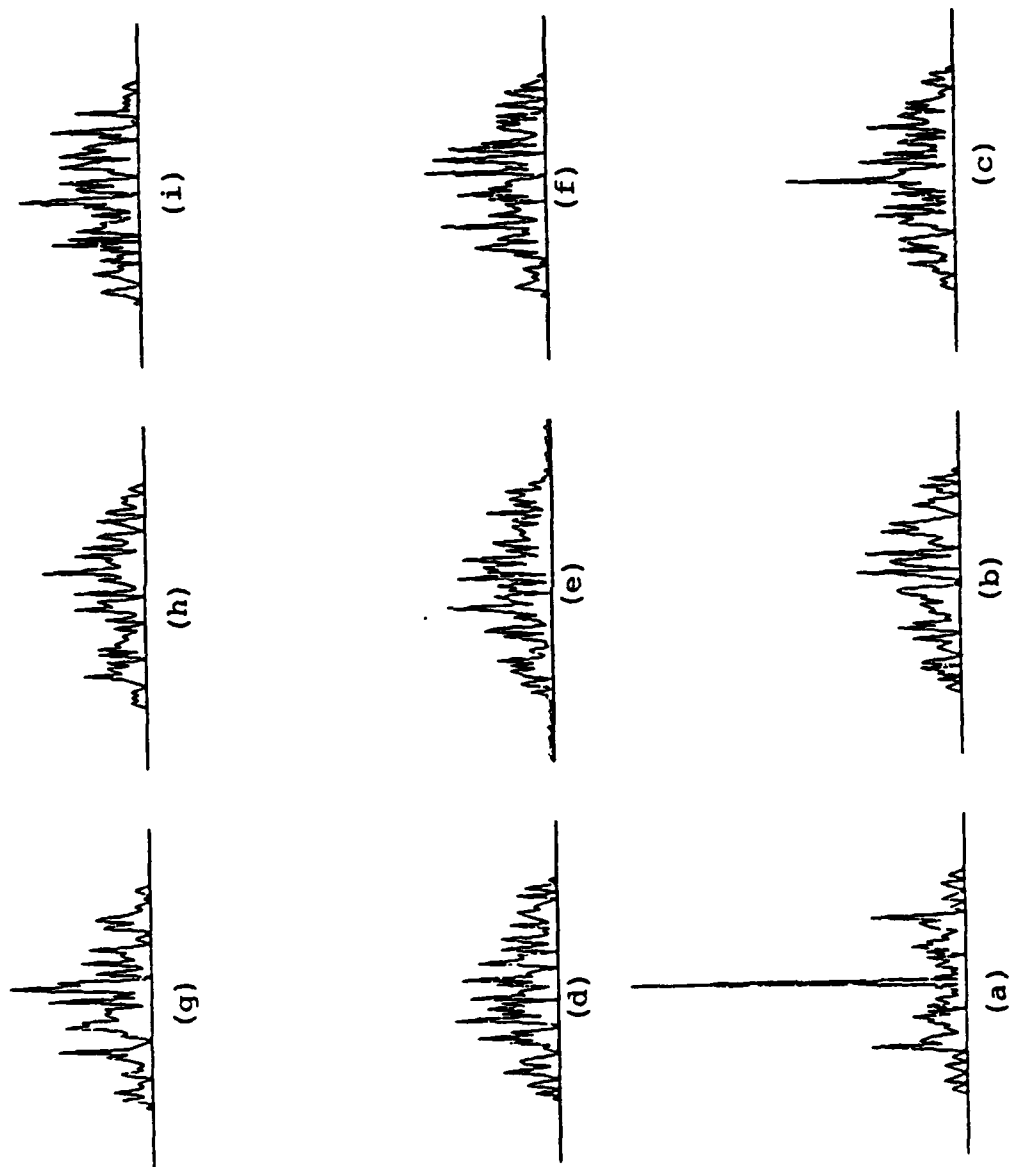


Figure 2-1. Autocorrelation and crosscorrelations of 42 central bits of 127 bit Gold codes.

output when only one of the transfer functions is recorded and played back using a Gold code. This simulation is done to assess the distortion in the impulse responses due to non ideal auto correlation of the codes. The program plots the outputs of these simulations as well as the impulse responses used. The results of these simulations for three sets of impulse responses are shown in Figs. (2-2), (2-3) and (2-4). The impulse responses used in the first simulation consists of two disjoint inputs as shown in Figs. (2-2)a and b. The outputs when the transfer functions of these impulse responses are recorded and played back using a Gold code one at a time are shown in Figs. (2-2)c and d. Note that due to non-ideal auto-correlation of the Gold codes, the output impulse responses are considerably distorted. This distortion is due solely to the auto-correlation and the effects of cross correlation are not included. Figures (2-2) e and (2-2)f show the outputs when both the transfer functions are multiplexed in a single array and then an attempt to retrieve the impulse responses individually are made. These outputs are distorted much more than the outputs of Figs. (2-2)c and d because of the cross talk between the holograms due to non zero cross-correlations in addition to the non ideal auto-correlations of the Gold codes. Finally the result when both the transfer functions are accessed simultaneously by two phase coded reference

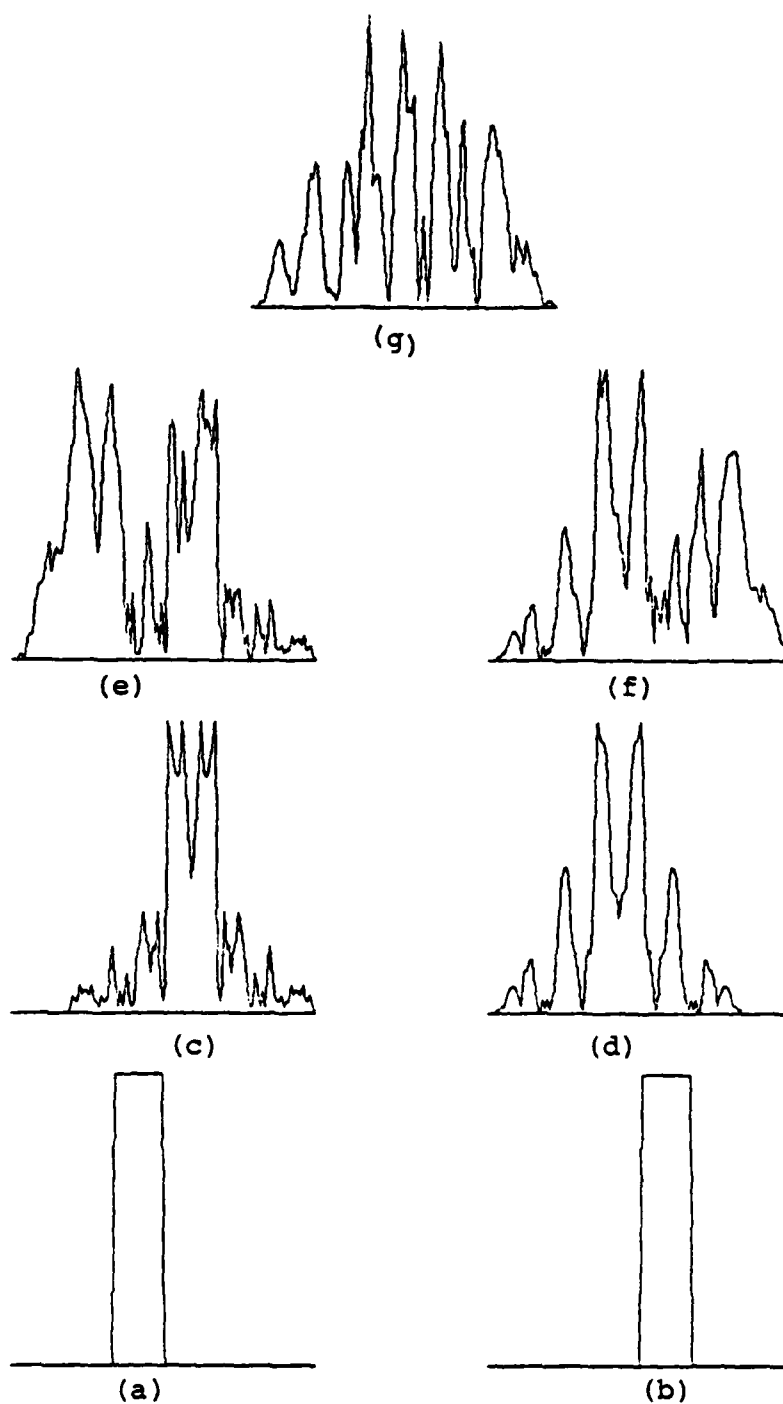


Figure 2-2. Simulation of multiplex holography using 42 central bits of 127 bit Gold codes. (Disjoint impulse responses.)

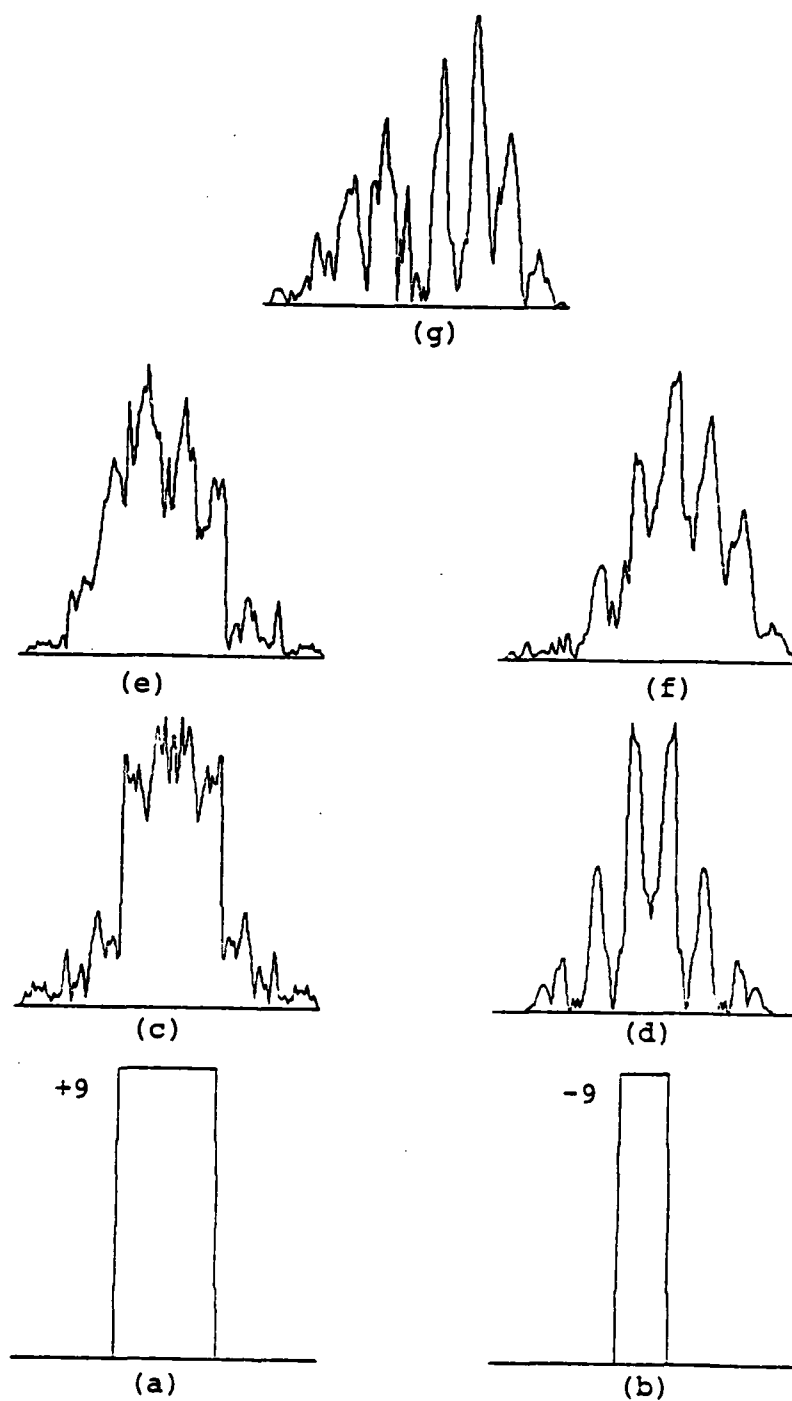


Figure 2-3. Simulation of multiplex holography using 42 central bits of 127 bit Gold codes (overlapping impulse responses).



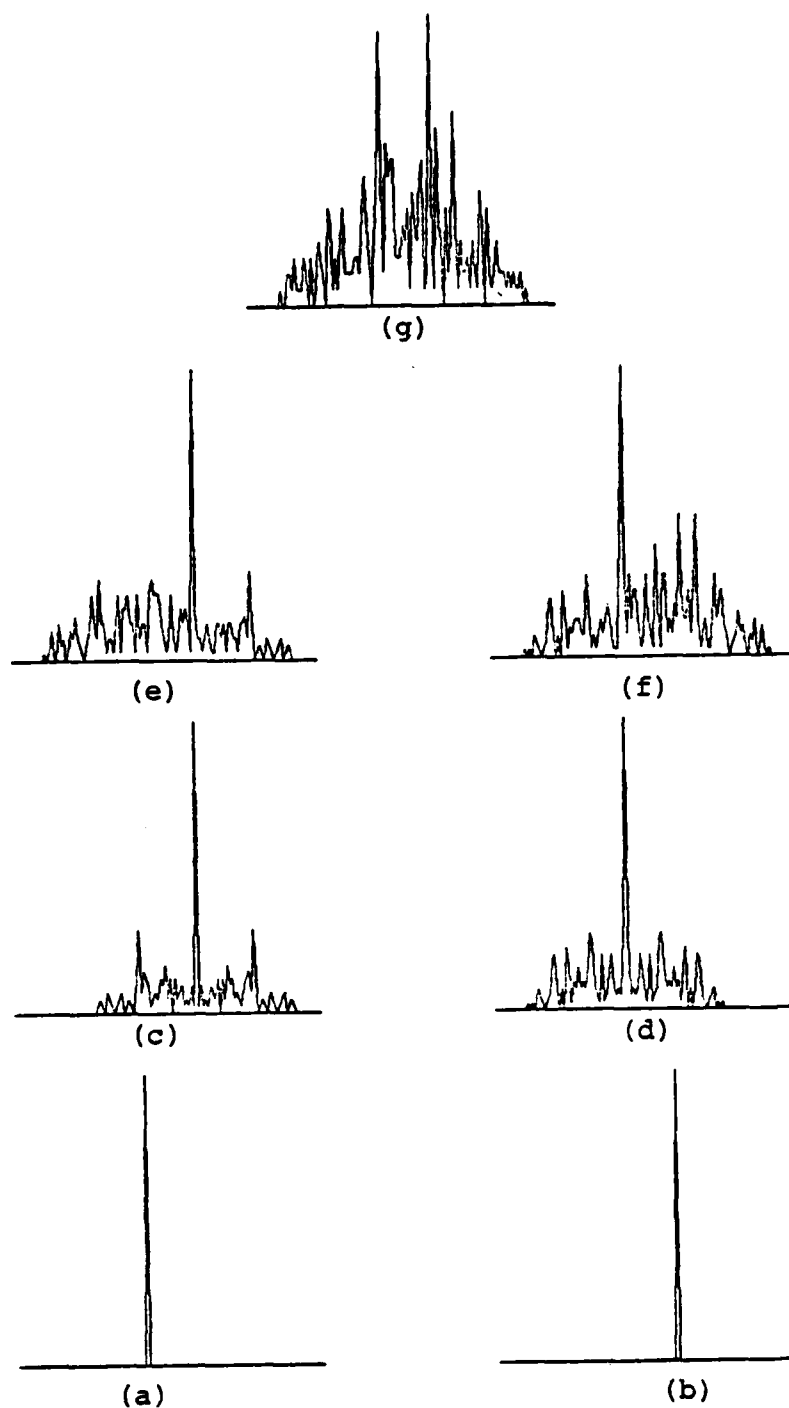


Figure 2-4. Simulation of multiplex holography using 42 central bits of 127 bit Gold codes. (Delta like impulse responses.)

beams is shown in Fig. (2-2)g. The corresponding outputs when two overlapping impulse responses, one with a positive amplitude and the other with a negative amplitude, as shown in Figs. (2-3)a and b, are used as inputs to the simulator are shown in the Figs. (2-3)c through g. In the next simulation two impulse responses with values similar to delta functions are used as inputs and the corresponding outputs are shown in Fig. (2-4). Note that in this case the outputs, although containing a substantial number of noise terms, have a term that may be attributed to the desired output. These simulations show that the undesired terms in the correlations of the 42 central bits of the 127 bit codes are too large and hence result in a poor playback. This is because an arbitrary segment of the Gold code does not exhibit the same degree of randomness as the full code. Thus further simulations to study the correlation properties of the 127 bit codes when the entire length of the codes are used for multiplexing were carried out. This was done by altering the size of the arrays in the computer program to accommodate the larger size of the outputs as determined by the Eqns. (2-10) and (2-11). The results of these simulations are shown in Figs. (2-5) through (2-8). Figure (2-5) shows the auto and cross-correlations of the 127 bit Gold code. A comparison of this output with that of Fig. (2-1) indicates a substantial reduction in the magnitudes of the undesired components. The impulse responses used in the simulation of multiplex holography using all the 127 bits

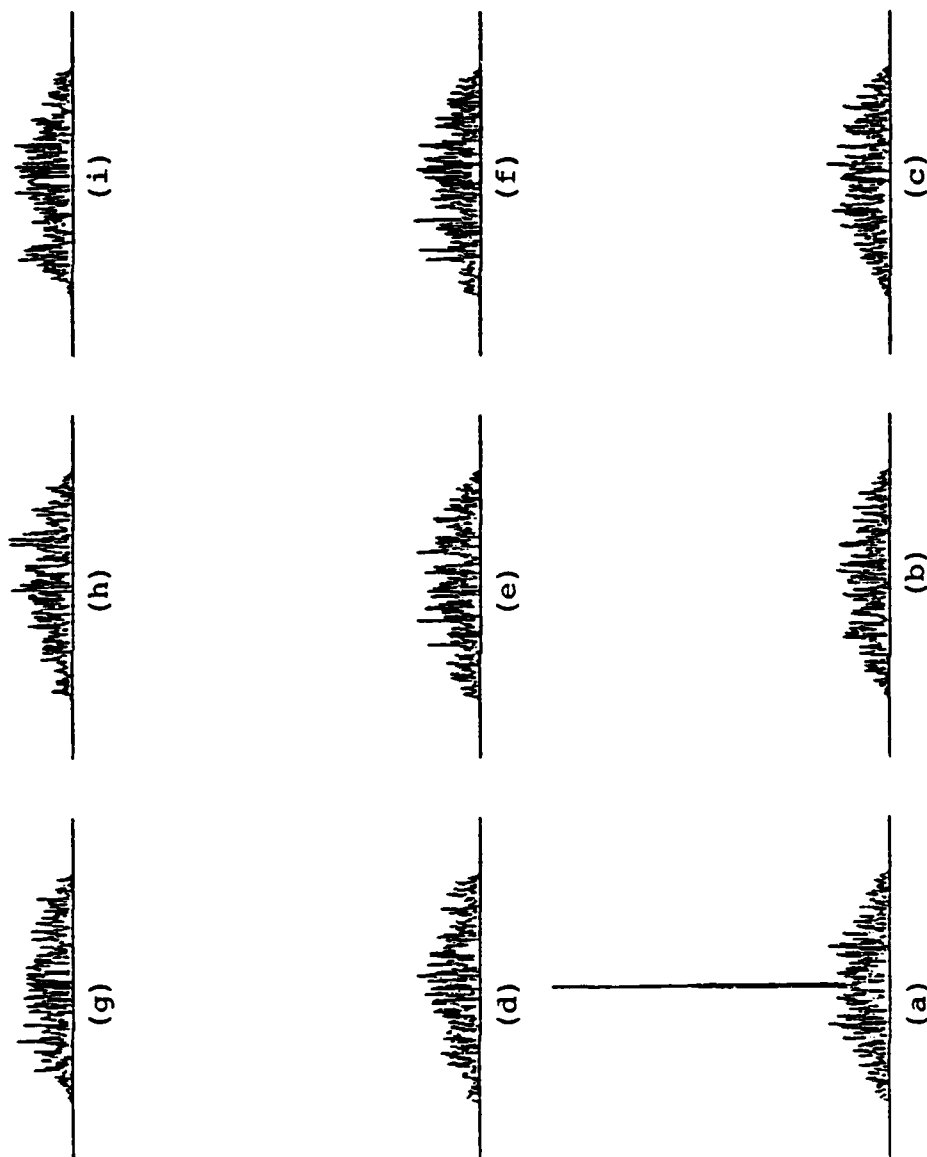


Figure 2-5. Autocorrelation and crosscorrelations of 127 bit Gold codes.

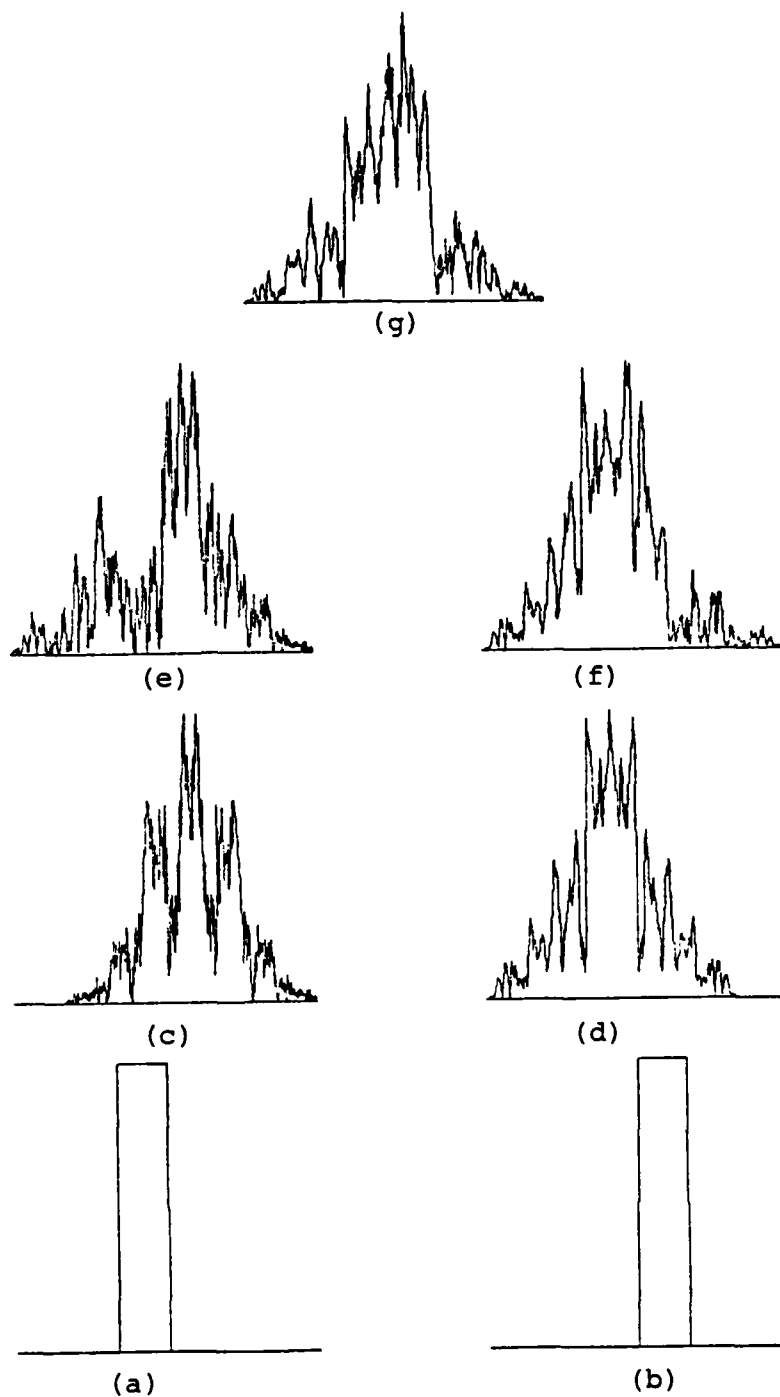


Figure 2-6. Simulation of multiplex holography using 127 bit Gold codes (disjoint impulse responses).

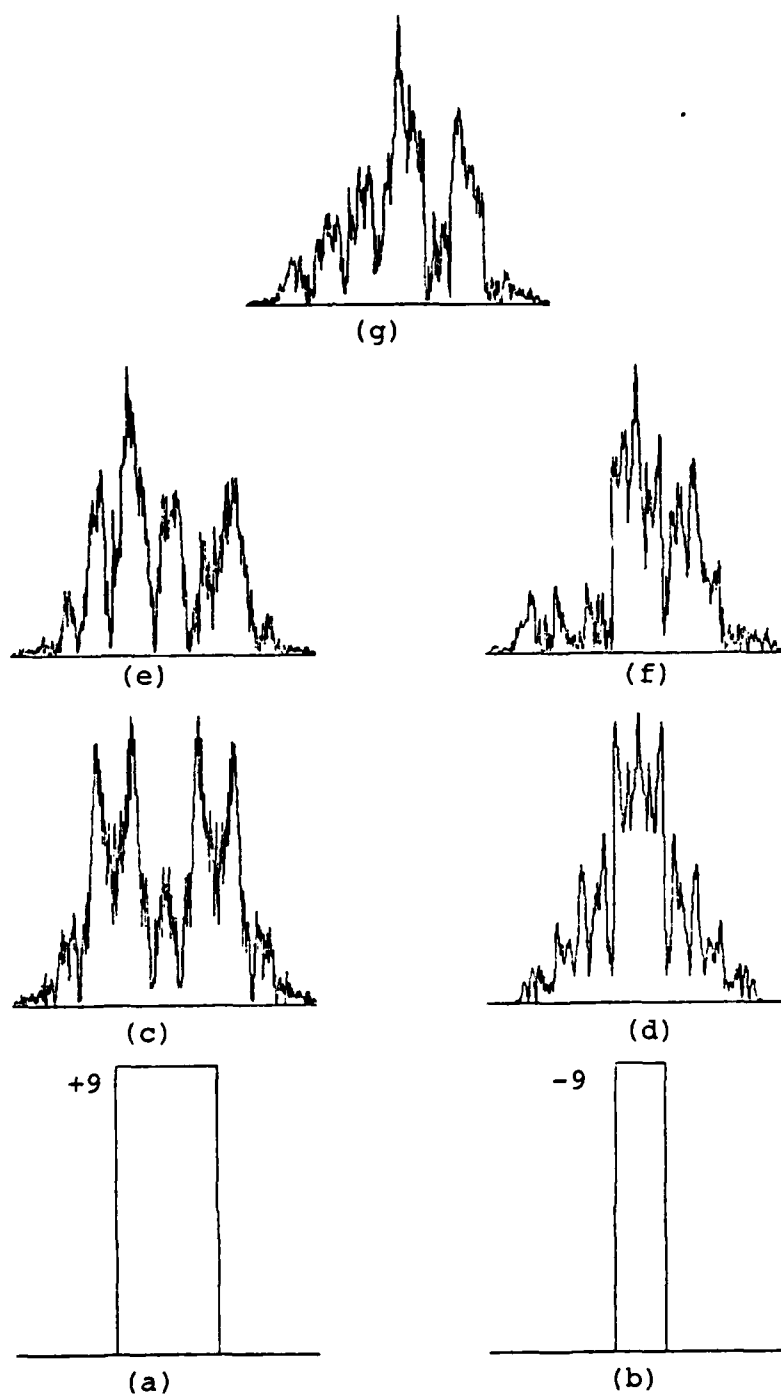


Figure 2-7. Simulation of multiplex holography using 127 bit Gold codes (overlapping impulse responses).

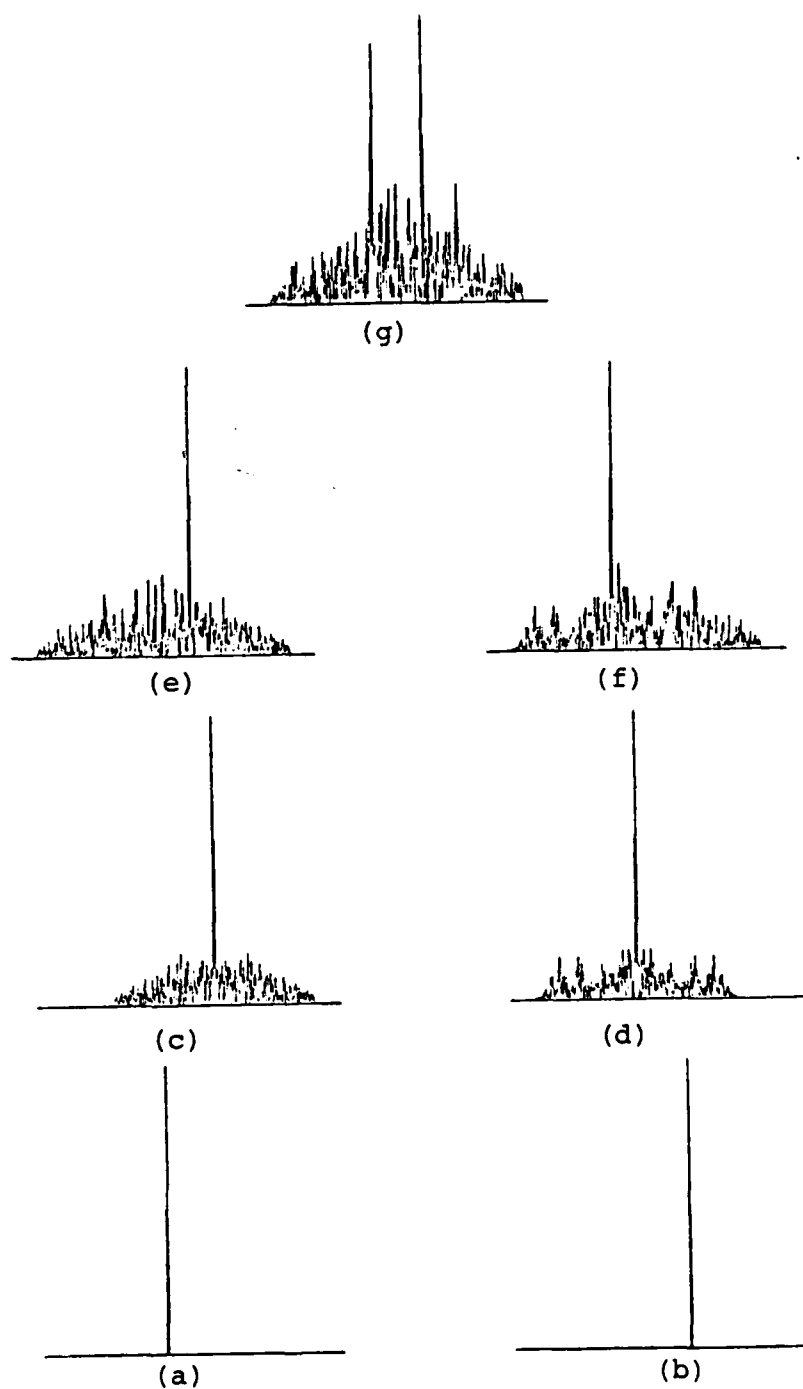


Figure 2-8. Simulation of multiplex holography using 127 bit Gold codes (Delta like impulse responses).

of the Gold codes are similar to the ones used in the simulation when only a part of the codes was used in the computation. Note that the outputs when the impulse responses are delta like functions have noise terms at much lower magnitudes compared to the outputs in Fig. (2-4). Finally the results of evaluation of correlations and simulation of multiplex holography when Gold codes of length 511 bits were used are shown in Figs. (2-9) through (2-12). The Gold codes used in these computations are the outputs of the program CODE described in Section 2.1. Here again note that the magnitudes of the undesired terms in the correlation outputs are much smaller than the outputs for codes of smaller lengths. There is also a substantial improvement in the output when delta function like impulse responses are used in the simulation of multiplex holography compared to the outputs using smaller length codes. However there is no improvement in the outputs when the impulse responses are broader. This may be attributed to the fact that although the magnitudes of the individual noise elements in the correlation outputs are small, the number of such terms are large with larger length of codes and their collective contributions when convolved with the impulse responses may be quite high. A major problem may be the fact that the Gold codes, unlike the maximal length cyclic codes from which they are derived, are not balanced to have the same number of +1's and -1's. Thus the expected value of a bit is not

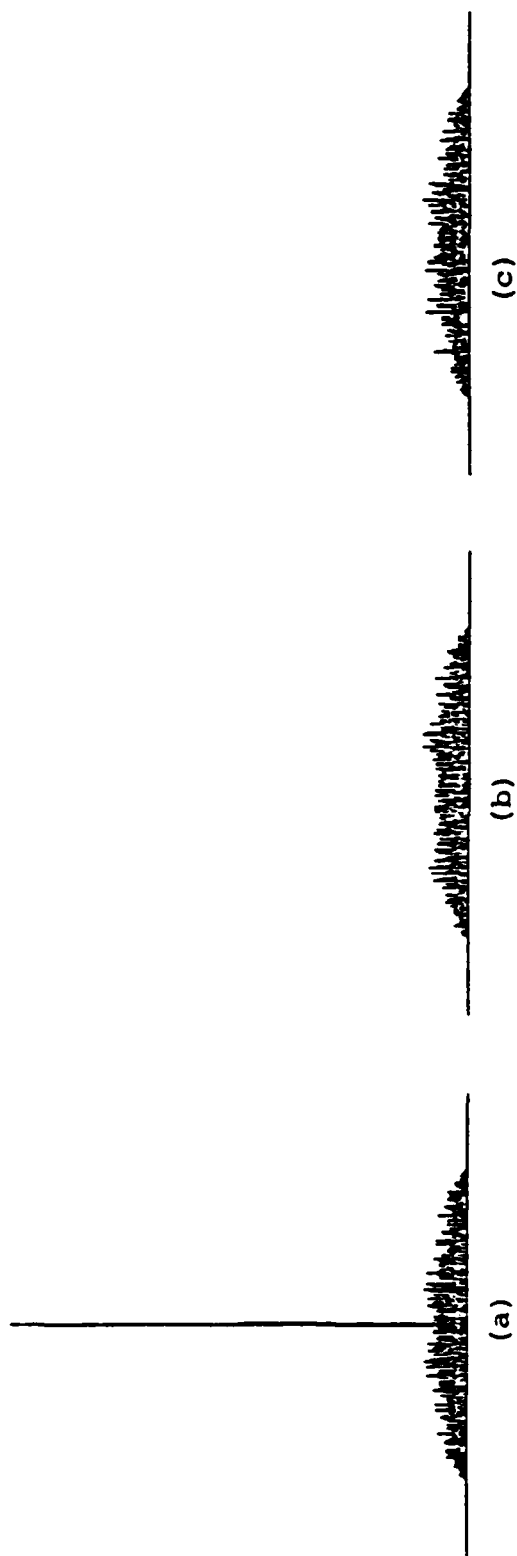


Figure 2-9. Autocorrelation and crosscorrelations of 511 bit Gold codes.



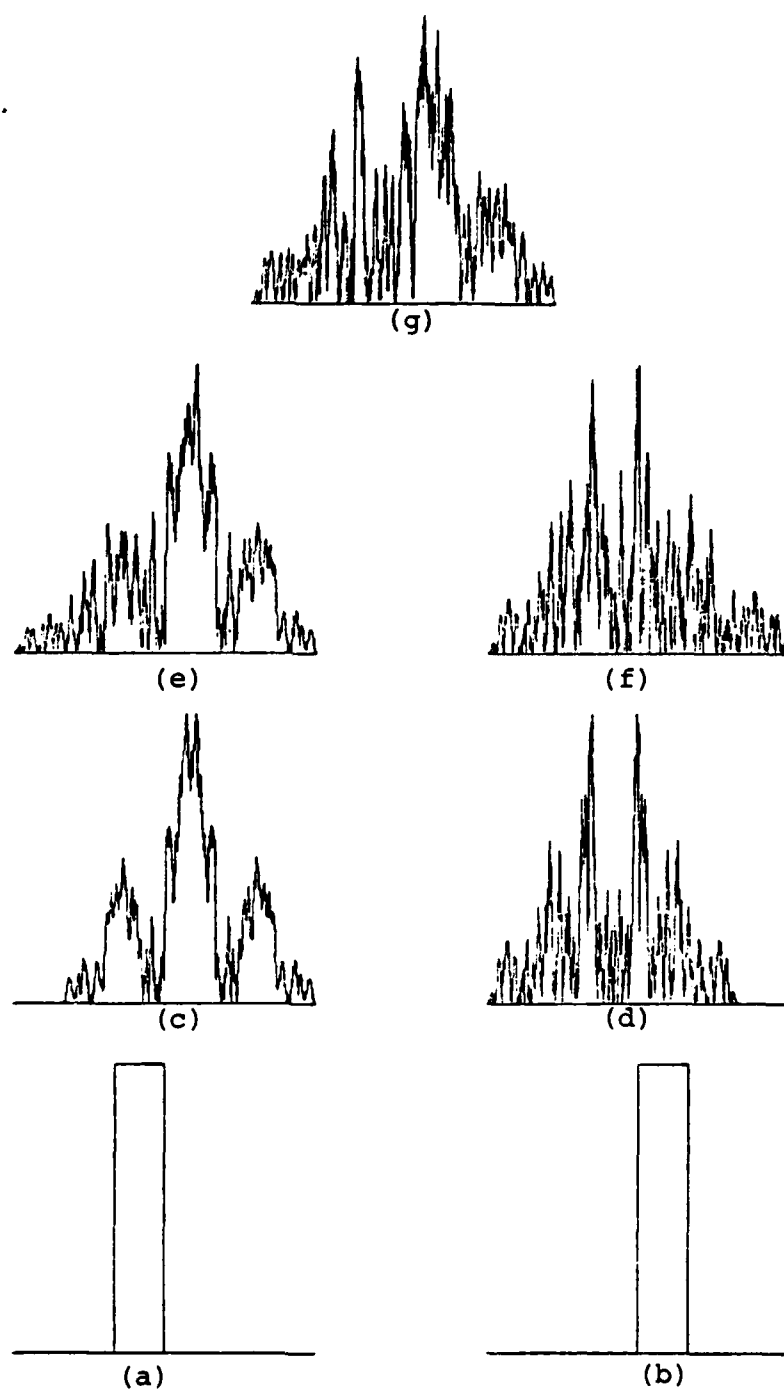


Figure 2-10. Simulation of multiplex holography using 511 bit Gold codes. (Disjoint impulse responses.)

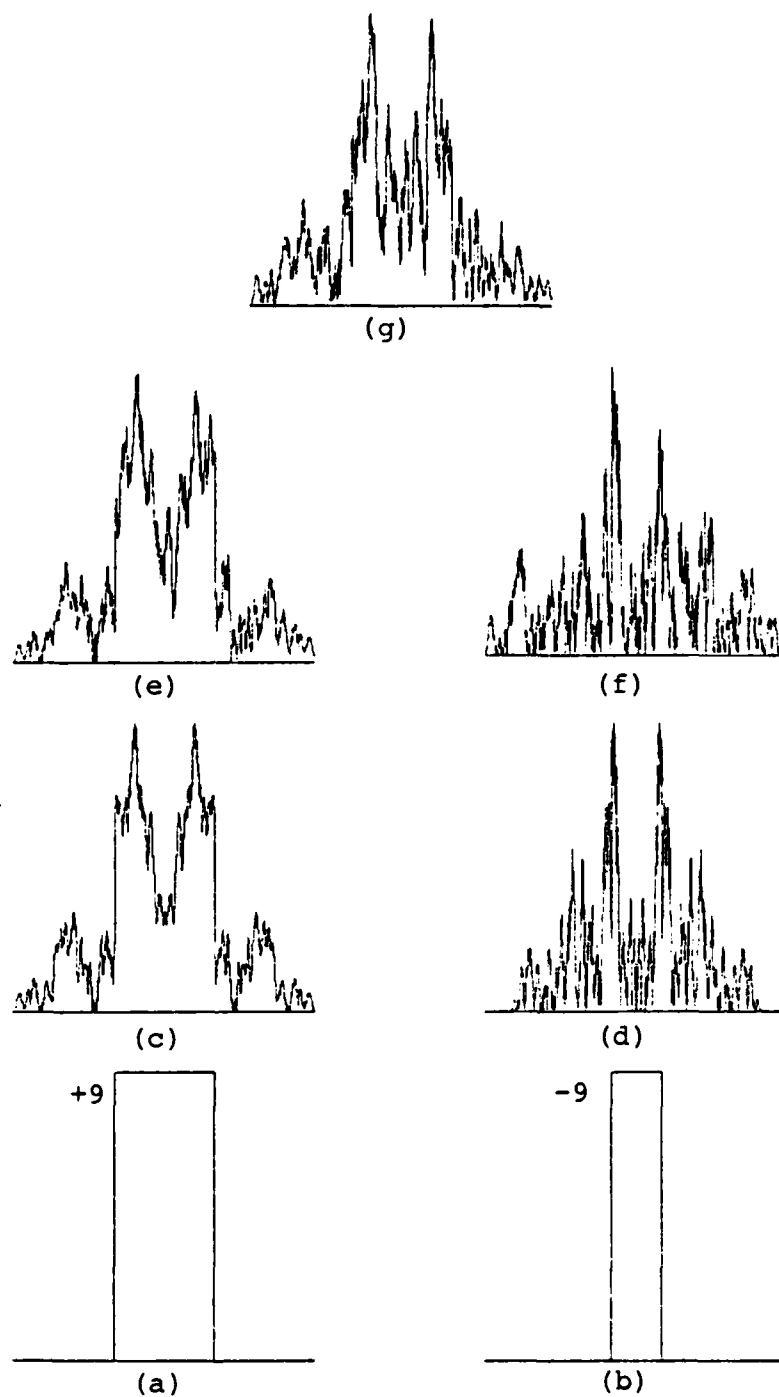


Figure 2-11. Simulation of multiplex holography using 511 bit Gold codes (overlapping impulse responses).

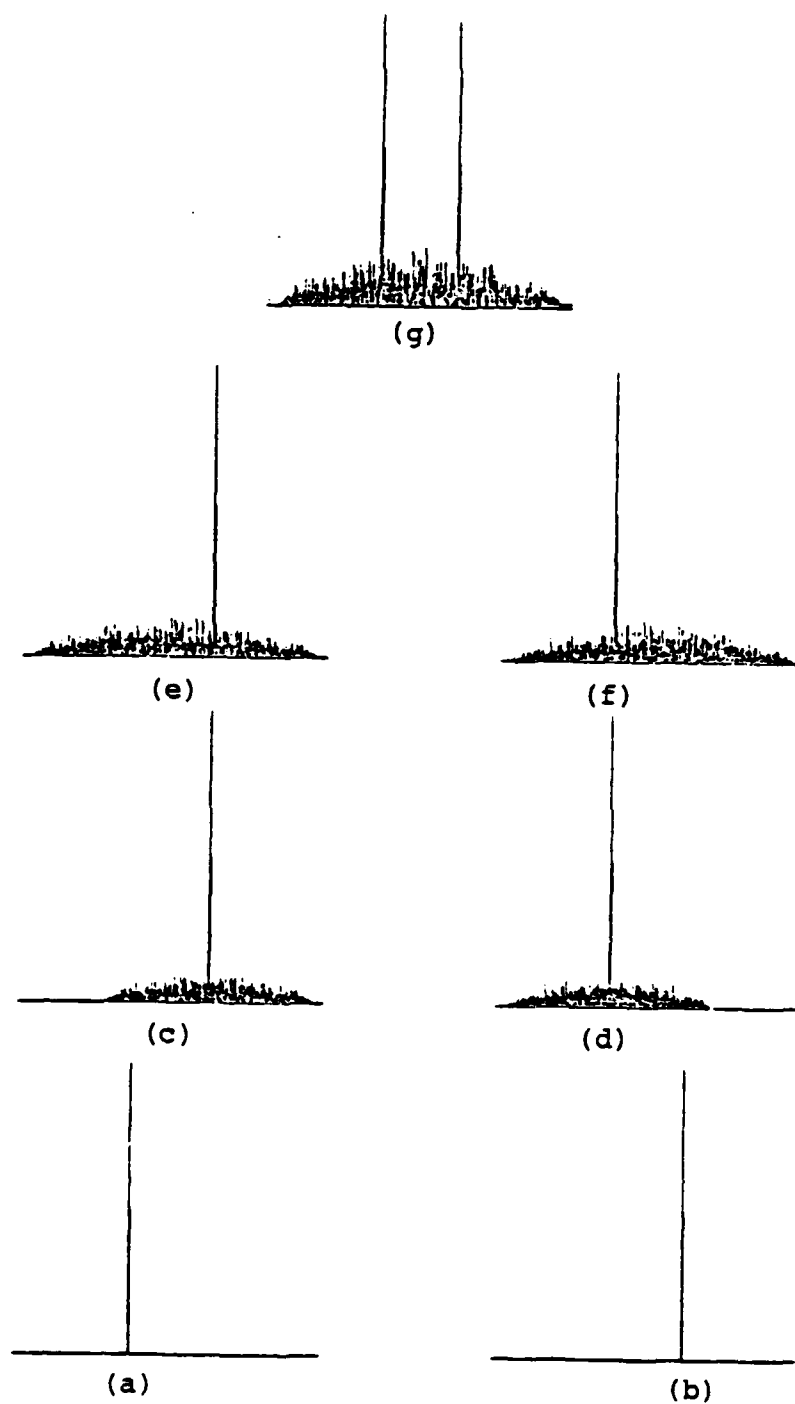


Figure 2-12. Simulation of multiplex holography using 511 bit Gold codes (Delta like impulse responses).

zero, and there is a built-in bias. The outputs of these simulations suggest that the method of space-variant system representation using phase coded reference beams is more suitable for space-variant systems having narrow impulse responses. An example of such a system is a magnifier which transforms points in the input plane to points in the output plane.

All the simulations described so far have been done under the assumption that the Gold code masks used in the system for recording and playback are pure phase masks with exactly  $180^\circ$  phase difference between the elements in the code. However it is generally difficult to fabricate such a perfect phase mask. For this reason an evaluation of the performance of a system using non perfect phase masks and binary amplitude masks was carried out and the results are presented in the next subsections.

#### 2.2.2 Results of Evaluation of Gold Codes as Amplitude

Masks and Non Perfect Phase Masks: An amplitude mask of a binary Gold code may be easily fabricated using any high contrast copy film. The transmittance of these masks has values of 0 and 1 instead of +1 and -1 for a perfect phase mask. The auto-correlation and the cross-correlations of such amplitude masks with code lengths of 127 bits are shown in Fig. (2-13). Note that the magnitudes of the correlation terms are very large toward the center of the output array and then tail off rather slowly. The outputs of simulation of multiplex holography for the same

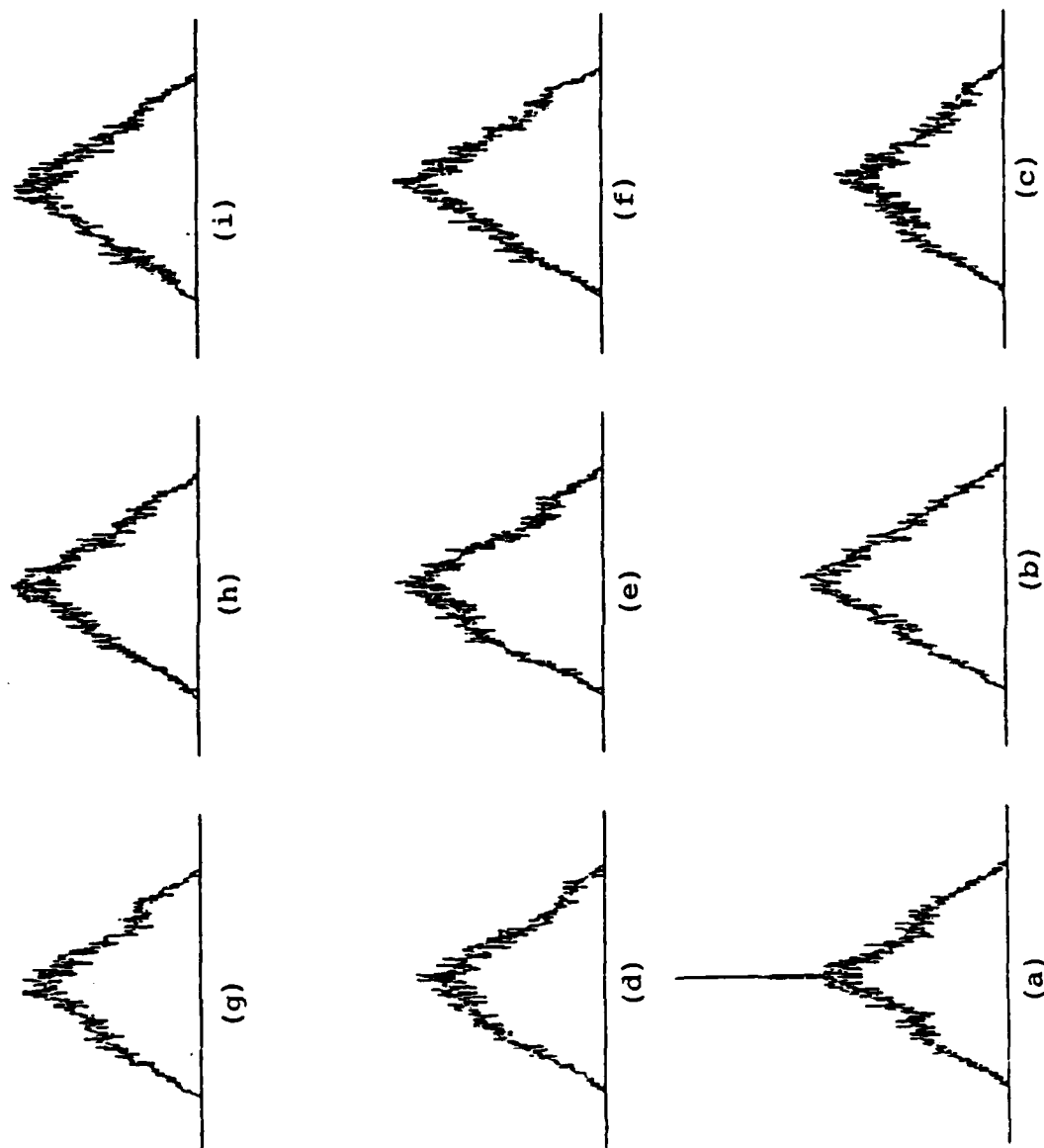


Figure 2-13. Autocorrelation and crosscorrelations of 127 bit Gold codes used as binary amplitude masks.

inputs used in the case of pure phase masks are shown in Figs. (2-14) through (2-16). Comparison of these outputs with those of Figs. (2-5) through (2-8) reveals that the phase masks are much superior in performance to amplitude masks. However as mentioned earlier it is difficult to fabricate phase masks with phase difference of exactly 180 degrees between the elements. Thus a study was made to determine an acceptable level of tolerance in the value of the phase difference. The program SPACEVAR of Appendix B was modified to account for non perfect phase masks with phase differences of 172°, 162°, 150°, and 120°. The output of auto-correlation of a 127 bit mask with itself and the cross-correlation with two other 127 bit masks were computed and plotted. The plots for various degrees of non perfectness is shown in Fig. (2-17). From these outputs it may be concluded that it is desirable that the phase differences between the elements of the code should be within 10% of 180°. In the next subsection the results of evaluation of Gold codes when a spherical wavefront is used during recording and playback are presented.

### 2.2.3 Results of Evaluation of Gold Codes Illuminated by

Spherical Wavefront: It has been reported [16] that the use of spherical wave illumination instead of plane wave illumination in an optical processing system implementing the phase coded reference beam multiplexing tech-

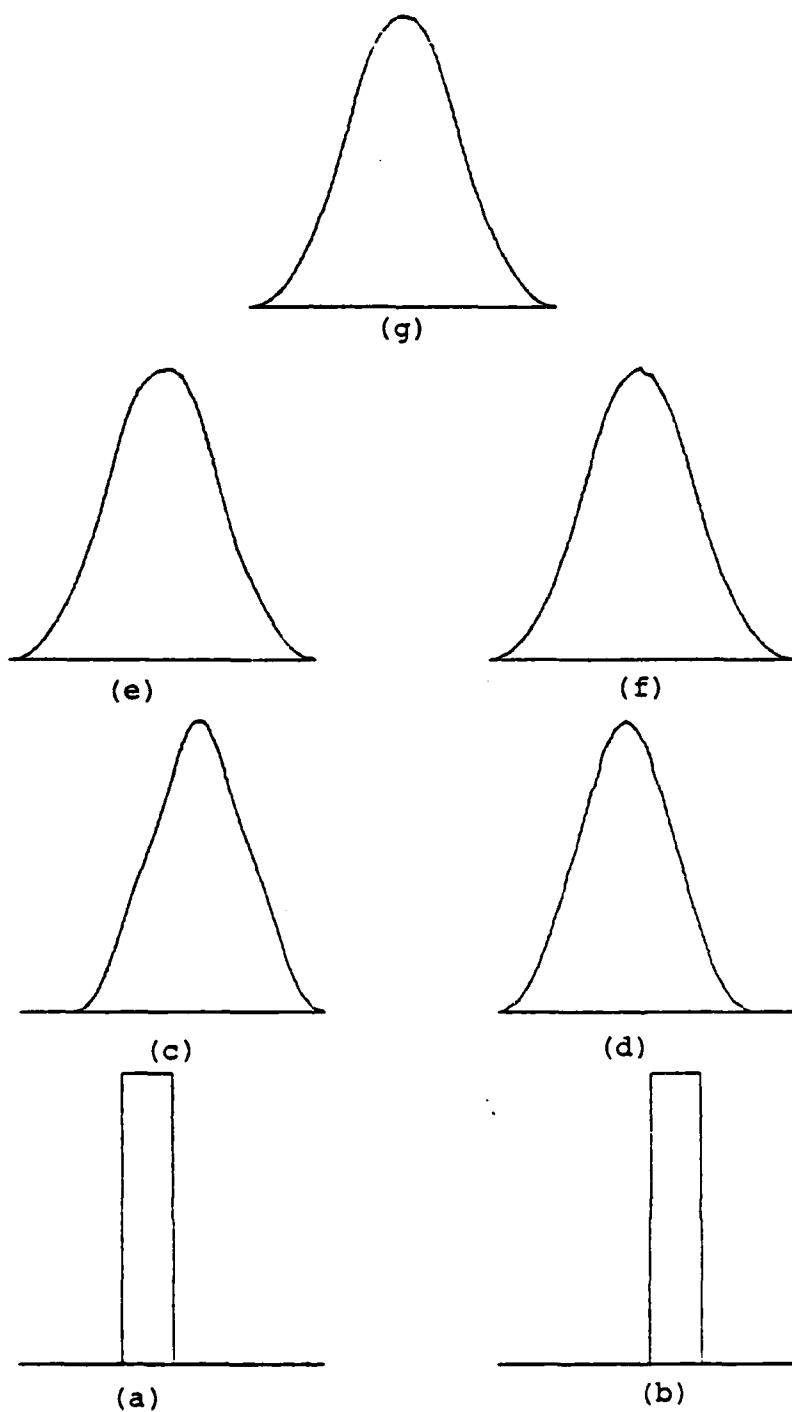


Figure 2-14. Simulation of multiplex holography using 127 bit amplitude masks (Disjoint impulse responses).

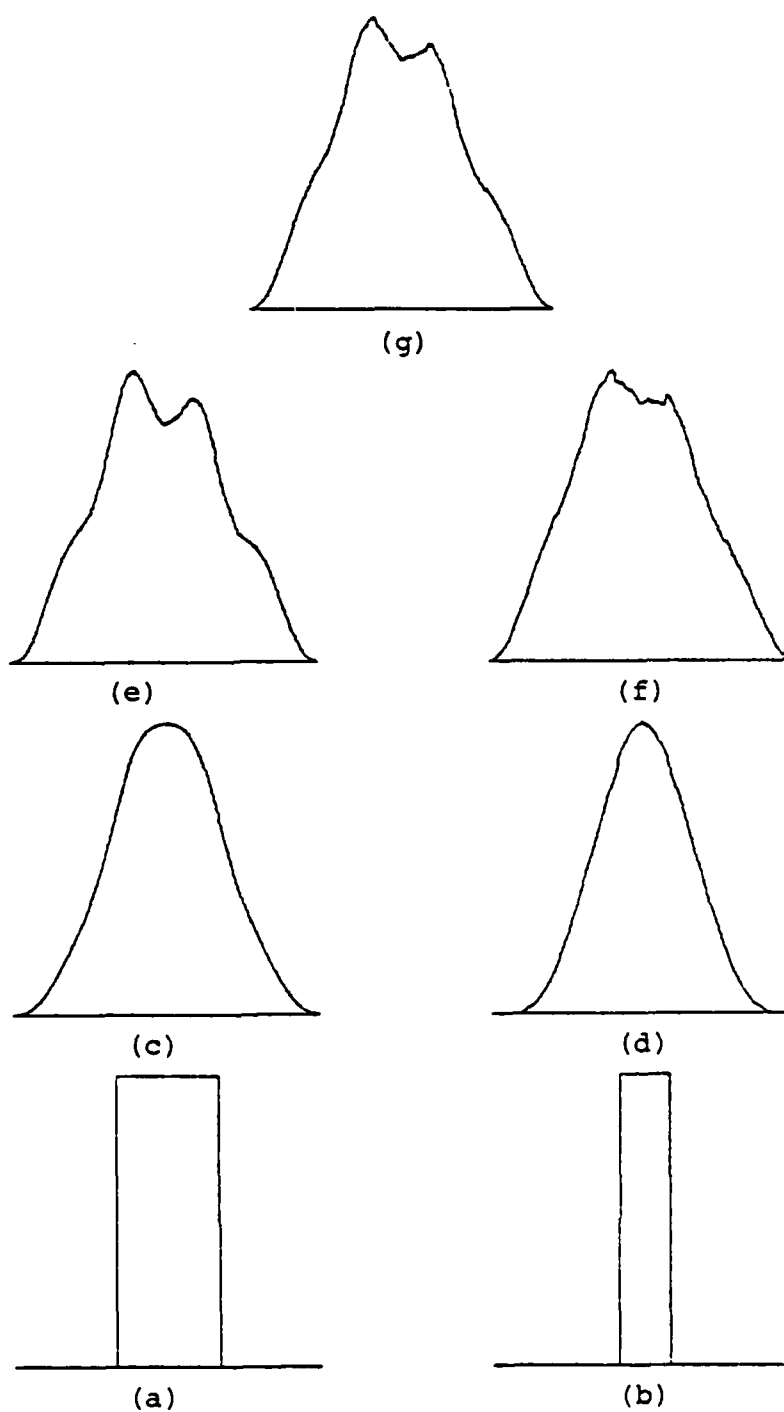


Figure 2-15. Simulation of multiplex holography using 127 bit amplitude masks (overlapping impulse responses).



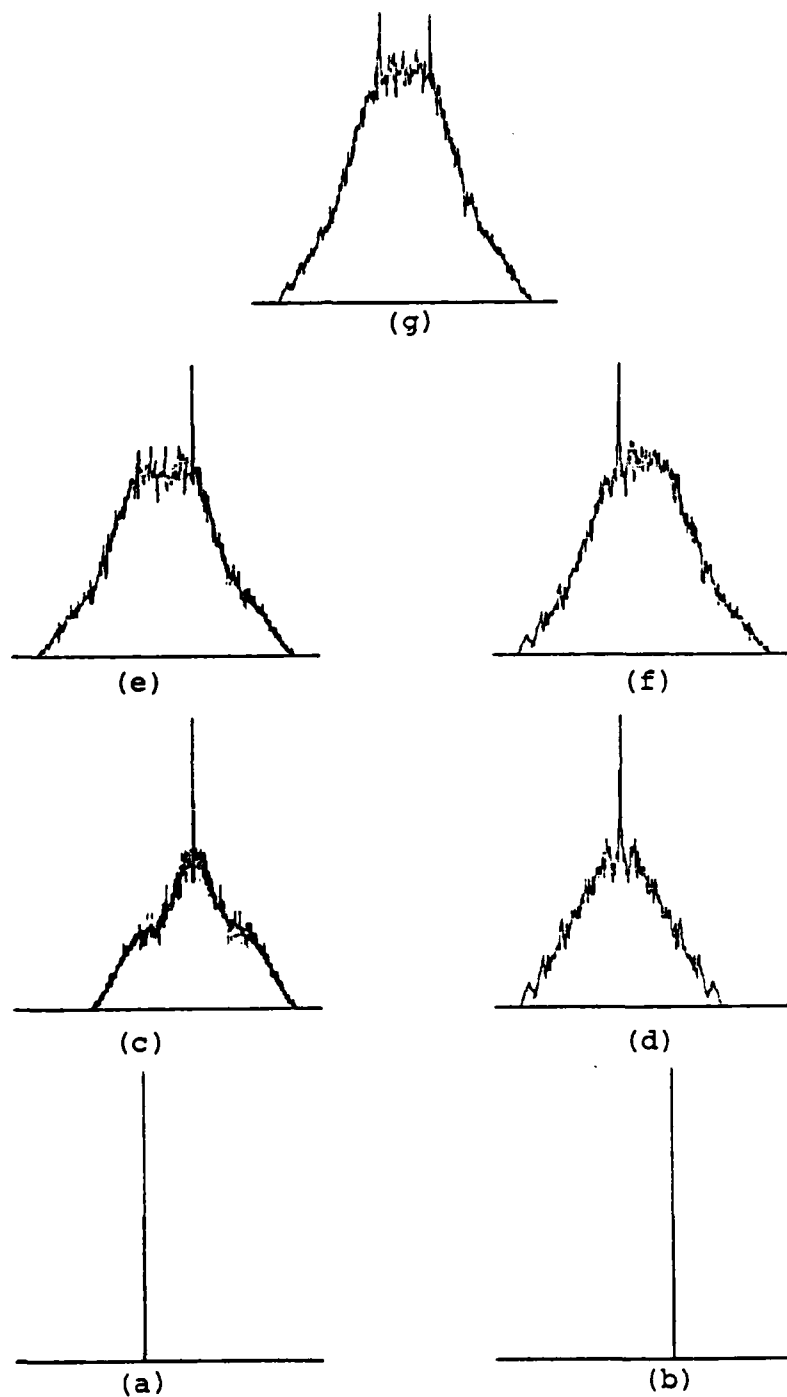


Figure 2-16. Simulation of multiplex holography using 127 bit amplitude masks (Delta like impulse responses).

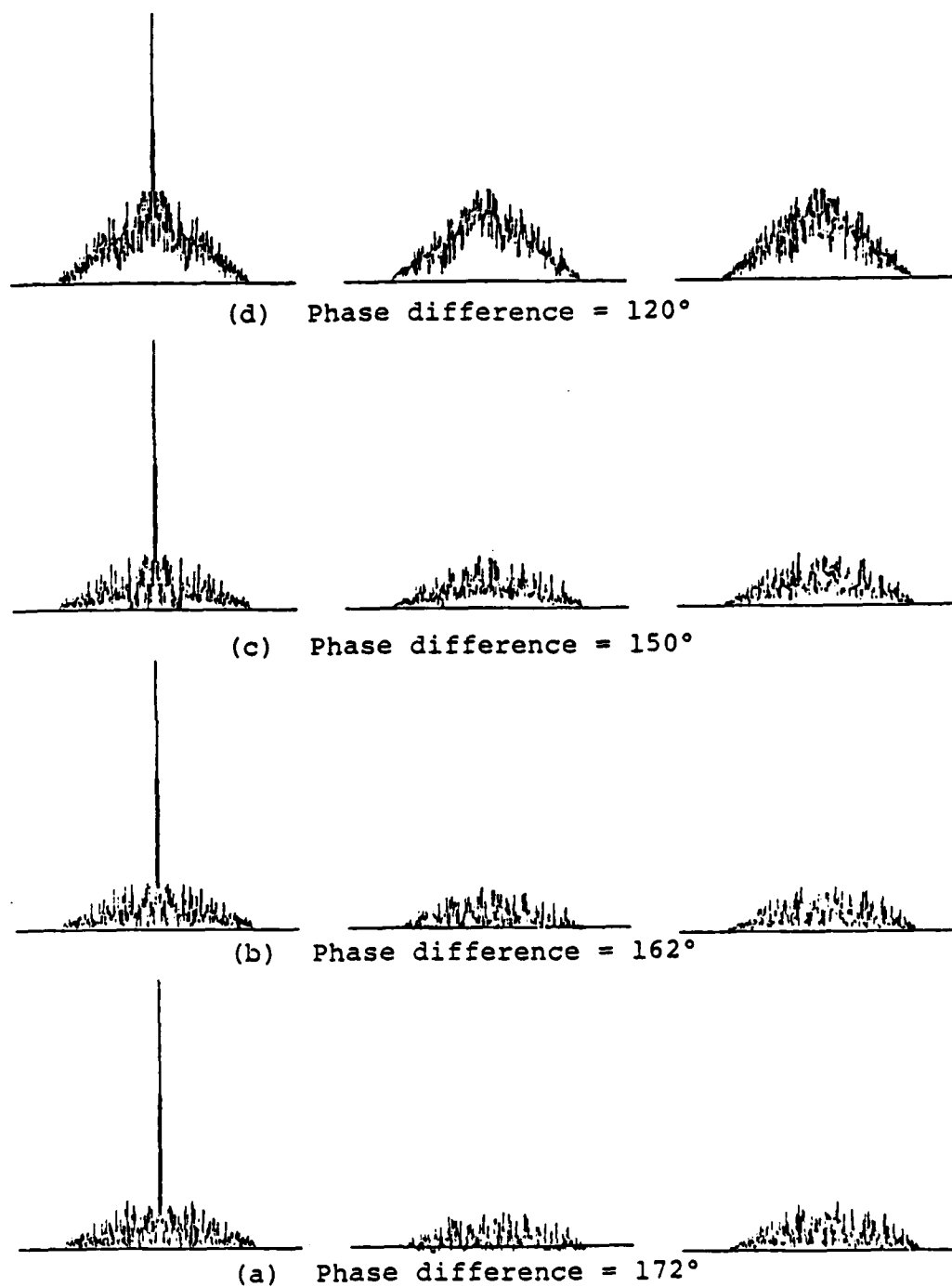


Figure 2-17. Autocorrelation and crosscorrelation of 127 bit Gold codes used as non perfect phase masks.

nique results in a reduction in the magnitudes of the cross-talk terms during playback. A computer program SPHWAVE given in the Appendix D was used to compute the auto and cross-correlations of two 127 bit masks when illuminated by spherical waves of different values of chirp, i.e., different radii of curvature and the width of mask.

The method for calculating the chirp at each element of the mask is shown in the Fig. (2-18). Let  $R$  be the radius of curvature of spherical wave in millimeters, and let  $w$  be the width of the mask in millimeters; the path difference  $\Delta l$  between the wave front at a point  $n$  elements from the center of the array is then given by

$$\Delta l = \sqrt{R^2 + \left(\frac{2nw}{N}\right)^2} - R, \quad (2-12)$$

where  $N$  is the total number of elements in the entire array.

The phase difference  $\theta$  in radians at the center of the element with reference to the center of the array when using an illumination of wavelength equal to  $\lambda$  millimeters is given by

$$\theta = \left(\frac{\Delta l}{\lambda} - n\right) 2\pi, \quad (2-13)$$

where  $n$  is an integer chosen such that  $0 \leq \theta < 2\pi$ .

At optical wavelengths the phase angle  $\theta$  changes very rapidly along the width of the phase mask. There will be

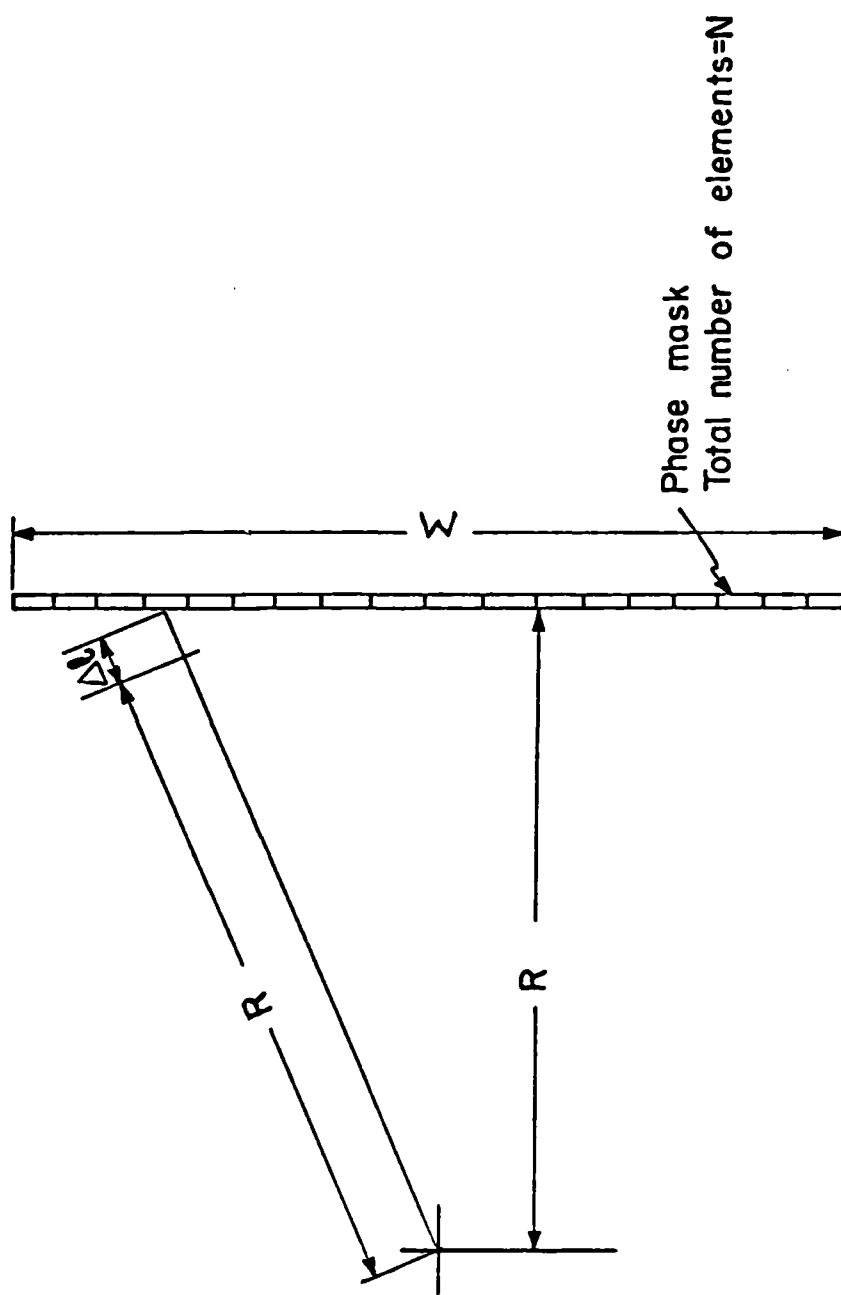


Figure 2-18. Calculation of phase-angle at an element due to spherical wavefront.

many complete cycles of phase change within each element of a 127 bit mask even for such small mask sizes as 3 mms. For this reason it is necessary to breakup each element of the code into several subcells as is done in the program. Then the value of each subcell is determined by the value of the originating element, corrected for the phase change due to the spherical wave front at the center of the subcell. The auto-correlation output of a 127 bit code and its cross-correlations with another 127 bit code for different values of chirp as determined by the radius of wavefront and the width of mask are shown in Figs. (2-19)a and (2-19)b respectively. These plots are scaled in width to account for the variation in the size of the masks. The heights are scaled so that the areas under each of the auto correlation peaks are equal in order to establish a criterion for comparison. Note that the illumination by a spherical wavefront has a tendency to reduce the amount of undesired terms in the correlation that are located away from the center of the peak of the auto-correlation. The terms near the center are not changed appreciably. Also note that as the radius of wavefront gets very large the correlation outputs approach that of a mask illuminated by a plane wave as obtained in Fig. (2-1). Further simulations are necessary to quantitatively establish the exact amount of improvement in the output that may be obtained by using the spherical



(iv)  $R = 15, W = 2.0$



(iii)  $R = 12.5, W = 3.81$



(ii)  $R = 15.0, W = 3.81$



(i)  $R = 999.0, W = 3.81$

(a)

(b)

Figure 2-19. Autocorrelation and crosscorrelations of 42 central bits of 127 bit Gold codes illuminated by a spherical wave of radius  $R$  and width of mask  $W$ .

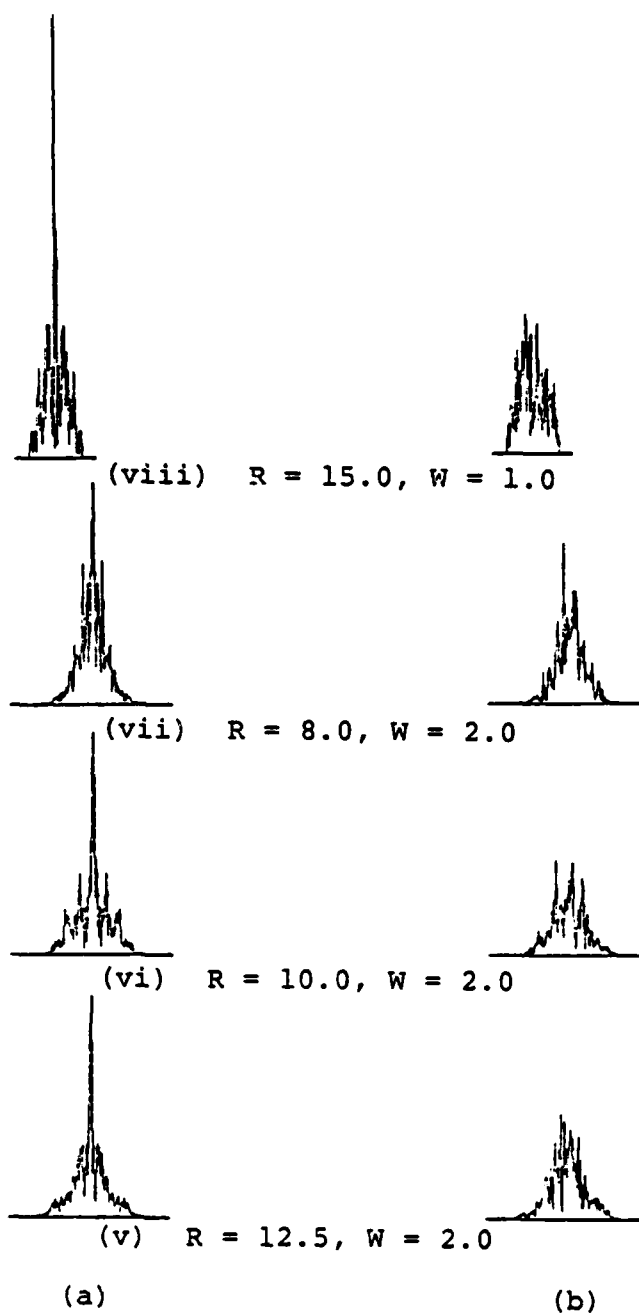


Figure 2-19 continued.

wave front as well as for determining the optimum relations between the width of the mask and the radius of curvature of the spherical wave front.

The results of the computer simulations presented in this chapter are useful in choosing a space-variant system for representation using the phase coded reference beam approach. The need for a good phase mask with phase differences between the elements close to  $180^\circ$  was also established. A technique for fabricating a two dimensional phase mask using Dichromated gelatin is described in Appendix G.

In the following two chapters an alternate multiplexing technique for generating a composite transfer function hologram is presented



## CHAPTER 3

### SAMPLED INPUT/SAMPLED TRANSFER FUNCTION APPROACH

#### 3.1 Space Division Multiplexing of Transfer Functions

Consider a system sampled at  $N$  points in the input plane, as determined by the sampling theorem of Eqn. (1-10). As a result we have  $N$  line spread functions representing the system. Thus after Fourier transformation there are  $N$  transfer functions in the holographic plane to be multiplexed in a single recording medium. When the system line spread functions are space limited, it is possible to sample their transfer functions at a rate determined by the modified version of the Whittaker-Shannon sampling theorem [11] and generate a composite hologram containing the samples of all the transfer functions. A typical space limited line spread function might be as shown in Fig. (3-1). The maximum spatial width of this function is  $2x_m^i$  where  $x_m^i$  is the larger of the values on either side of the axis of the optical system. Let  $x_M$  be the maximum of  $\{x_m^i\}$  for all  $i = 1, 2, \dots, N$ . Then the maximum sampling interval required in the transfer function plane is given by the Whittaker-Shannon sampling theorem:

$$\Delta f_x = \frac{1}{2x_M} \quad (3-1)$$

where  $\Delta f_x$  has the dimensions of spatial frequency; or in terms of linear dimensions,

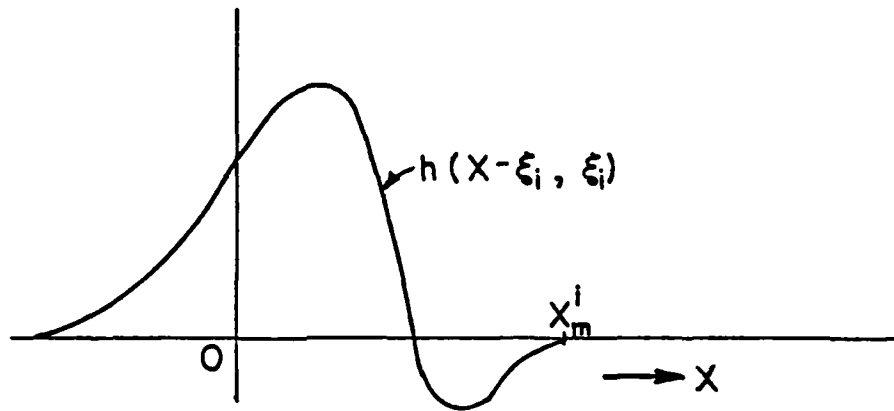


Figure 3-1. Typical line-spread function.

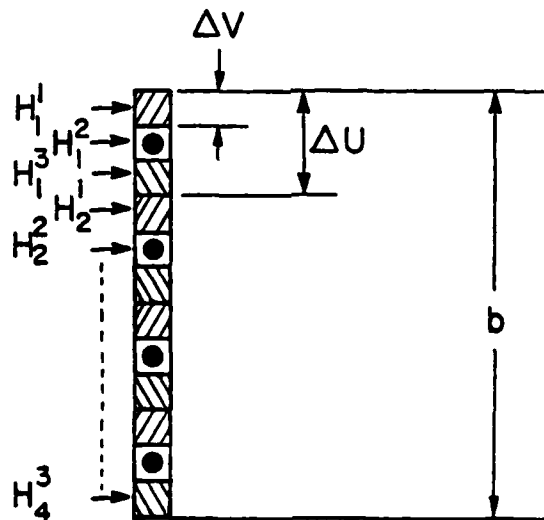


Figure 3-2. Typical arrangement of samples of transfer functions on hologram, when  $N = 3$  and  $M = 4$ .

$$\Delta U = \lambda f \Delta f_x \quad (3-2)$$

Where  $\lambda$  is the wave length of coherent light,  $f$  is the focal length of the Fourier transforming lens and  $\Delta U$  is the sampling interval in the holographic plane in units of length. Since we have  $N$  transfer functions to be multiplexed, the width of each individual sample is given by

$$\Delta v = \frac{\Delta U}{N} \quad (3-3)$$

Again if the magnitudes of the transfer functions are essentially zero beyond the width  $|u| \geq b/2$ , the transfer functions may be approximately represented by limiting the number of samples to

$$M = \frac{b}{\Delta U} = \frac{2bx_M}{\lambda f} \quad (3-4)$$

instead of the infinite number of samples required by the sampling theorem.

An example of sampling a transfer function and the spatial distribution of samples in the holographic plane, for  $N = 3$  and  $M = 4$ , is shown in Fig. (3-2). Each sample is marked as  $H_j^i$ , when  $i$  represents the  $i^{\text{th}}$  transfer function being multiplexed and  $j$  represents the  $j^{\text{th}}$  sample of the  $i^{\text{th}}$  transfer function.

### 3.2 An Optical Recording And Playback Scheme

A scheme for implementing the multiplexing technique

just described is shown in Fig. (3-3). During recording, a binary mask with the width of each of the  $N$  transparent areas equal to  $\Delta v$  spaced at intervals of  $\Delta U$  is placed immediately in front of the recording medium. This mask samples the transfer function hologram at intervals of  $\Delta U$ . The mask is moved by a distance of  $\Delta v$  after recording each hologram. Thus at the end of recording and processing, assuming that the resultant transmittance after processing is proportional to intensity, the transmittance of the hologram is given by

$$t(u) = \sum_{i=1}^N [|H^i(u) + R(u)|^2] [\text{Rect}(\frac{u}{\Delta v}) * \text{Comb}(\frac{u-i\Delta v}{\Delta U})] \quad (3-5)$$

where  $*$  represents convolution,

$$\text{Comb}(x) \triangleq \sum_{n=-\infty}^{\infty} \delta(x-n) \quad (3-6)$$

and  $\text{Rect}(x)$  is as defined in equation (1-8).

For playing back this multiplexed hologram the scheme is as shown in Fig. (3-4). The binary mask used in the recording step is now replaced by a multiple input function transparency with transmittance equal to  $f(\xi_i)$  at all  $M$  points that are directly in front of the samples of the  $i^{\text{th}}$  transfer function. The transmittance of this transparency may be represented as

$$s(u) = \sum_{i=1}^N f(\xi_i) \text{Rect}(\frac{u}{\Delta v}) * \text{Comb}(\frac{u-i\Delta v}{\Delta U}) \quad (3-7)$$

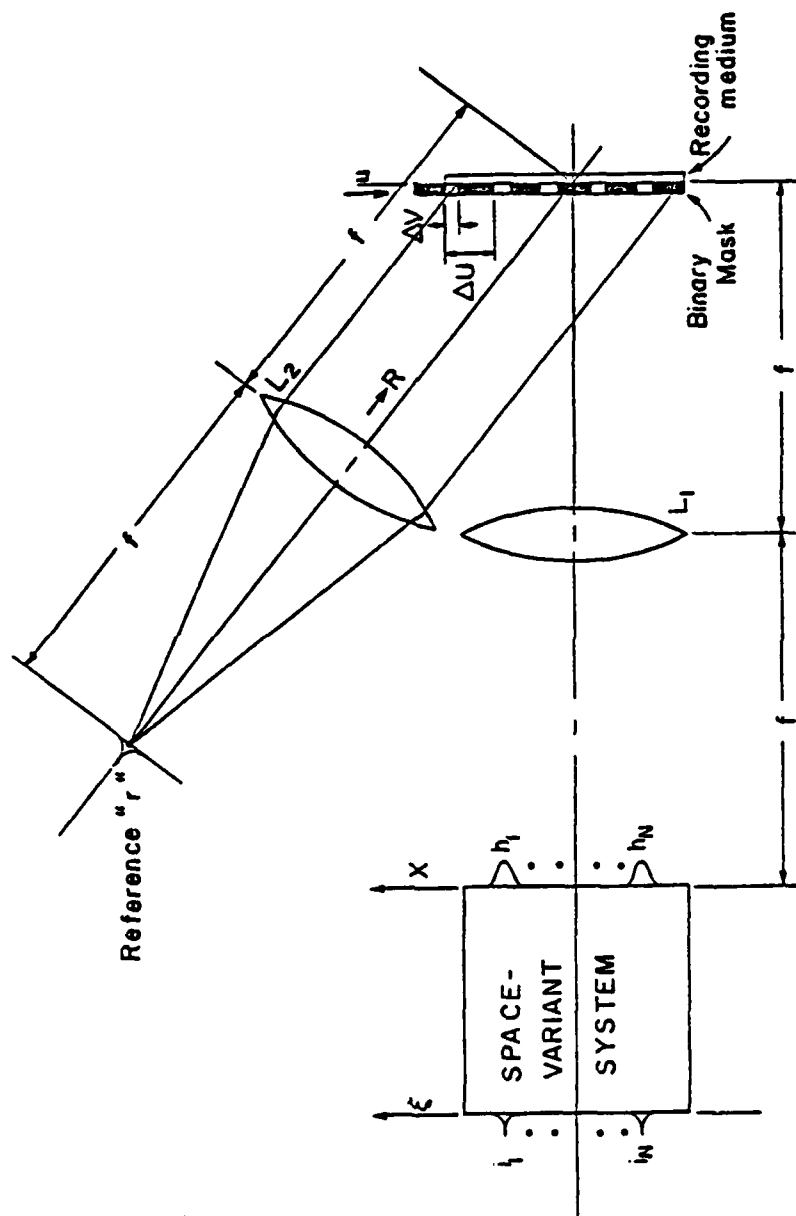


Figure 3-3. Scheme for optically recording the multiplex hologram.

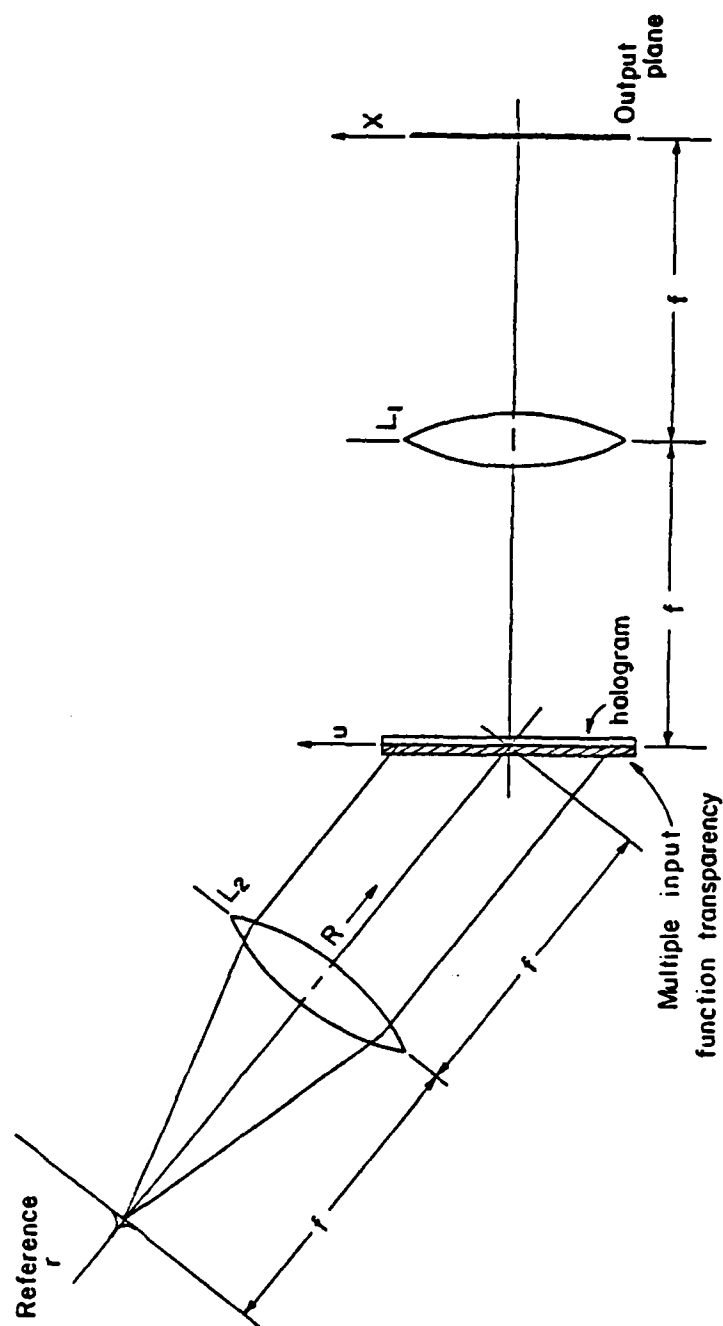


Figure 3-4. Scheme for the playback of multiplexed hologram.

When this transparency is illuminated by the reference beam  $R$ , the reconstructed wavefront to the right of the hologram is given by

$$\begin{aligned} G(u) &= R(u) S(u) t(u) \\ &= \sum_{i=1}^N R(|H^i + R|^2) f(\xi_i) \text{Rect}\left(\frac{u}{\Delta v}\right) * \text{Comb}\left(\frac{u-i\Delta v}{\Delta u}\right). \end{aligned} \quad (3-8)$$

Now out of the four terms in the expansion of  $R|H^i + R|^2$  (Eqn. (1-13)) only the term  $RR^*H_i$  is diffracted by the hologram in the direction of the output plane as a result of the offset in the reference beam. Thus the output after Fourier transformation by the lens  $L2$  is given by

$$\begin{aligned} g'(x) &= F^{-1} \left[ \sum_{i=1}^N H^i R R^* f(\xi_i) \text{Rect}\left(\frac{u}{\Delta v}\right) * \text{Comb}\left(\frac{u-i\Delta v}{\Delta u}\right) \right] \\ &= \sum_{i=1}^N K h_i * (r \star r) * \left[ f(\xi_i) \text{Sinc}\left(\frac{x}{2nx_M}\right) \left( \text{Comb}\left(\frac{x}{2x_M}\right) \right) \right], \end{aligned} \quad (3-9)$$

where  $\star$  represents correlation.

Here  $K$  is a scaling factor due to Fourier transformation.

In this equation the term  $r \star r$  approaches a delta function if the reference source  $r$  approaches a delta function. The term  $\text{Sinc}\left(\frac{x}{2nx_M}\right)$  is due to the finite size of the sample width in the frequency plane, and approaches a constant in the limit as  $\Delta v \rightarrow 0$ . Finally the term  $\text{Comb}\left(\frac{x}{2x_M}\right)$  is present

because of the sampling carried out for multiplexing the holograms. Thus under the assumption that the width of each sample  $\Delta v$  is small, and that  $r$  is a delta function, the equation for  $g'(x)$  is given by

$$g'(x) \approx \sum_{i=1}^N f(\xi_i) h_i * \text{Comb}\left(\frac{x}{2x_M}\right) \quad (3-10)$$

The required output  $g(x)$  is

$$g(x) = \sum_{i=1}^N f(\xi_i) h_i \quad (3-11)$$

Hence to recover the output  $g(x)$  from  $g'(x)$  we need a mask in the output plane with a slit which passes one of the multiple images.

All the mathematical derivations carried out so far has been in 1-D for clarity of presentation. Extensions to two dimensions are straightforward.

This method of multiplexing does not require the multiple reference beams that were necessary in the encoded reference beam approach described in Section 1.2. However the need exists for preparing a multiple input function mask for the spacelimited input  $f(\xi)$ . This mask is used during the playback as explained in the previous paragraphs. This mask generates coherent replications of the input function to illuminate the hologram. Some of the schemes for achieving this objective are described in Section 3.4. In the next section the results of 1-D computer simulations



carried out to verify the sampled transfer function multiplexing technique are described.

### 3.3 One-Dimensional Computer Simulations

The computer program used to simulate the sampled transfer function multiplexing technique is given in Appendix E. In this simulation the number of samples in the input plane is taken as  $N = 4$ . Thus there are four transfer functions to be multiplexed in a single hologram. A one dimensional array of 128 elements is used to represent each impulse response. This array is used as the input to the discrete Fast Fourier Transform routine (FFT) to generate a 128 element array of Fourier components. This transfer function array is sampled at an interval of four elements and the samples are stored at their corresponding positions in another array representing the composite hologram. The above steps are repeated for all the four impulse responses, resulting in a final composite array of 128 elements. This composite array is played back by using it as the input to a second Fourier transform routine. As the composite array is not multiplied by any term representing the input function, the result after Fourier transformation should be the sum of the individual impulse responses. In fact this simulation is equivalent to a situation when the input is a constant for all the impulse responses. The output of the system when the transfer functions are accessed one at a time is also simulated.

The four impulse responses used in this experiment are shown in Fig. (3-5a). Note that since we have four transfer functions to be multiplexed in a composite array of 128 elements, the maximum extent  $x_M$  of any of these impulse responses should be less than 16 elements on either side of the center of the array, i.e.,  $2x_M \leq 128/4 = 32$  elements; otherwise aliasing problems will result in the output plane when the multiplexed transfer function array is played back. The magnitudes of the transfer functions of each of these impulse responses are shown in Fig. (3-5b). These transfer functions are sampled by selecting the 1<sup>st</sup>, 5<sup>th</sup>, 9<sup>th</sup> .... elements of the first transfer function, 2<sup>nd</sup>, 6<sup>th</sup> .... elements of the second transfer function, 3<sup>rd</sup>, 7<sup>th</sup> .... elements of the third transfer function and 4<sup>th</sup>, 8<sup>th</sup> .... elements of the last transfer function. These samples are placed in their respective positions in another composite array. The magnitude of the elements in this array is shown in Fig. (3-6a). This array is then Fourier transformed and the output is shown in Fig. (3-6b). This output represents the system output when illuminated by an input function  $f(\xi)$  which is a constant over all the sample points in the input plane. Note that the output, which is a sum of all the four impulse responses, is replicated four times in the output plane. This is because of the  $\text{Comb}(x/2x_M)$  term in Eqn. (3-10). The coordinate reversal is due to the consecutive application of two Fourier transformation operations. Next,

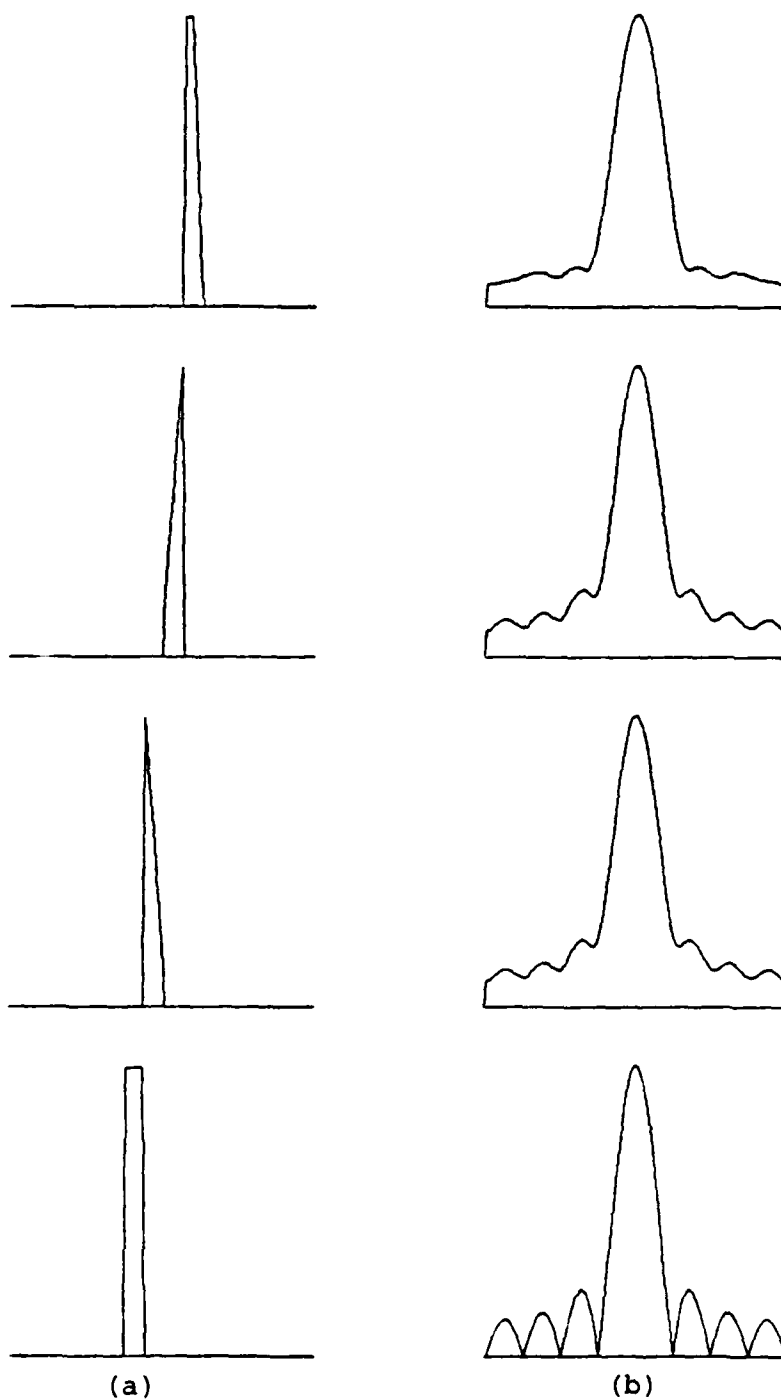


Figure 3-5. Impulse responses and their Fourier transforms used in the simulations.

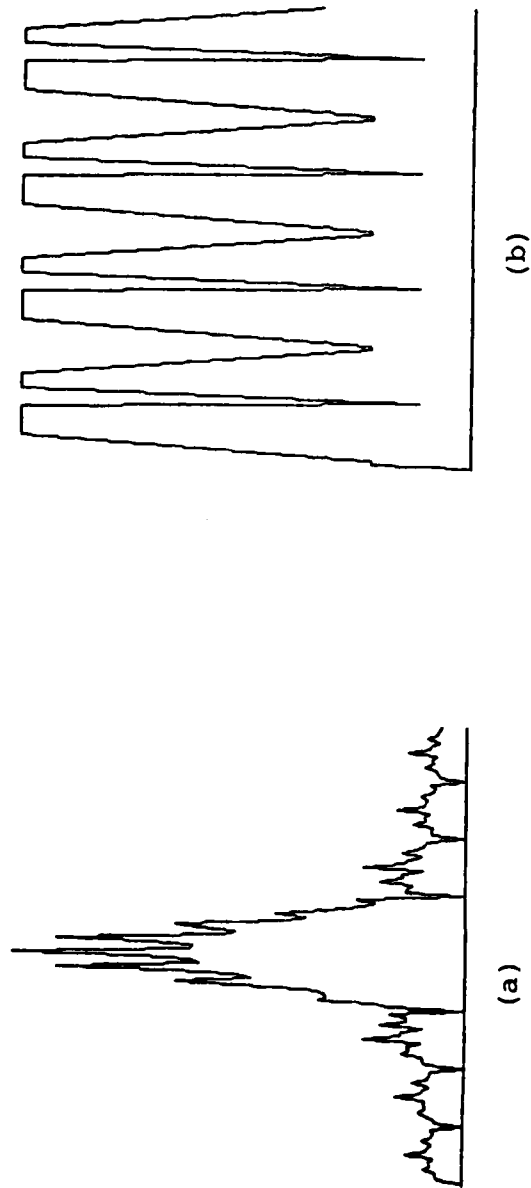


Figure 3-6. Composite hologram and the resultant output.

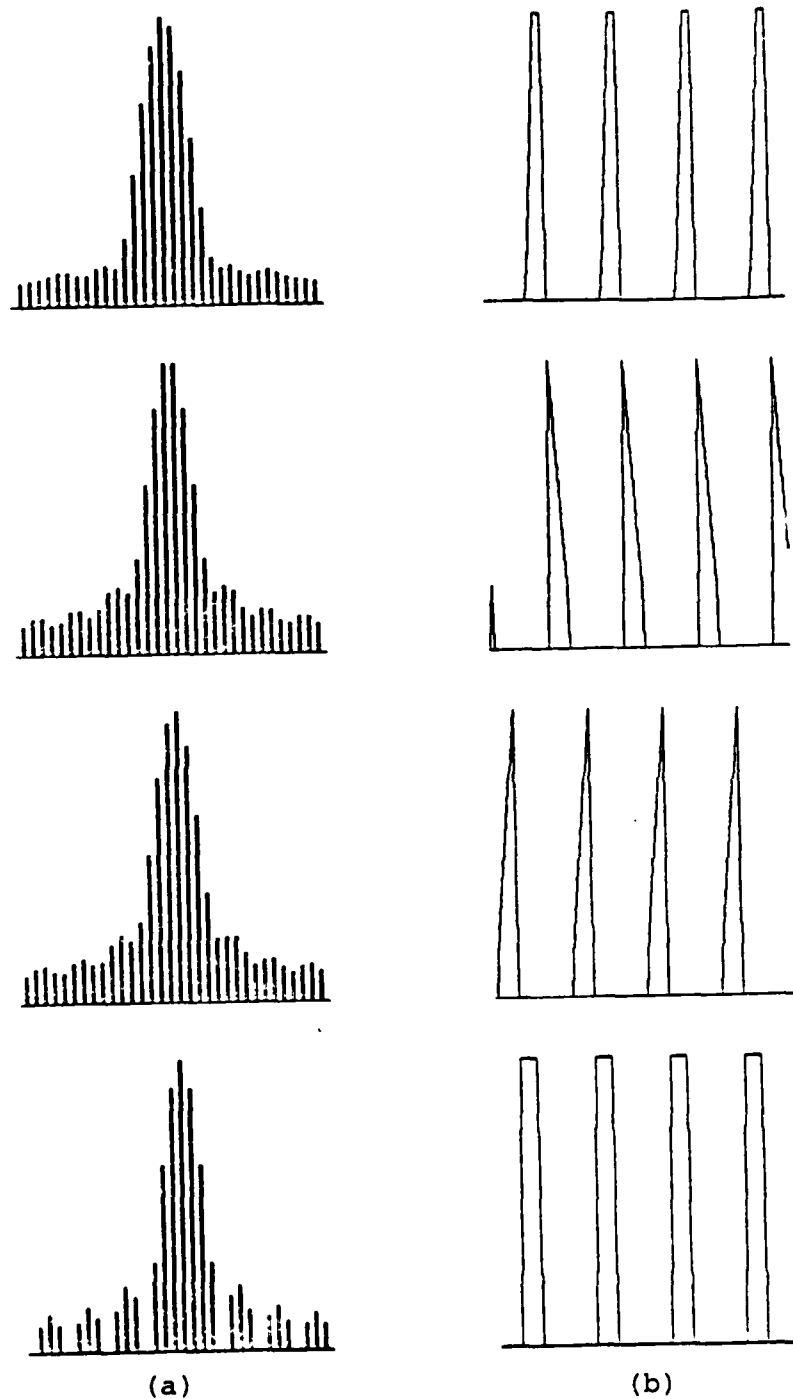


Figure 3-7. Sampled transfer functions and the corresponding outputs.

to simulate individual access of each impulse response, the samples belonging to each transfer function are recovered from the composite array and are placed in another array. The plot of the magnitudes of the elements in this array is shown in Fig. (3-7a). The results of Fourier transforming these arrays are shown in Fig. (3-7b). This simulation is equivalent to the situation when the input function  $f(\xi)$  has a magnitude of 1 at the input sample point corresponding to the impulse response being accessed and zero at all the other sample points. Again note that the output is replicated four times in the output plane. This program was written in the Fortran 63 language for use with a CDC 1604 Computer and Cal-Comp drum type plotter.

### 3.4 Schemes for the Generation of Multiples of the Input Function

In this section some of the schemes for generating multiple images of the input function are briefly described.

3.4.1 Multiple Image Transparencies: Multiple copies of the sampled values of the input function  $f(\xi)$  are prepared on a film using a step-and-repeat process or other methods. A typical transparency for a given function  $f(\xi)$  is shown in Fig. (3-8). The disadvantages of this method are (a) Separate masks are required for each of the input functions, (b) the process is slow.

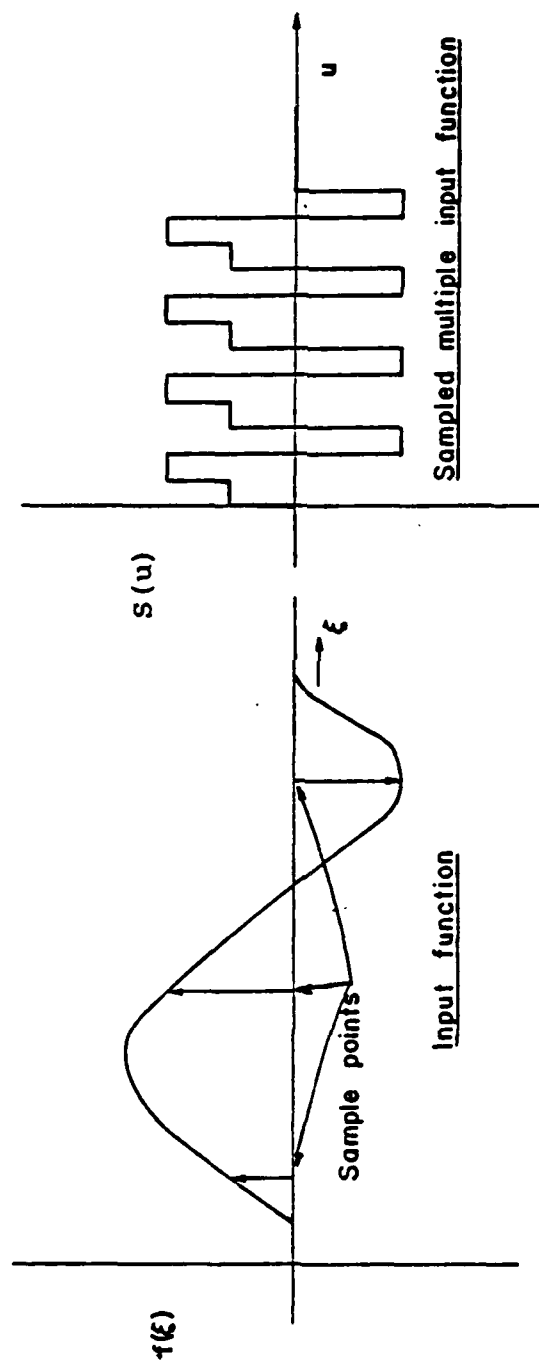


Figure 3-8. Typical input function  $f(\xi)$  and the corresponding sampled multiple input function when  $N = 3$  and  $M = 4$ .

3.4.2 Multiple Imaging Using Beam Splitters: An array of beam splitters may be set up to generate multiple images of the input function. The requirement, however that all the images should have the same amplitude and be coherent with one another requires high precision in the values of transmittance and reflectance of each of the elements as well as in the optical path lengths.

3.4.3 Multiple Imaging Using Phase Holograms: The use of phase holograms to produce equally bright multiple images in the fabrication of integrated circuits has been reported [17]. Similar techniques to produce multiple coherent images may be possible.

3.4.4 Use of Fiber Optic Elements: Bundles of equal lengths of fiber optic elements may be arranged as shown in Fig. (3-9) to generate multiple images of the sampled input function when illuminated by a plane wave.

3.4.5 Use of Liquid Crystal Devices: The property of liquid crystal devices by which local changes in the periodicity of a phase grating becomes proportional to the light variation incident on the device has been used in optical computing [18]. This property may be used in conjunction with other techniques described earlier to generate coherent multiple images.



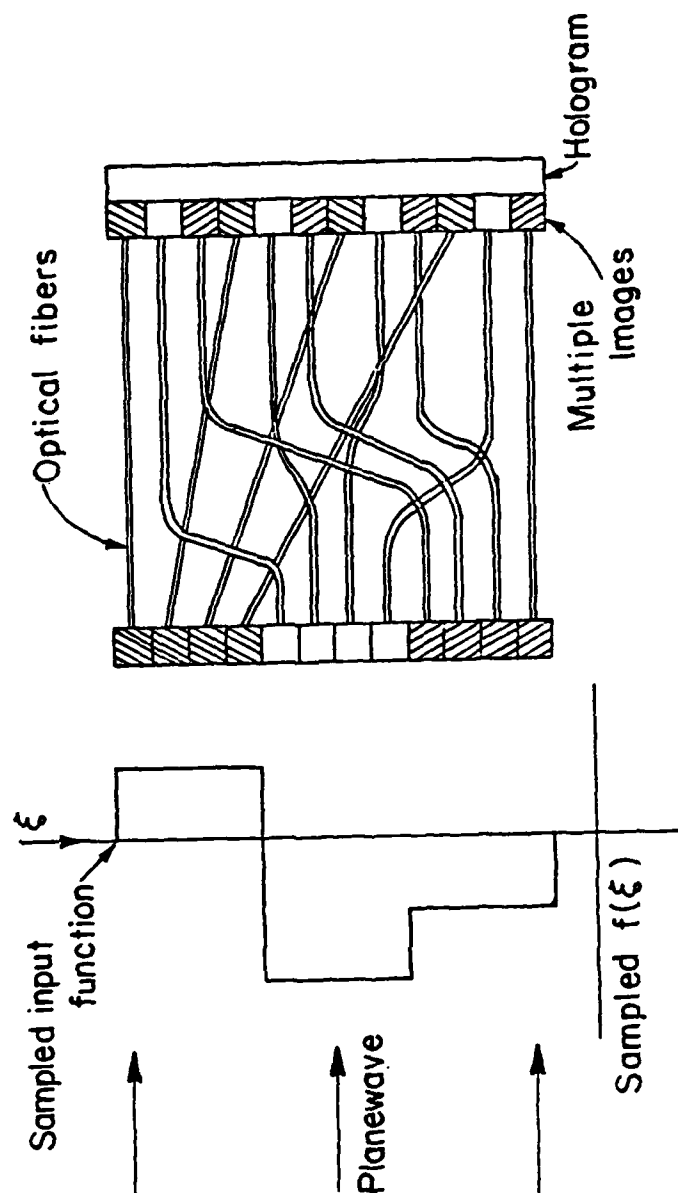


Figure 3-9. Use of optical fibers to generate multiple images of the input function.

In the next chapter the experimental results obtained using 2-D computer multiplexed holograms are presented.

## CHAPTER 4

### EXPERIMENTAL RESULTS USING COMPUTER MULTIPLEXED HOLOGRAMS

The technique of representing a space-variant system using a thin recording medium has the advantage of allowing computer generation of the system transfer function hologram instead of using the optical recording schemes described in section (3-2). In this chapter the results of 2 experiments using computer multiplexed holograms are presented. The experiments were conducted to verify the technique of multiplexing the transfer functions using the sampling method described in Chapter 3. In these experiments the number of samples  $N$  in the input plane was taken to be 2 in each dimension, thus requiring the multiplexing of  $N \times N = 4$  transfer functions on a single hologram.

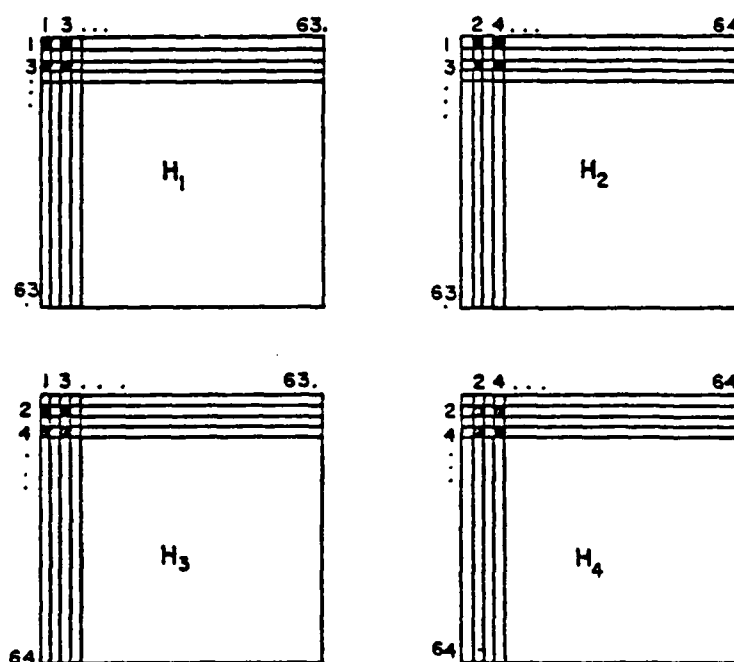
#### 4.1 Computer Generation and Playback of the Multiplexed Hologram

The computer program used to generate the transfer function hologram and to simulate the playback of the system is given in Appendix F. In this program a 2-D array of  $64 \times 64$  elements is used to represent an impulse response. The four impulse responses are Fourier transformed using the discrete Fast Fourier Transform (FFT) subroutine to result in four transfer function arrays of  $64 \times 64$  elements each. These four transfer function arrays are multiplexed

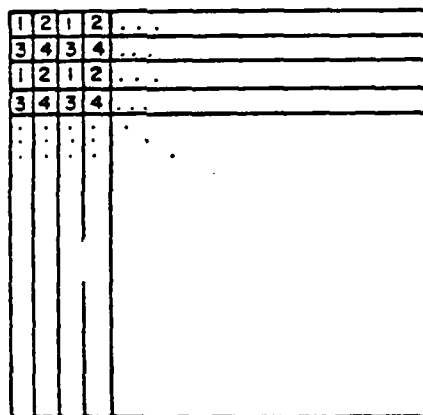
into a single composite array of 64 x 64 elements by selecting every alternate element from each of the arrays in both direction as shown in Fig. (4-1) i.e., the 1<sup>st</sup>, 3<sup>rd</sup>, 5<sup>th</sup>, etc. element from the 1<sup>st</sup>, 3<sup>rd</sup>, 5<sup>th</sup>, etc., rows of the transfer function  $H_1$  are selected and placed in their corresponding positions in the composite array. Similarly the 2<sup>nd</sup>, 4<sup>th</sup>, 6<sup>th</sup>, etc. element from the 1<sup>st</sup>, 3<sup>rd</sup>, 5<sup>th</sup>, etc. rows of the transfer function  $H_2$ , 1<sup>st</sup>, 3<sup>rd</sup>, 5<sup>th</sup>, etc. elements from the 2<sup>nd</sup>, 4<sup>th</sup>, 6<sup>th</sup>, etc. rows of the transfer function  $H_3$  and 2<sup>nd</sup>, 4<sup>th</sup>, 6<sup>th</sup>, etc. elements from the 2<sup>nd</sup>, 4<sup>th</sup>, 6<sup>th</sup>, etc. rows of the transfer function  $H_4$  are selected and are placed in their corresponding positions in the composite array. Thus in this scheme the sampling interval in the transfer function plane is 2 elements. This implies that the maximum size of the impulse response in either direction from the center of the array must be less than  $64/(2 \times 2) = 16$  elements in order to satisfy the sampling theorem. In general if  $N$  transfer functions are to be multiplexed in each dimension the maximum extent of the impulse response from the center of the array is given by

$$X_M = \frac{b}{2N} \quad \text{elements,} \quad (4-1)$$

where  $b$  is the number of elements in the array in each dimension. If this condition is not satisfied aliasing errors will result during the playback step.



(a) Selection of samples from the transfer functions.



(b) Position of components from the four transfer functions in the composite array.

Figure 4-1. Scheme for computer multiplexing the transfer functions.

At the end of the multiplexing step we have one composite array of  $64 \times 64$  elements representing the multiplexed hologram. The magnitude and phase of the elements in this array are plotted using Burckhardt's 3 vector method [19] in cells of size  $0.15'' \times 0.15''$ , resulting in a plot of size  $9.6'' \times 9.6''$ . Since the resolution of the plotter was limited to  $0.01''$  the magnitudes of the elements in the array are quantized to a total of 15 levels. Thus all elements whose magnitudes are less than  $1/15$ th of the magnitude of the largest element in the array are set to zero. These quantized vectors are resolved into components along 3 vectors  $120^\circ$  apart as shown in Fig. (4-2). Each of these components are represented on the plot by three subcells of  $0.05''$  width. The height of these subcells is proportional to the magnitude of the component. The plot of one such cell corresponding to the element having magnitude and phase as shown in Fig. (4-2) is given in Fig. (4-3).

The plot of the encoded sampled transform array is reduced to a size of  $0.4'' \times 0.4''$  using high contrast copy film and is used in the optical system shown in Fig. (4-4). The optical playback system consists of lens  $L_1$  placed at a distance of one focal length from both the hologram and the output plane. The hologram is placed in the plane U and the output, after Fourier transformation by lens  $L_1$ , appears in the X plane. A photograph of the optical setup is given in Fig. (4-5). In this setup an additional lens is

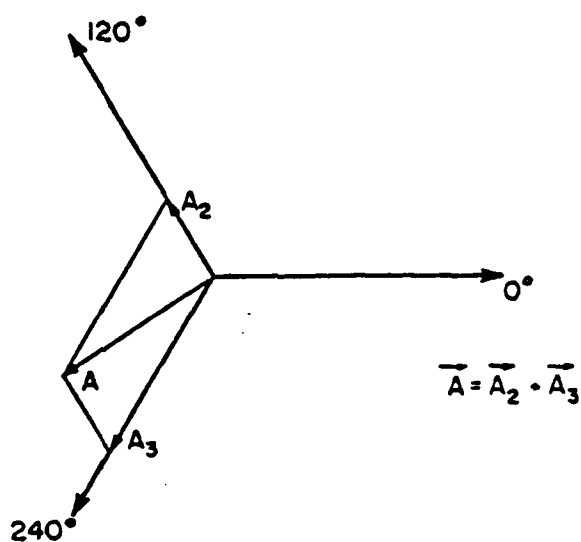


Figure 4-2. Resolving the component values of transfer function along 3 vectors.

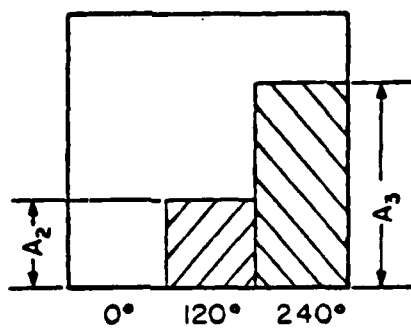


Figure 4-3. Typical cell representing the magnitude and phase using 3 vector method.

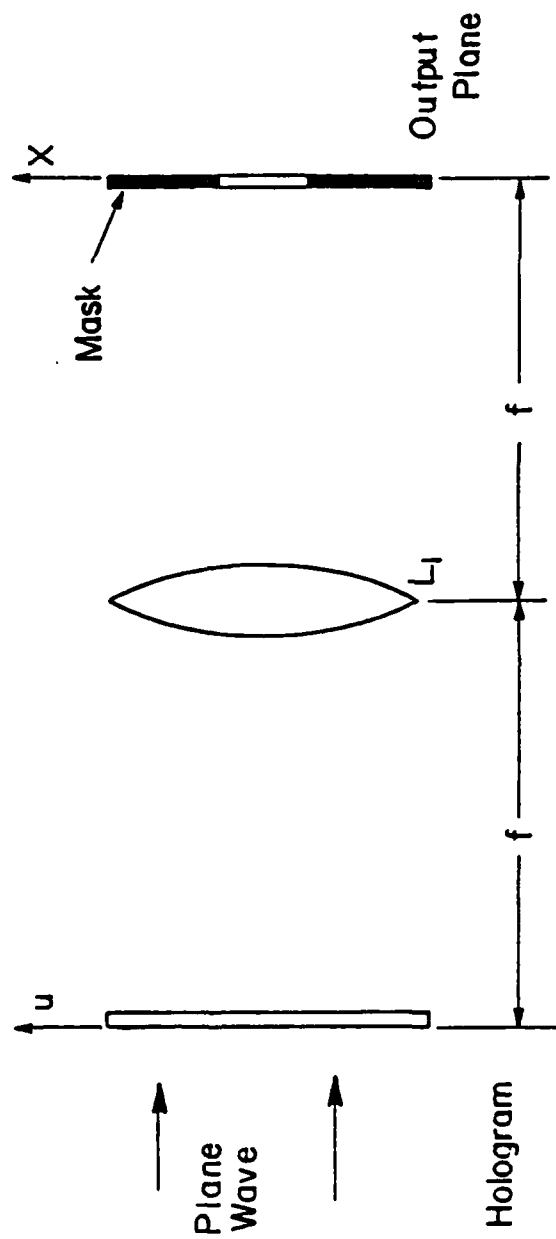


Figure 4-4. Optical system for playback.





Figure 4-5. Photograph of the Optical System used for the playback of computer multiplexed holograms.

used to project enlarged images in the output plane. The entire hologram is illuminated by a plane wave of constant amplitude. This is equivalent to the situation when the input function  $f(\xi_i)$  in Eqn. (3-10) is constant for all the impulse responses  $h_i$ ,  $i = 1, 2, 3, 4$ . The output is observed as an intensity distribution in the output plane. The computer program also simulates the playback of the optical system. This is done by using the composite transfer function array as the input to the Fast Fourier Transform routine and the magnitude of the output is plotted as before.

Next, to simulate the playback of only one impulse response the components belonging to one of the transfer function from the composite array are selected and placed in their respective position in another array with magnitudes of all other elements set to zero. A hologram of this transfer function array is prepared as before using a high contrast copy film. This hologram is used in the optical system of Fig. (4-4) and the output is observed as an intensity distribution in the output plane. This is equivalent to the situation when the input function  $f(\xi_i)$  in Eqn. (3-10) is nonzero at only the point corresponding to the impulse response  $h_i$  being accessed and zero at all other points. In the following sections the results obtained using this computer multiplexing technique are presented.

#### 4.2 Experimental Results Using Disjoint Impulse Responses

The four disjoint functions representing the impulse responses used in this experiment are shown in Fig. (4-6). Note that the maximum extent of these impulse responses in either x or y direction with respect to the center of the array is less than 16 elements and hence satisfies the constraints imposed by Eqn. (4-1). These impulse responses are used as inputs to the computer program described in the previous section. The composite hologram generated by the computer is shown in Fig. (4-7). The result of playback of this hologram in the optical system of Fig. (4-4) is shown in Fig. (4-8). The binary mask shown in Fig. (4-4) was not used while recording this output. The multiple outputs seen in this output are due to two reasons. First, as a result of the sampling in the transfer function plane multiple images are produced in the output plane as illustrated by Eqn. (3-10). Second, the Fast Fourier Transform subroutine assumes that the object at the input is one period of a periodic function in both x and y directions so that the output is limited to the size of one period of the array. The result of optical playback using the binary mask as shown in Fig. (4-4) to pass only one of the multiple images is shown in Fig. (4-9). Note that this output is a sum of all the four impulse responses. This simulation is equivalent to accessing all the impulse responses by an

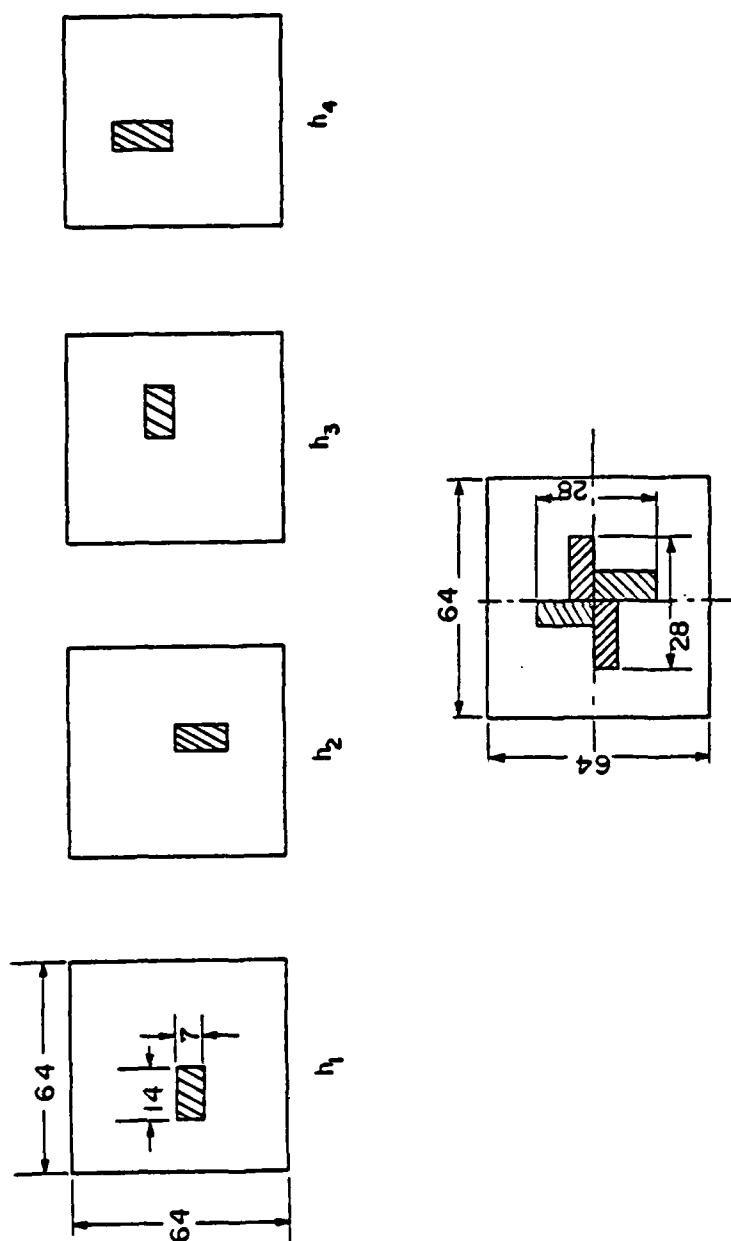


Figure 4-6. Four disjoint impulse responses used in experiment 1 and their sum.

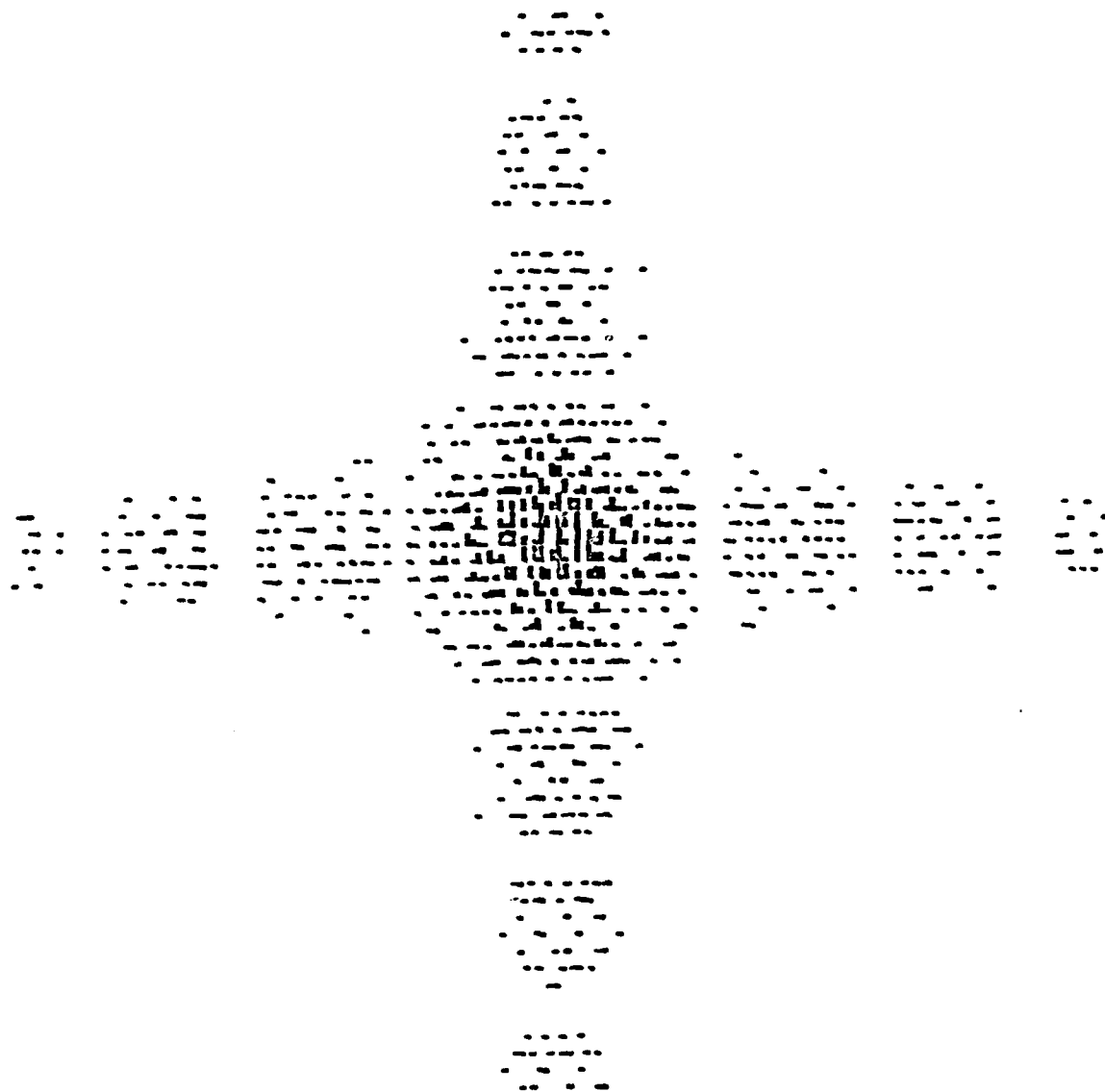


Figure 4-7. Computer multiplexed hologram using impulse responses of Fig. 4-6.



Figure 4-8. Output of the Optical System  
when the hologram of Fig. 4-7  
is played back.



Figure 4-9. Enlarged output of the Optical System when the hologram of Fig. 4-7 is played using a binary mask to pass only one of the multiple images.

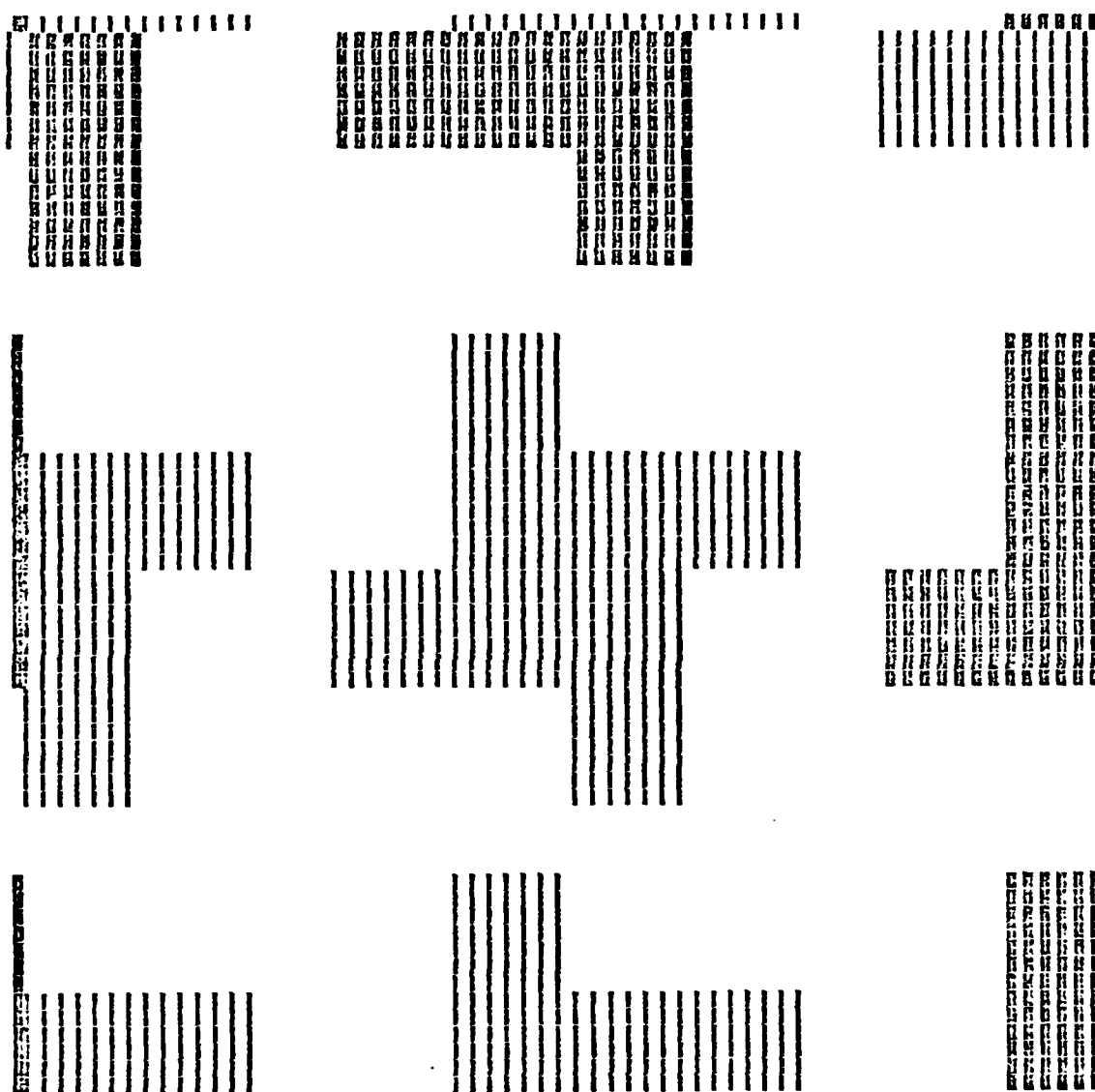


Figure 4-10. Computer-simulated output when all the impulse responses of Fig. 4-6 are played back.





Figure 4-11. Output of the Optical System when only one of the impulse responses of Fig. 4-6 is played back.



Figure 4-12. Output of the Optical System when one of the impulse responses of Fig. 4-6 is played back using a binary mask to pass only one of the multiple images.

input function which is constant at all the sample points in the input plane. The result of a computer simulation of the playback is shown in Fig. (4-10). As explained in the previous section the components belonging to one of the transfer functions are selected from the composite array and a hologram is prepared. The result of playback of this hologram is shown in Fig. (4-11). Again an enlarged output of one of the multiple images in the output plane is shown in Fig. (4-12). This simulation is equivalent to the situation when the input function accesses only one of the impulse responses.

#### 4.3 Experimental Results Using Overlapping Impulse Responses

The impulse responses used in this experiment are shown in Fig. (4-13). The first and second functions are made up of two disjoint right angle triangles with the values of elements within these triangles equal to -1 and zero everywhere else. Similarly the elements within the inverted triangles of the 3<sup>rd</sup> and 4<sup>th</sup> function have a value of +1. It is clear that the set of functions 3 and 4 partially overlap the set of functions 1 and 2. Thus when all the functions are added together a central hexagonal area of zeros are generated surrounded by a star like outer pattern. This experiment was conducted to verify whether the property of coherent addition is retained when the transfer functions are multiplexed using the sampled transfer function approach.

AD-A087 285

TEXAS TECH UNIV LUBBOCK OPTICAL SYSTEMS LAB F/G 14/5  
SPACE-VARIANT PROCESSING USING PHASE CODES AND FOURIER-PLANE SA--ETC(U)  
JUN 80 R KASTURI AFOSR-79-0076  
SCIENTIFIC-1

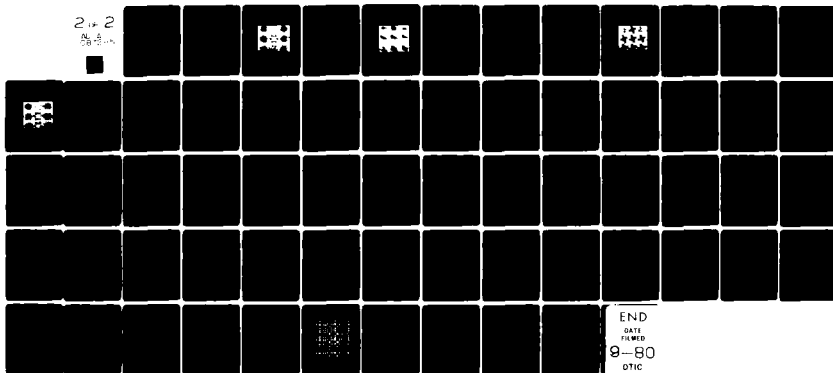
UNCLASSIFIED

AFOSR-TR-80-0557

NL

2 of 2

Page 2



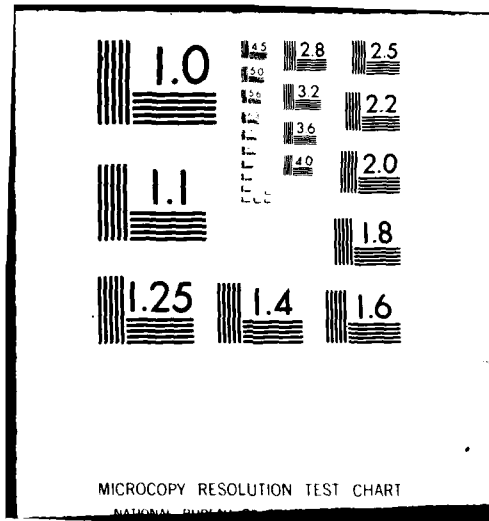
END

DATE

FILED

9-80

DTIC



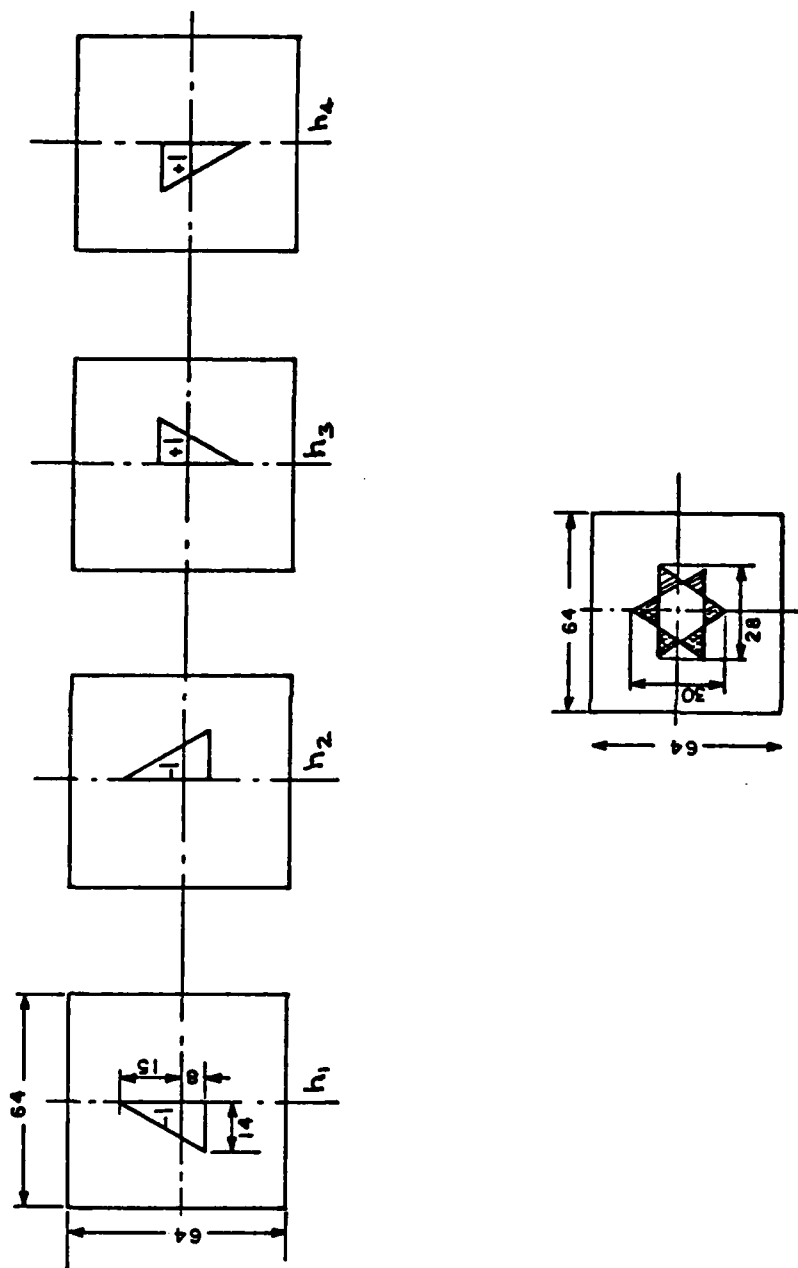


Figure 4-13. Four overlapping impulse responses used in experiment 2 and their sum.

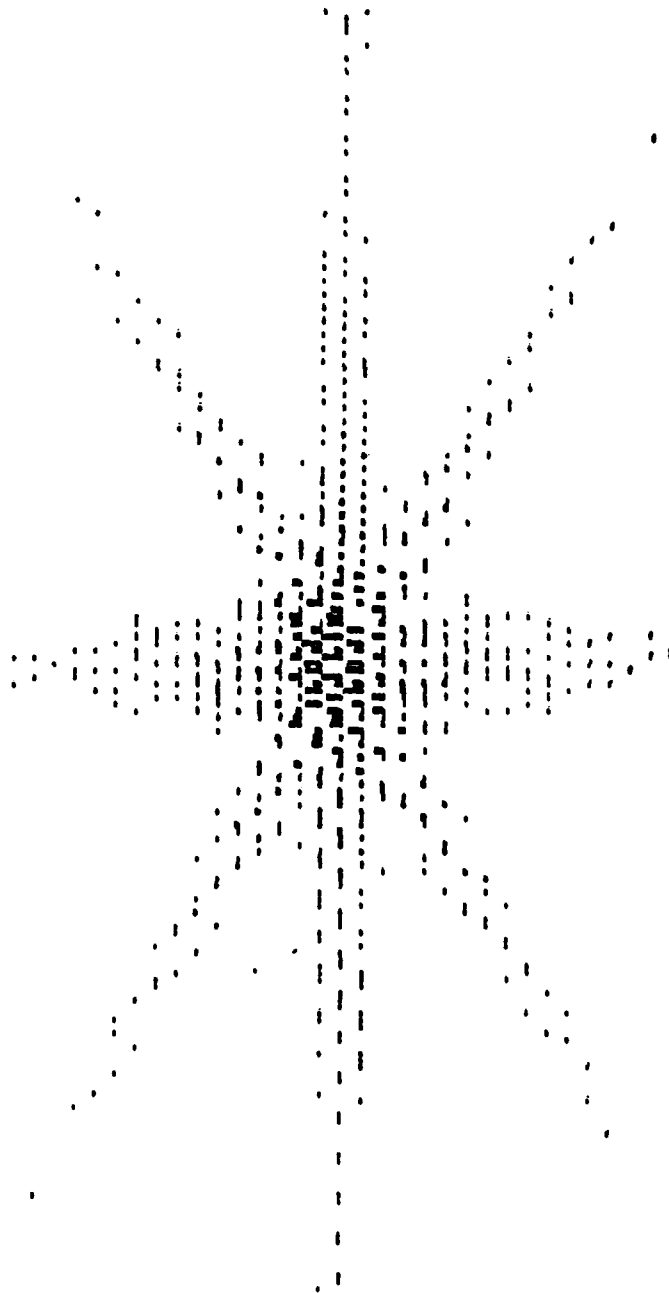


Figure 4-14. Computer multiplexed hologram using impulse responses  
of Fig. 4-13.



Figure 4-15. Output of the Optical System when the hologram of Fig. 4-14 is played back.

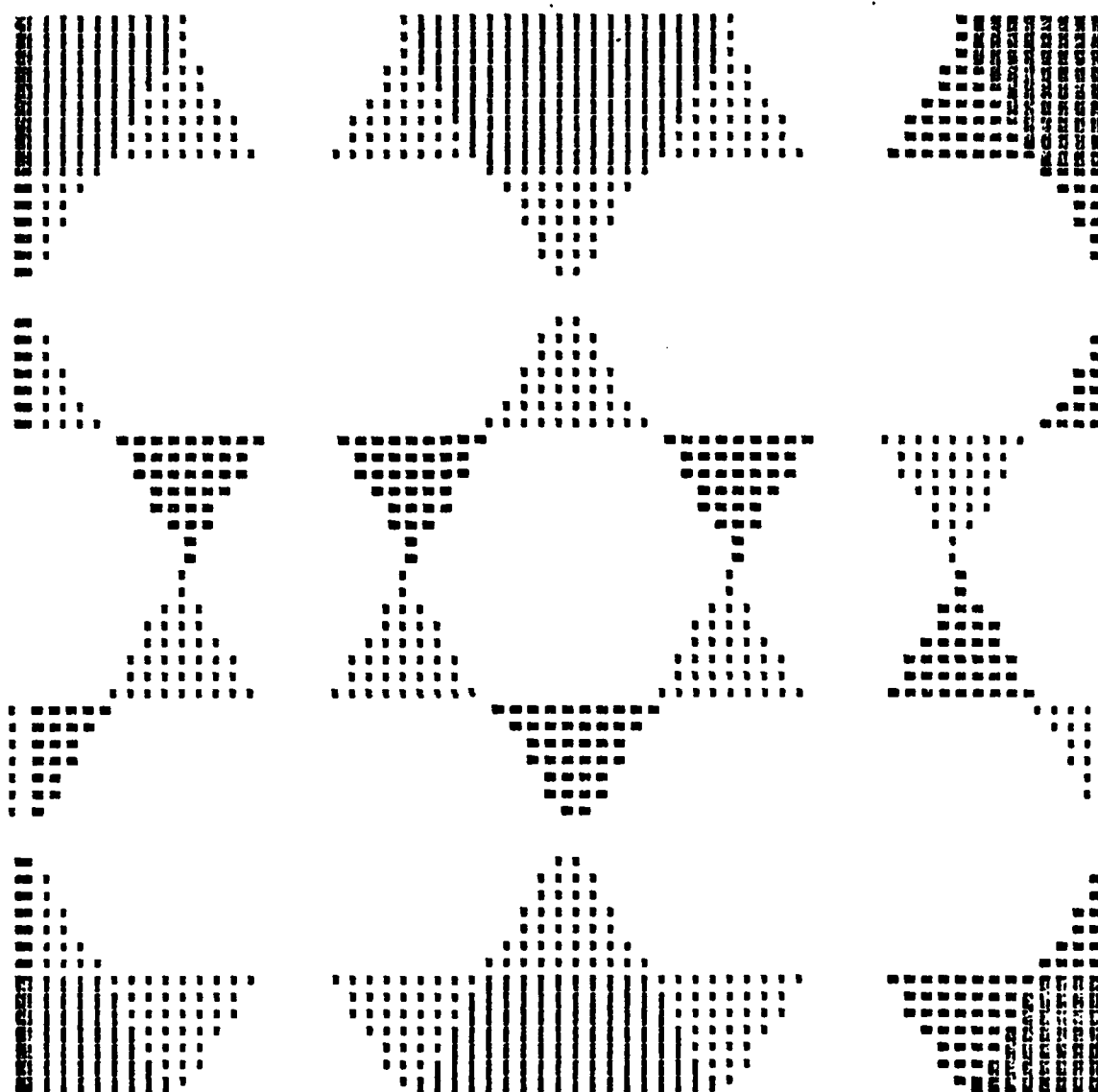


Figure 4-16. Computer simulated output when all the impulse responses of Fig. 4-13 are played back.



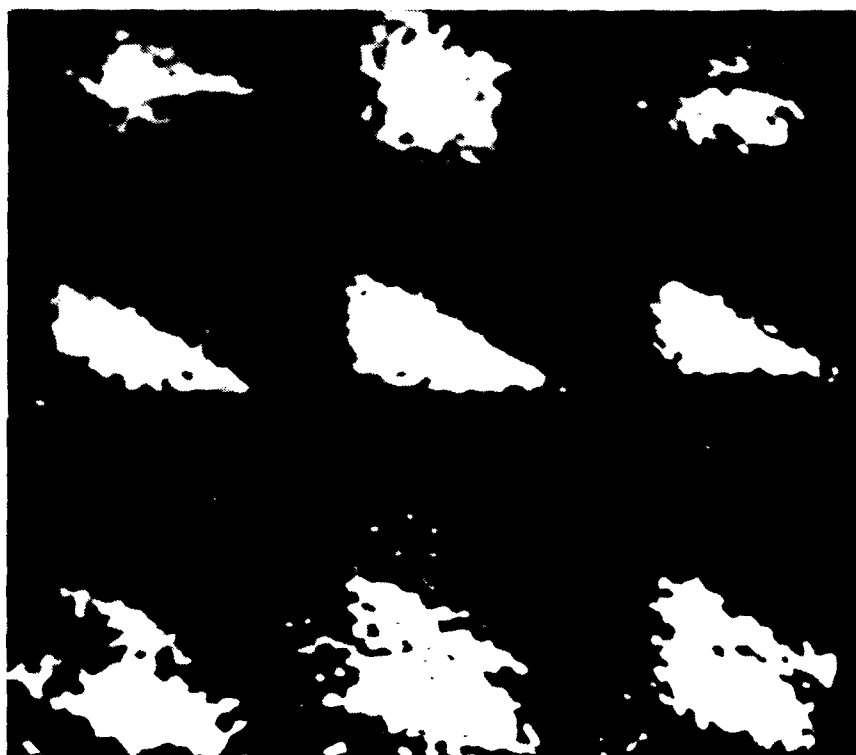


Figure 4-17. Output of the Optical System when only one of the impulse responses of Fig. 4-13 is played back.

The plot of the composite transfer function is shown in Fig. (4-14). The result of optical playback of this composite transfer function is shown in Fig. (4-15) and the computer simulated output is shown in Fig. (4-16). Note that the output contains a central hexagonal array of zeros and hence verifies the coherent addition property. The result of playback of one of the impulse responses is shown in Fig. (4-17).

#### 4.4 Multiplication of Impulse Responses by a Phase Function

It was mentioned in section 4-1 that some of the terms in the composite transfer function array are set to zero if their magnitude is less than  $1/15$  times the magnitude of the largest component in the array. This results in the loss of many terms especially when the transfer function has a dominating term of very large magnitude (usually the zero frequency term). This results in a computer hologram plot with only a few terms. The playback of such a hologram results in poor reconstruction. To circumvent this problem the impulse responses are multiplied by a phase function having magnitudes of  $+1$  and  $-1$  arranged in a checkerboard pattern as shown in Fig. (4-18). In general this operation spreads the components in the Fourier plane more evenly and the plot of the hologram after quantization contains more components. However multiplication of the impulse responses by this phase function will not result in any change in the

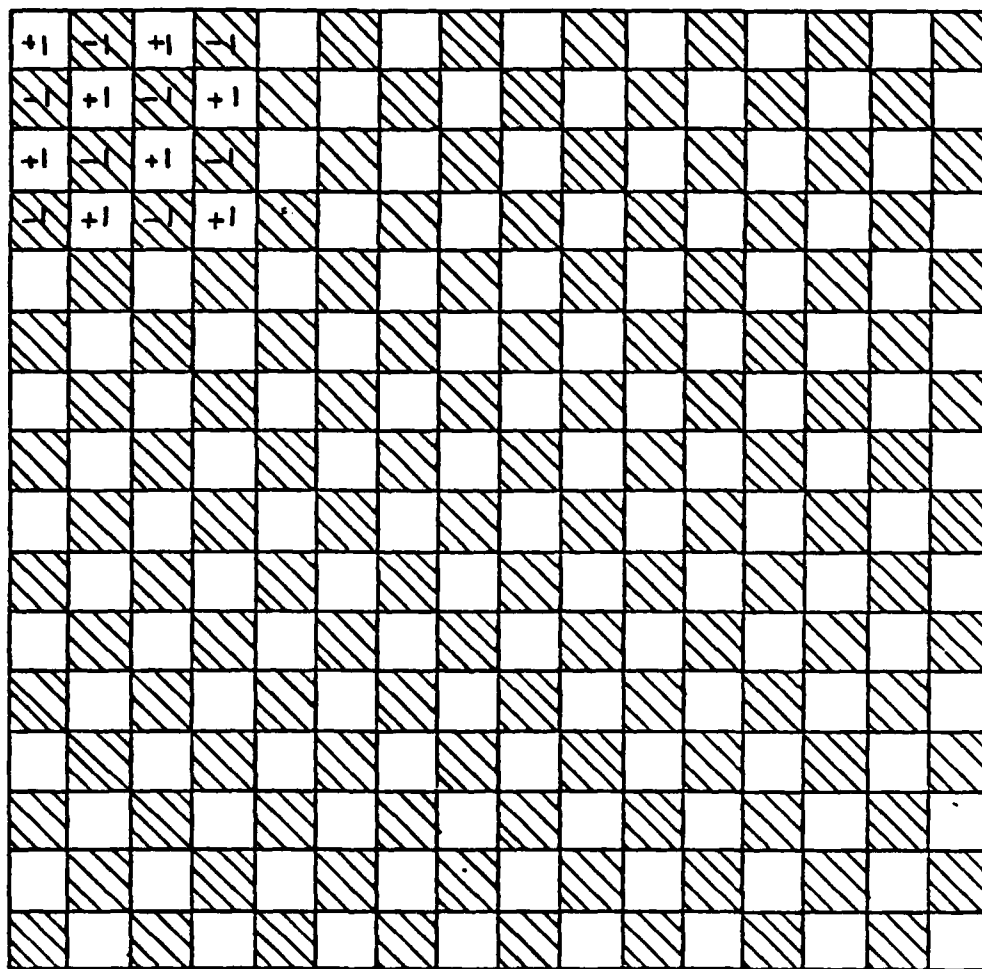


Figure 4-18. Phase mask used to multiply the impulse responses.

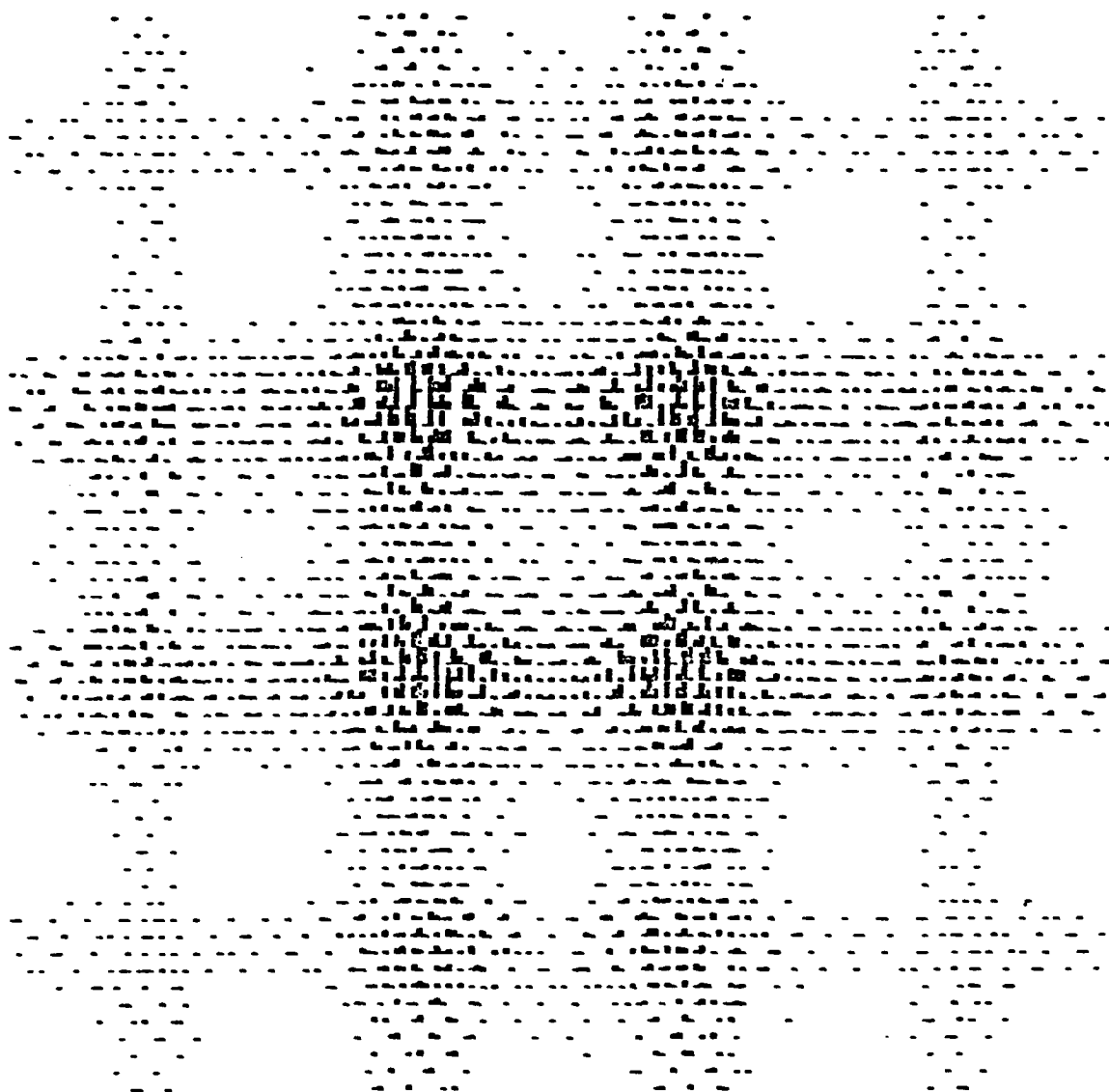


Figure 4-19. Composite hologram when the impulse responses of Fig. 4-6 are multiplied by the phase mask of Fig. 4-18.

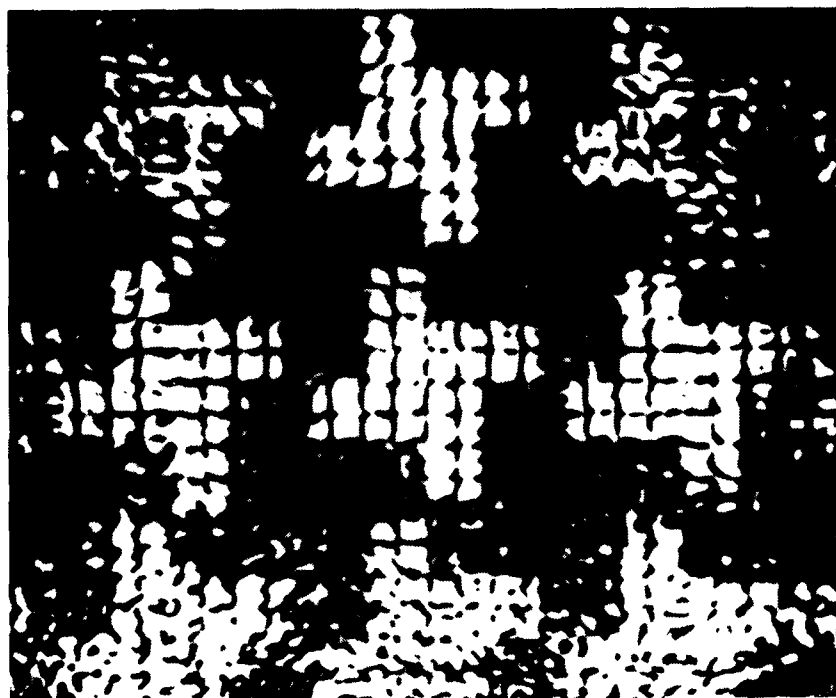


Figure 4-20. Output of the Optical System when the hologram of Fig. 4-19 is played back.

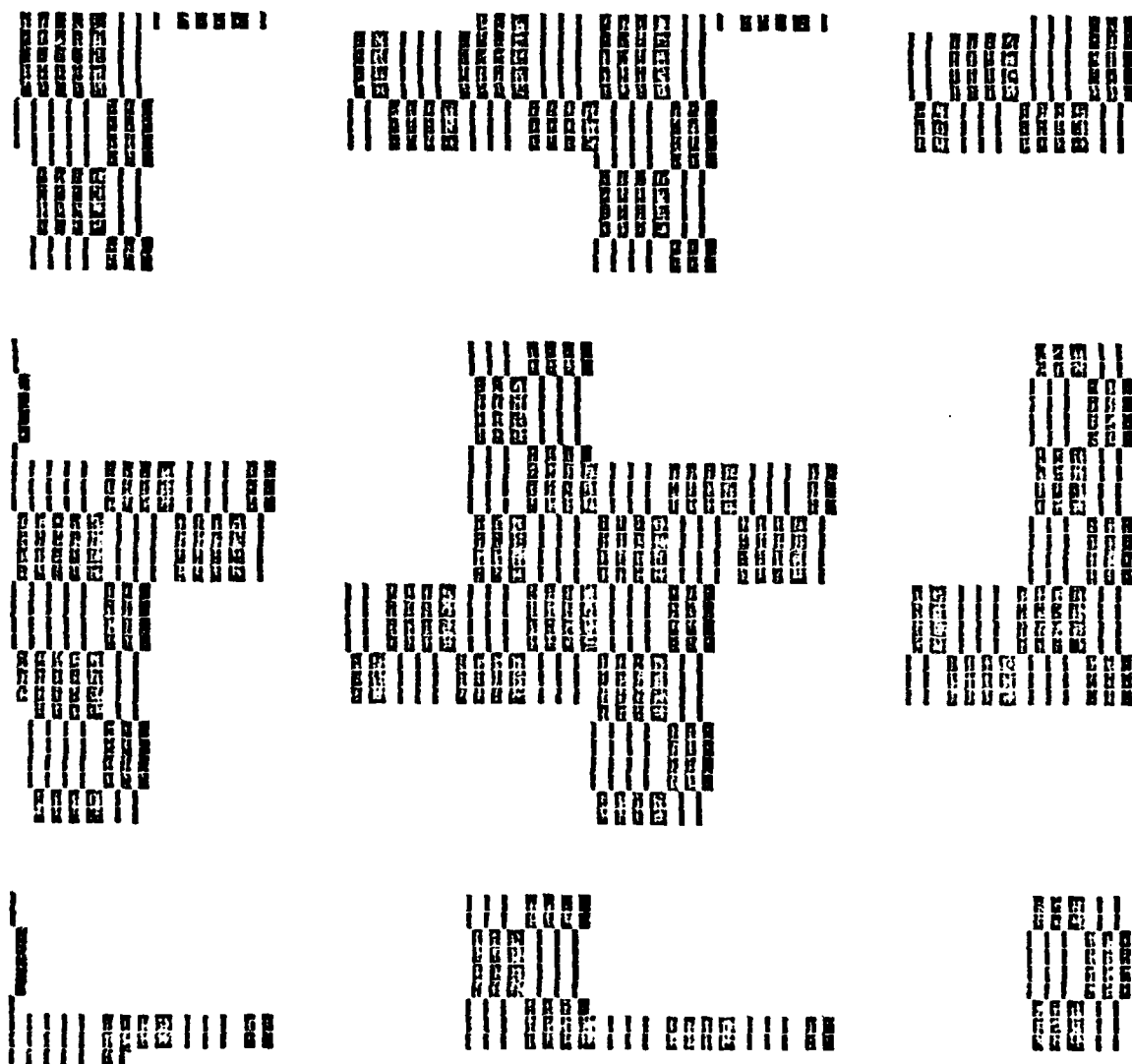


Figure 4-21. Computer simulated output when all the impulse responses of Fig. 4-6 premultiplied by the phase mask of Fig. 4-18 are played back.

observed distribution in the output plane during playback since the output is observed as an intensity distribution. Also a better reconstruction is obtained as more components are present in the hologram. The plot of the composite transfer function corresponding to the impulse responses of Fig. (4-6) using the phase mask as premultiplier is shown in Fig. (4-19). One may compare this plot with that of Fig. (4-7) which was produced without premultiplication by the phase mask. The result of optical playback of this hologram is shown in Fig. (4-20). The result of computer simulation of this output is shown in Fig. (4-21). Similarly the plot of the composite transfer function, the optical playback of the composite transfer function and the computer simulated output when the impulse responses of Fig. (4-13) are multiplied by the phase function of Fig. (4-18) are shown in Figures (4-22), (4-23), and (4-24) respectively. The block like structure of the output pattern could be removed by using a random phase premultiplexing mask rather than a periodic one.

#### 4.5 Computer Multiplexing Using Low Pass Filtered Transfer Functions

When the magnitudes of the high spatial frequency components of the transfer functions representing the space-variant system are small, the quantized composite transfer function array contains components only in the central region.

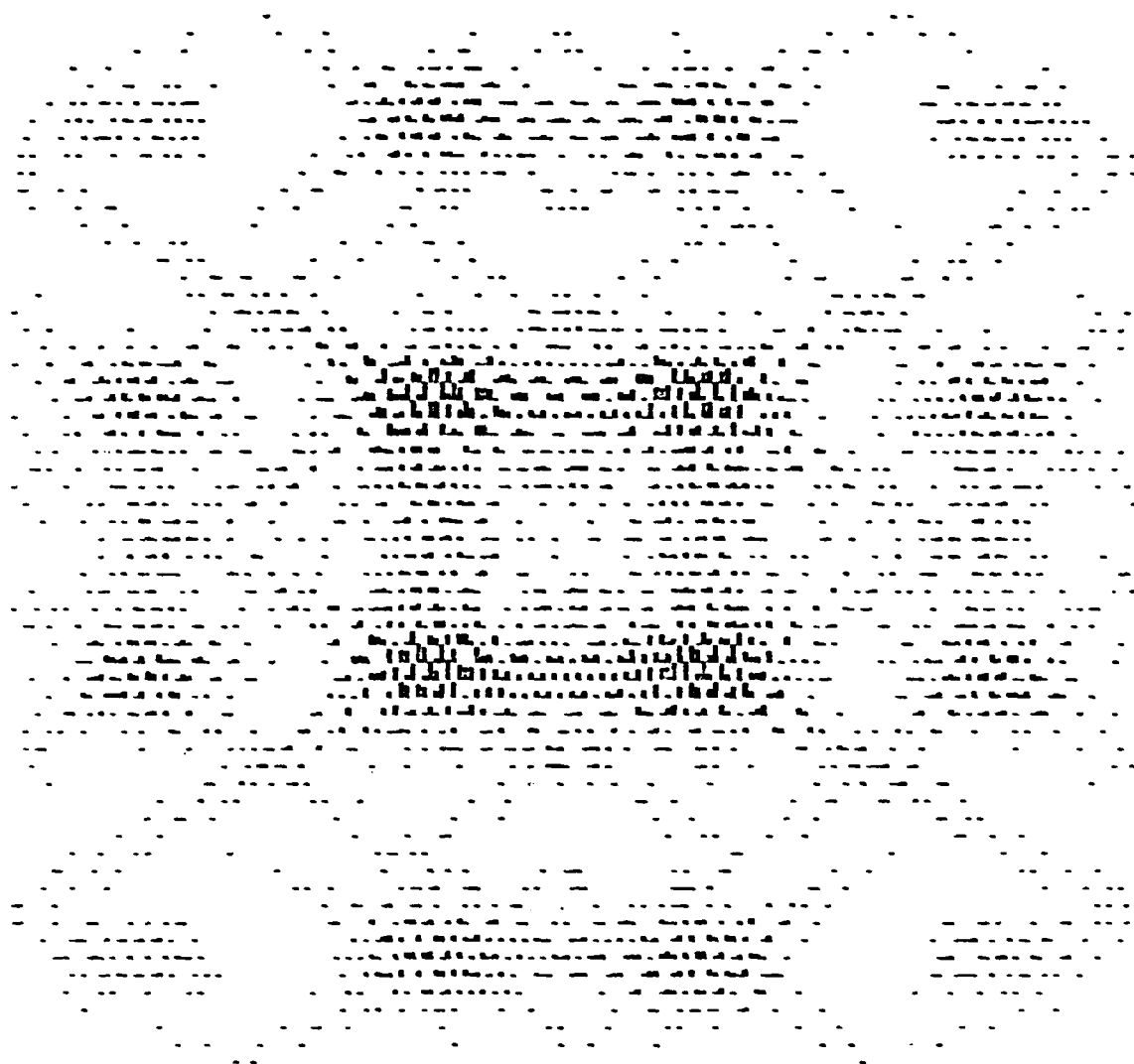


Figure 4-22. Composite hologram when the impulse responses of Fig. 4-13 are multiplied by the phase mask of Fig. 4-18.





Figure 4-23. Output of the Optical System when the hologram of Fig. 4-22 is played back.

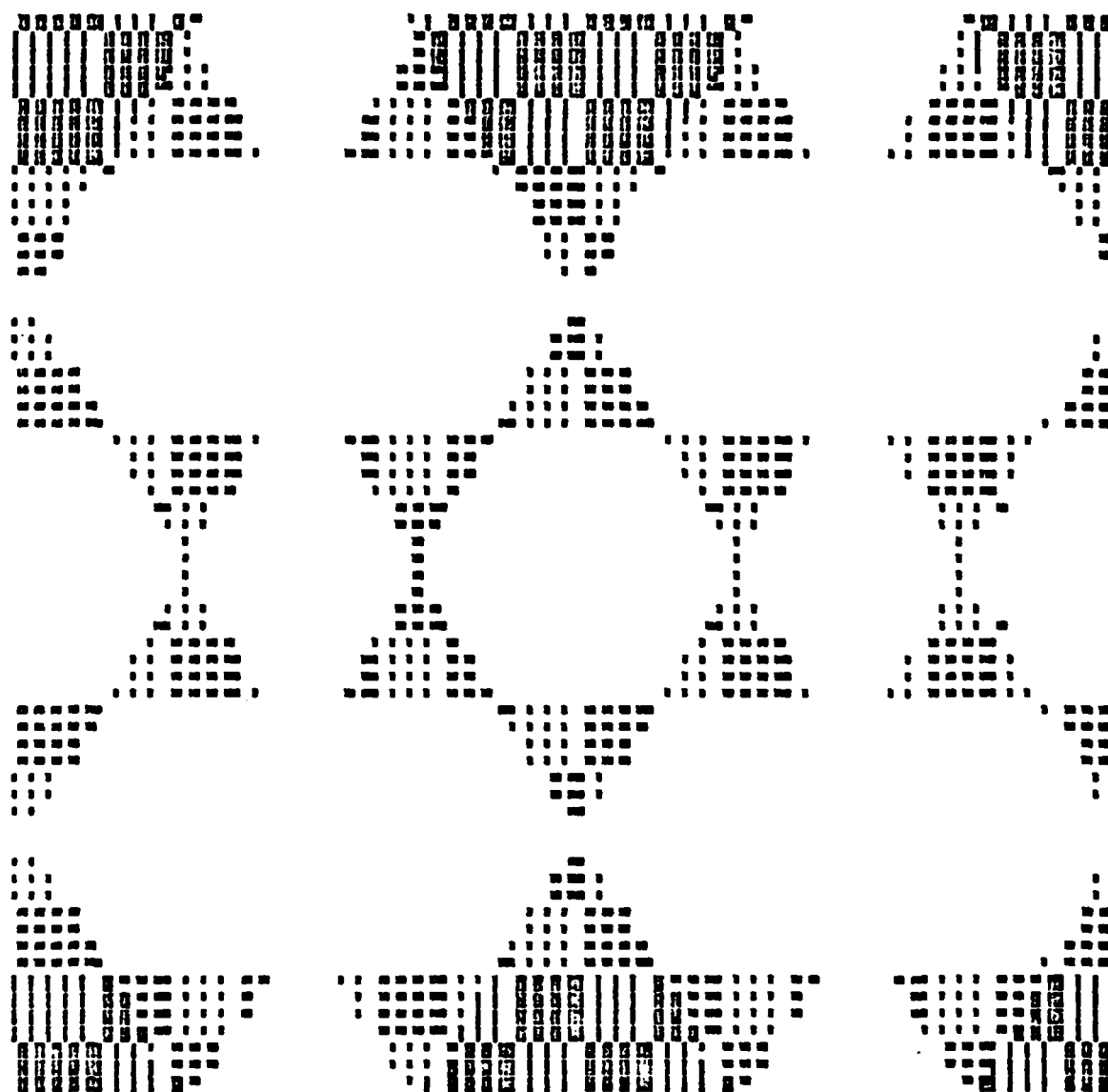
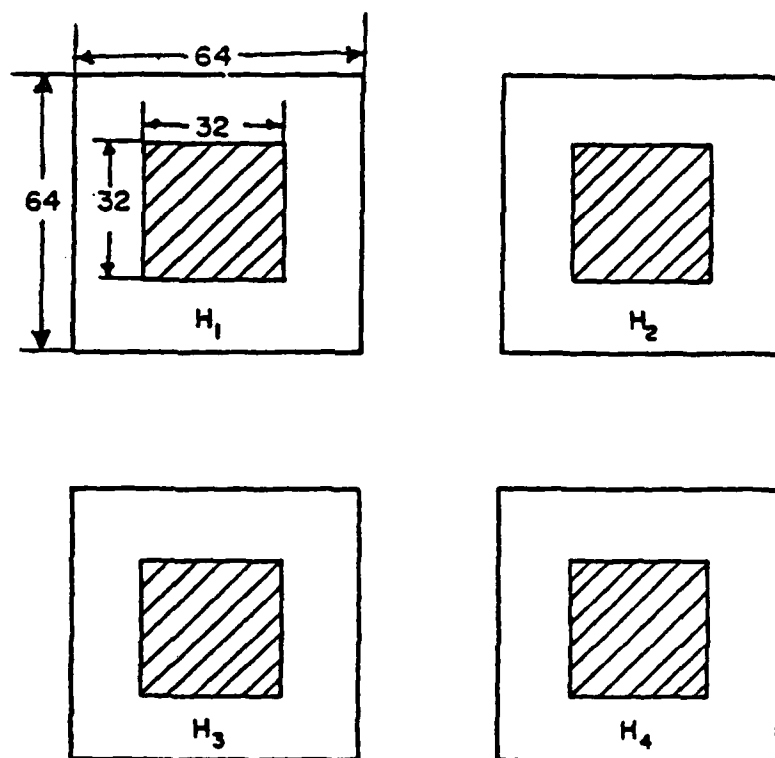
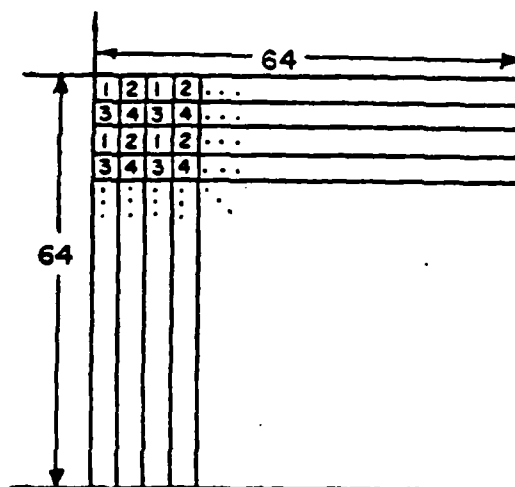


Figure 4-24. Computer simulated output when all the impulse responses of Fig. 4-13 premultiplied by the phase function of Fig. 4-18 are played back.

In such a situation a different scheme for selecting the samples from the transfer function arrays for multiplexing maybe employed. In this scheme the central  $32 \times 32$  elements from each of the transfer function arrays  $H_1$  through  $H_4$  are selected and repositioned in a composite transfer function array of  $64 \times 64$  elements as shown in Fig. (4-25). This scheme is different from the one described in section (4-1) in which alternate elements in both directions were selected as samples and were placed in their corresponding positions in the composite array. The present scheme is equivalent to low pass filtering the transfer functions and hence information about high frequency components, such as sharp edges, is lost. Since all the elements in the center of the transfer function array are used, however, effectively no sampling is being done in the Fourier plane, and hence the restriction on the size of the impulse responses given by Eqn. (4-1) is not valid. As such the impulse responses need not be space limited and may extend up to the edge of the array representing the impulse responses. However as the number of transfer functions being multiplexed increases, the size of the central array passed by the low pass filter becomes smaller and results in the loss of more and more components. In general if  $N$  transfer functions are being multiplexed in each dimension, the size of the central square array  $U$  in each dimension passed by the low pass filter is given by



(a) Low pass filtering of transfer functions: central 32 x 32 elements are selected from each transfer function.



(b) Repositioning of the selected elements in the composite array.

Figure 4-25. Generation of composite transfer function array using low pass filtering technique.

$$U = \frac{b}{N} , \quad (4-2)$$

where  $b$  is the size of the composite transfer function array. Also, since the elements from the central portion of the transfer function array are repositioned throughout the composite array as shown in Fig. (4-25) the spatial frequency scale in the composite transfer function is changed by a factor of  $N$  relative to the spatial frequency scale of the individual transfer functions. This results in a reduction in the size of the impulse responses during playback by the same factor. This multiplexing scheme is suitable for computer multiplexing only as it requires repositioning of elements and it is not possible to devise a simple optical equivalent of this multiplexing technique for recording the composite hologram. An experiment to verify this multiplexing method was carried out using the impulse responses shown in Fig. (4-26). Note that the impulse responses extend upto the edges of the array in both  $x$  and  $y$  directions. The composite hologram generated by the computer is shown in Fig. (4-27). The result of a computer simulation of the playback of this composite transfer function is shown in Fig. (4-28). Note that the edges of the function are not sharp due to the loss of high frequency components during the multiplexing step. Note also that the size of the combined impulse response during playback is only  $32 \times 32$  elements compared to the original size of  $64 \times 64$  elements as a result of scaling in the Fourier plane.

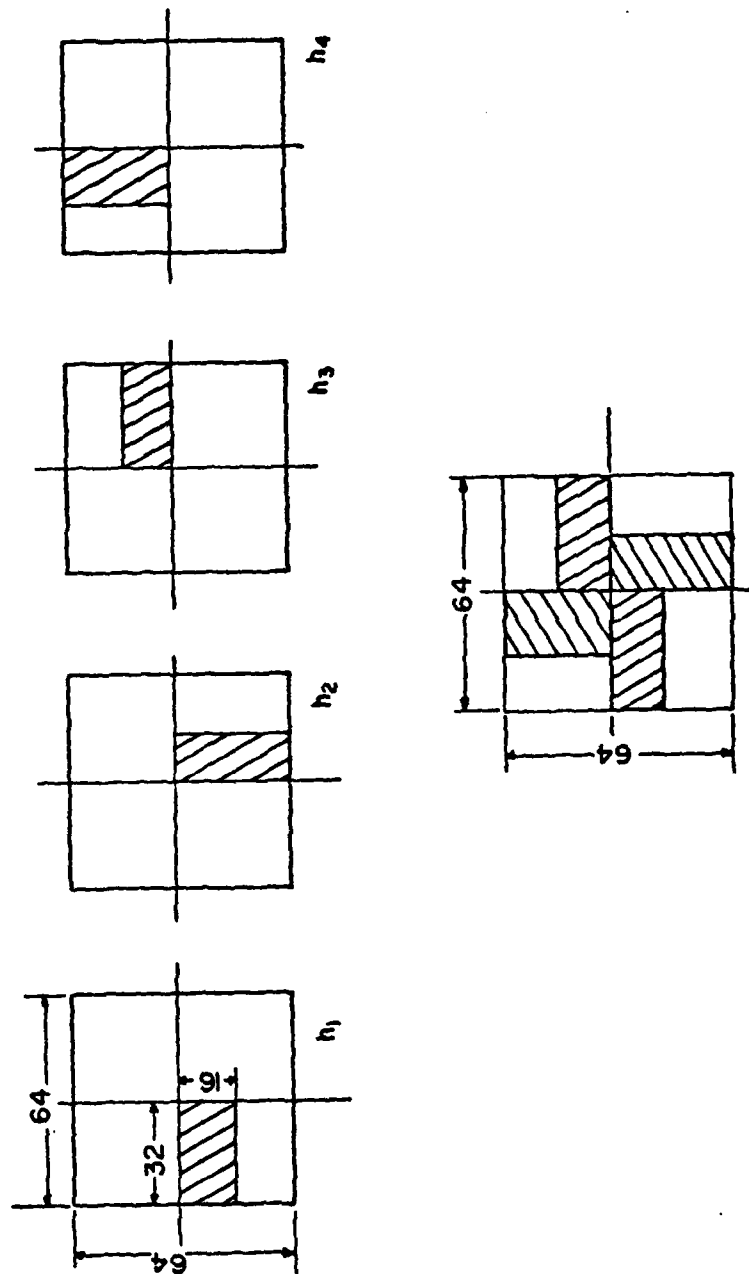


Figure 4-26. Four impulse responses used in "Low Pass Filter" multiplexing scheme.

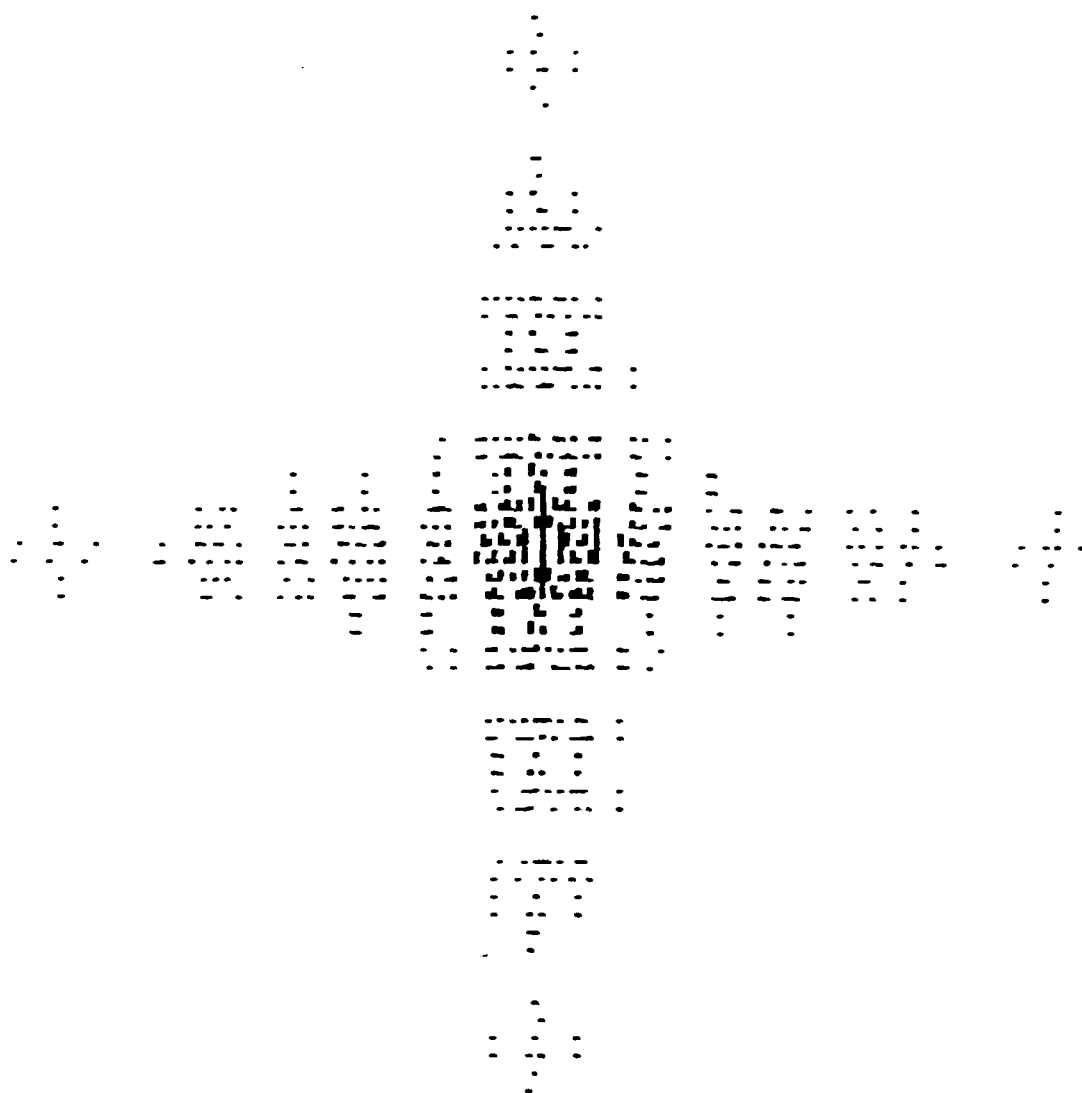


Figure 4-27. Composite hologram generated using low pass filtering technique.

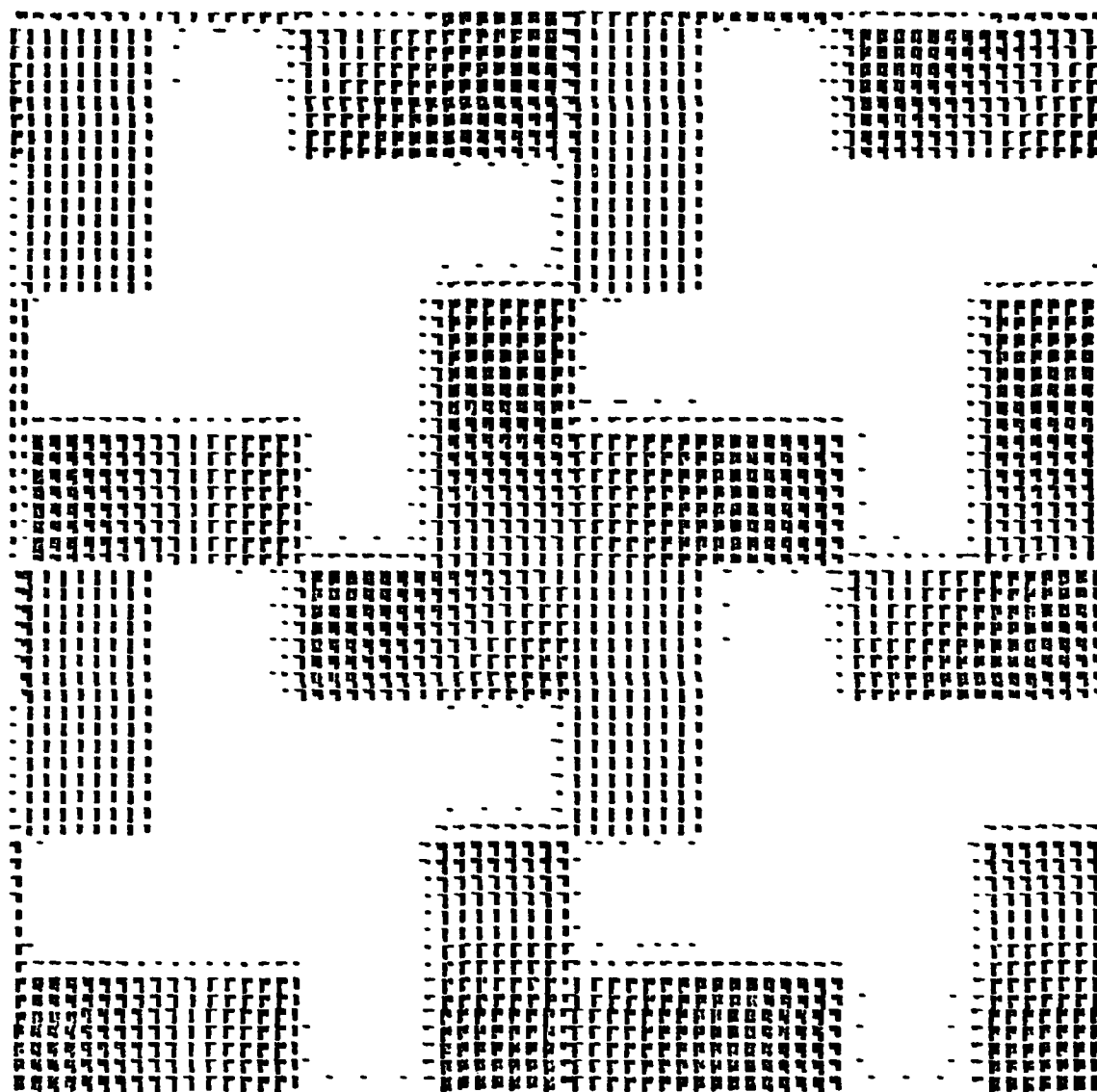


Figure 4-28. Computer simulated output when all the impulse responses of Fig. 4-26 are played back.



## CHAPTER 5

### CONCLUSIONS

The representation of space-variant systems using encoded reference beams requires diffusers with good correlation properties. One of the objectives of this report has been to evaluate the correlation properties of a family of binary phase codes for use as diffusers in multiplex holography. In Chapter 2 the results of extensive computer simulations to compute the autocorrelation and the crosscorrelations of a set of codes described by Gold for use in spread spectrum communication systems was presented. Simulations of multiplex holography using Gold codes of different lengths were also carried out. The results of these simulations indicate that, due to non ideal correlation properties of the Gold codes, the magnitudes of the crosstalk terms are quite large resulting in poor reconstruction. However it was observed that when the impulse responses have very small spatial widths, acceptable levels of the signal-to-crosstalk ratio were obtained. Thus it may be concluded that the method of space-variant system representation using the Gold codes as diffusers is more suitable for applications involving space-variant systems such as magnifiers which transform points in the input plane to points in the output plane, resulting in delta function like impulse responses.

The effect of chirped wave illumination was briefly described and the need for fabricating near perfect phase dif-

fusers was also demonstrated. A technique for fabricating phase masks using dichromated gelatin is discussed in Appendix G. Additional work needs to be done in this area to perfect this fabrication process as well as to determine simpler measuring techniques for evaluating the quality of the resultant phase masks.

Another objective of this research was to develop an alternative multiplexing technique to generate composite holograms representing the system transfer functions. In Chapter 3 a technique in which the transfer functions are sampled in the Fourier plane and repositioned to represent a composite hologram was presented. The multiplexed hologram generated by this technique contains samples of the transfer functions in nonoverlapping regions and hence the problem of hologram-to-hologram crosstalk is completely eliminated. The method also requires a single reference beam, unlike the encoded reference beam approach that required a number of reference beams. However this technique requires generation of multiple images of the input function during the playback step. Several schemes which permit generation of these coherent multiple images were briefly described. Additional research to implement these or other methods for multiple imaging needs to be done in order for this multiplexing technique to become practicable for the representation of space-variant systems characterized by a large number of impulse responses.

Experimental results using computer multiplexed holograms to represent a space-variant system sampled at  $2 \times 2$  points in the input plane were presented in Chapter 4. The experiments were conducted for both disjoint impulse responses as well as for overlapping impulse responses. The property of coherent addition that is required in the case of overlapping impulse responses was also verified through these experiments. A slight variation of this multiplexing technique using a low pass filter in the transfer function plane followed by repositioning of the filtered components was also presented. A combination of these techniques may be adopted to multiplex larger number of transfer functions in a single composite array. Multiplication of the impulse responses by a random phase mask to distribute the transfer functions more evenly so as to reduce the quantization losses of small components during the generation of computer multiplexed holograms was also demonstrated. The computer simulations and the experimental results presented in this report demonstrate the ability of the sampled input/sampled transfer function approach to effectively represent any slowly varying, linear, space-variant system with finite spatial extent of the impulse responses. However implementation of this method for very large size sampling arrays in the input plane requires high precision in the alignment of the multiple images of the input function during playback and is likely to be a limiting factor in practical systems.

## REFERENCES

- [1] R. J. Marks, J. F. Walkup, and M. O. Hagler, "A sampling theorem for space-variant systems," J. Opt. Soc. Am., 66, 918-921 (1976).
- [2] R. J. Marks, J. F. Walkup, and M. O. Hagler, "Sampling theorems for linear shift-variant systems," IEEE Trans. Ckts. & Sys., CAS-25, 228-233 (1978).
- [3] L. M. Deen, J. F. Walkup, and M. O. Hagler, "Representation of space-variant optical systems using volume holograms," Applied Optics, 14, 2438-2446 (1975).
- [4] T. F. Krile, R. J. Marks, J. F. Walkup, and M. O. Hagler, "Holographic representations of space-variant systems using phase coded reference-beams," Applied Optics, 16, 3131-3135 (1977).
- [5] T. F. Krile, M. O. Hagler, W. D. Redus, and J. F. Walkup, "Multiplex holography with chirp modulated binary phase-coded reference-beam masks," Applied Optics, 18, 52-56 (1979).
- [6] M. I. Jones, J. F. Walkup, and M. O. Hagler, "Multiplex holography for space-variant optical computing," Proc. Soc. Photo Opt. Inst. Engrs., 177, 16-21 (1979).
- [7] E. L. Kral, "Correlation properties of diffusers for multiplex holography," M. S. Thesis, Texas Tech University, (1978).
- [8] C. Irby, "Computer generated multiplex holography," M. S. Thesis, Texas Tech University, (1980).
- [9] W. D. Redus, "Two dimensional phase codes for multiplex holography," M. S. Thesis, Texas Tech University (1978).
- [10] A. W. Lohmann, and D. P. Paris, "Space-Variant image formation," J. Opt. Soc. Am., 55, 1007-1013 (1965).
- [11] J. W. Goodman, "Introduction to Fourier optics," Mc-Graw Hill, 21-25 (1968).
- [12] R. Gold, "Optimal binary sequences for spread spectrum multiplexing," IEEE trans. inform. theory, IT-13, 619-621 (1967).
- [13] W. W. Peterson, and E. J. Weldon, Jr., "Error-correcting codes," 2nd Ed., M.I.T. Press, Cambridge, Mass, 476 (1972).

- [14] D. E. Carter, "On the generation of pseudonoise codes," IEEE trans. Aerospace and Electronic Systems, AES-10, 898-899 (1974).
- [15] Redus, pp 72-73.
- [16] Redus, pp 32-38.
- [17] H. Dammann, and K. Gortler, "High-efficiency in-line multiple imaging by means of multiple phase holograms," Optics Communications, 3, 312-315 (1971).
- [18] A. Armand, A. A. Sawchuk, and T. C. Strand, "Real time nonlinear optical processing with LC devices," Proc. Intl. Opt. Comp. Conf., 153-158 (1978).
- [19] C. B. Burckhardt, "A simplification of Lee's method of generating holograms by computer," Applied Optics, 4, 1949 (1970) [Erratum, pp 2813 (1970)].
- [20] Redus, pp. 83.
- [21] Redus, pp. 89-97.
- [22] L. H. Lin, "Hologram formation in hardened dichromated gelatin films," Applied Optics, 8, 963 (1969).
- [23] C. D. Leonard, and B. D. Guenther, "A cookbook for dichromated gelatin holograms," Technical report T-79-17, U.S. Army missile research and development command (1979).
- [24] B. J. Chang and C. D. Leonard, "Dichromated gelatin for the fabrication of holographic optical elements, Applied Optics, 18, 2407-2417 (1979).
- [25] B. J. Chang, "Post processing of developed dichromated gelatin holograms," Optics Communications, 17, 270-272 (1976).
- [26] B. J. Chang, "Dichromated gelatin as a holographic storage medium," Proc. Soc. Photo Opt. Inst. Engrs., 177, 71-81 (1979).
- [27] H. M. Smith, ed., "Holographic recording materials," Topics in Applied Physics, 20, Springer-Verlag, 75-99, (1977).

## APPENDIX A

Computer Program to Generate Gold Codes of Length  
511 Bits and a Set of Nine Codes Generated by the Program.

```

PROGRAM CODE
C THIS PROGRAM GENERATES A SET OF THE GOLD CODE
C SEQUENCES OF LENGTH 512 BITS EACH. THE REQUIRED
C INPUTS TO THE PROGRAM ARE (1) THE SHIFT REGISTER
C CONNECTIONS REPRESENTING THE POLYNOMIAL, (2) THE
C NUMBER OF CODES IN THE SET (LIMITED TO A MAXIMUM
C OF 25.) THE PROGRAM USES 000000000000000001 AS
C THE FIRST SEED FOR GENERATING THE FIRST CODE IN
C THE SET. SUBSEQUENTLY THE VALUE OF THE SEED IS
C INCREMENTED BY 1 AND THE NEW SEED IS CHECKED
C TO VERIFY WHETHER IT IS A SEGMENT OF THE CODES
C ALREADY GENERATED. IF SO THE SEED IS AGAIN
C INCREMENTED BY 1 AND AGAIN CHECKED. THE OUTPUT
C OF THE PROGRAM IS A SET OF UNIQUE CODES. THE
C PROGRAM PRINTS THE SEED USED AND THE CORRESPONDING
C GOLD CODE GENERATED.
    DIMENSION IZ(25,530),IA(18)
  5  FORMAT(////)
C READ THE SHIFT REGISTER CONNECTIONS.
C SHIFT REGISTER CONNECTIONS ARE ENTERED ON THE
C DATACARD STARTING FROM THE HIGHEST ORDER.
C FOR EXAMPLE  $1+x+x^{*3}+x^{*5}+x^{*6}+x^{*8}+x^{*11}+x^{*12}+x^{*15}$ 
C  $+x^{*16}+x^{*18}$  IS ENTERED AS 101100110010110101
C IGNORING THE CONSTANT 1.
    READ(5,10)(IA(I),I=1,18)
  10 FORMAT(18I1)
    WRITE(6,5)
    WRITE(6,15)(IA(I),I=1,18)
  15 FORMAT(5X,26HSHIFT REGISTER CONNECTIONS,/5X,18I1,////)
C READ THE DESIRED NUMBER OF CODES IN THE SET.
    READ(5,20)N
  20 FORMAT(I3)
    WRITE(6,25)N
  25 FORMAT(5X,20HNUMBER OF SEQUENCES=,I3,////)
C SET THE SEED FOR THE FIRST CODE AS 000000000000000001.
    I030J=1,17
  30 IZ(1,J)=0
    IZ(1,18)=1
    I0300 K=1,N
    IF(K.EQ.1)GO,50
C INCREMENT THE SEED USED FOR THE PREVIOUS CODE BY 1.
  50 I052 J=1 3
  52 IZ(K,J)=IZ(K-1,J)
  55 I0 60J=1,18
    IF((IZ(K,19-J)).EQ.1)GO,56
  56 IZ(K,19-J)=1
    IJ=J-1
    I058 JJ=1,IJ
  58 IZ(K,19-JJ)=0
    GOT062
  60 CONTINUE

```

```

C      VERIFY WHETHER THE NEW SEED IS A SEGMENT OF THE
C      PREVIOUSLY GENERATED CODES IN THE SET. IF SO RETURN
C      TO THE PREVIOUS STEP AND CHANGE THE VALUE OF THE
C      SEED. IF NOT USE THIS SEED FOR GENERATING
C      ANOTHER MEMBER IN THE SET.
62     DO70L=1,512
      KK=K-1
      DO70I=1,KK
      DO65J=1,18
      IF((IZ(K,19-J)).EQ.(IZ(I,18+L-J)))65,70
65     CONTINUE
      GOT055
70     CONTINUE
80     WRITE(6,85)(IZ(K,J),J=1,18)
85     FORMAT(5X,21HSEED FOR THE SEQUENCE, /5X,18I1,////)
C      GENERATE THE GOLD CODE USING THE SEED
C      PREVIOUSLY SELECTED.
      DO150I=19,530
      M=0
      DO90J=1,18
90     M=IA(J)*IZ(K,J+I-19)+M
      R=M/2.0
      MM=R
      R=R-MM
150    IZ(K,I)=R*2.0
      WRITE(6,180)
180    FORMAT(5X,26HGOLD CODE FOR THIS SEED IS,/)
      WRITE(6,200)(IZ(K,J),J=19,530)
200    FORMAT(5X,48I1 )
300    WRITE(6,5)
      END

```



SHIFT REGISTER CONNECTIONS  
101100110010110101

NUMBER OF SEQUENCES= 9

SEED FOR THE SEQUENCE  
000000000000000001

GOLD CODE FOR THIS SEED IS

1101110102110001101110000101110000100101101001101  
001110011001111100000010000110110111101110001101  
010000011010010000110101001101000100111000010000  
00100101000011000111101110010001011010001010010  
10111000000010110110000110100011000100100110110  
1000011100000100011101111010000001111010000100  
0011010111011110110011011101101100001001000010  
11101110100110101000010010011111110011000001100  
110111111011001101100010100010110001001001001000  
110011010100011100010001010101010111011011100110  
1011001011101000000000000000000001

SEED FOR THE SEQUENCE  
000000000000000010

GOLD CODE FOR THIS SEED IS

011001111001001011001000111001001101110111010111  
010010101010000010000110001011011000110010010111  
11000010111011000101111110111001101001000110000  
011011110001010010001100010110011101110011110111  
11001000000011101101110111100101001101101011011  
10001001110011001001100011100000010001110001100  
0101111001110000110101011001111011001101100111  
00110011101011110001101101000000010101000010101  
011000001101010110100111100111010011011011001  
0101011111001001001100111111111001101100101011  
1101011100111000010000000000010

SEED FOR THE SEQUENCE  
000000000000000101

GOLD CODE FOR THIS SEED IS

000100100101010000101001100101011111000011100011  
101011001001111010001110010000000110001010100010  
11000100011111001000101110001001110101001110000  
111110110010010101100011011110110000110110111101  
00101000000110000001110001101001011111110000001  
100101001101110101000111001100000101100110011100  
100010011000111000011000010000000100111111001100  
1000100111000101100111111011111011001000100110  
00011110000110000010110110110001011111111111010  
0110001011010101110110101010100100000010110001  
00011100100110000000000000000101

SEED FOR THE SEQUENCE  
00000000000000110

GOLD CODE FOR THIS SEED IS

10101000101101101011001001011010110011001111001  
11011111111001011000101001110110100100110111000  
010001110011010011100001111001010111011001010000  
101100010011110110010100111010100110010100011000  
01011000001001101100111100101111010110111101100  
100110100101010110101000100100000110010010010100  
111000100101000101111110101011100101101001001  
010101001111000010010110111000000111111000111111  
10100010011111011101000101001110101101101101011  
1111100010110110101010000000001010110101111100  
01111001010010000000000000000110

SEED FOR THE SEQUENCE  
000000000000001000

GOLD CODE FOR THIS SEED IS

0100001100111010100110111000111100111110000010000  
000100110001110110011010101011010100100111010010  
01001010000101010100100010001110000011011010001  
1001100100111100100101010101111100011110001101  
10011000001111101100000100011111110010001011000  
101000000111011000010110000100001001000010110101  
01001101001011001110010100110111101100101011110  
001000000010010010110010000111110100111001011001  
01011100111001011111100111111111100100100101101  
100100100110001111011110101011100011101001001001  
11101110000010000000000000000001000

SEED FOR THE SEQUENCE

00000000000001011

GOLD CODE FOR THIS SEED IS

1111100111001100111101011011101110101010001010  
 0110000001000010101111010011011101111011001000  
 11001001000111010010001000101111001101011110001  
 11010011010001101011110100111101010111100101000  
 1110100001101011010100010111000111011000110101  
 10101110111111011111001101100001010110110111101  
 001001101111001110000011111101100101110111011011  
 11111010101000110111011001000001000001001000000  
 1110001110000110011100111010011110110110111100  
 000010001110110111111100000001011111011110000100  
 1000101110110000000000000001011

SEED FOR THE SEQUENCE

00000000000001100

GOLD CODE FOR THIS SEED IS

100011000001111110000101000001101000011110111110  
 100001100101110010010010111101100101000011111101  
 11001111110011011111001011111110101000101010001  
 010001110111011101010010000110000111111001100010  
 000010000100011011110111111101101001011101111  
 10110011111011110010011011110000110101111011101  
 1111000101001101010011100010110101010011010000  
 010001110111101110101001010111110001101001110011  
 100111010100111010110011110001011010010010011111  
 001111011110001101110010101000010110000011110  
 010000000111100000000000000100

SEED FOR THE SEQUENCE

00000000000001111

GOLD CODE FOR THIS SEED IS

0011011011111000111101010111100001000100100100  
 111101010110001110010010110000001010011111100111  
 010011001000010110011100100101100011111010010001  
 00001101011011110100101100011010001011011000111  
 011110000010100000010010010111011100000010000010  
 101110101100111100100110100001110101010100101  
 100110101001001000101000110000001101000001010101  
 100110100100111010100000011000001101011001101010  
 001000100010100001110110110100111000000000001110  
 10100111011111110011011111111101100000111010011  
 001001011010100000000000000001111

SEED FOR THE SEQUENCE

000000000000010001

GOLD CODE FOR THIS SEED IS

0101101100001001000111110000100011001101101101  
 0001111110100100101101110000001110100000101001  
 11010101100011101010010110110100100001110110011  
 000101111011000011101110100101110011101101001001  
 100010000111100000110110111001100100000110000111  
 1100011110101000010110111110001001111111101110  
 10101111101101100111100101000001011100001111110  
 10101110110100111110000010100001011110101011110  
 011001100111100010011011011101001000000000010011  
 111010011000000010101100100000110100001001110101  
 0110111011111000000000000000010001

APPENDIX B

Computer Program to Evaluate the  
Correlation Properties of the Gold Codes

```

C      PROGRAM SPACEVAR
C      THIS PROGRAM COMPUTES AND PLOTS THE AUTOCORRELATION
C      OF A GOLD CODE IN A SET OF NINE 128 BIT CODES AND
C      ITS CROSSCORRELATION WITH THE OTHER EIGHT MEMBERS
C      IN THE SET. THIS IS DONE BY MULTIPLYING THE FOURIER
C      TRANSFORMS OF THE CODES AND THEN FOURIER TRANSFORMING
C      THE PRODUCT. IN THIS PROGRAM ONLY THE CENTRAL 42
C      BITS OF THE 128 BIT CODE ARE USED IN THE CALCULATION
C      SO THAT THIS OUTPUT MAY BE COMPARED WITH THE OUTPUT
C      OF THE PROGRAM 4PXHOLD.
      DIMENSION A(128),G(128),H(128),T(128) ,B(9,128)
      TYPE COMPLEX G,H,T,CMPLX,CONJG
      CALLPLOTS(0,0,1)
      WRITE(6,220)
      DO3I=1,128
      H(I)=(0.0,0.0)
5      T(I)=(0.0,0.0)
C      READ THE 128 BIT CODE TO BE USED AS THE COMMON CODE
C      IN THE CALCULATION OF CORRELATION WITH A SET OF NINE
C      128 BIT CODES. THE CODE IS READ IN AS ZEROS AND TWOS.
      READ(5,10)(A(I),I=1,128)
10      FORMAT(64F1.0)
C      CONVERT THE VALUES IN THE CODE TO +1 AND -1 TO
C      REPRESENT A PHASE MASK WITH 180 DEGREES PHASE
C      DIFFERENCE.
      DO20I=44,85
      IF(A(I).GT.0)15,12
12      A(I)=-1.0
      GO TO 20
15      A(I)=1
20      CONTINUE
      DO30I=44,85
      H(I)=CMPLX(A(I),0.0)
30      CONTINUE
C      CALCULATE THE FOURIER TRANSFORM OF THE CODE .
      CALL FOURIER (H)
C      CALCULATE THE CONJUGATE OF THE FOURIER TRANSFORM OF
C      THE CODE AND STORE IN THE ARRAY T.
      DO 40 I=1,128
40      T(I)=CONJG(H(I))
C      THE FOLLOWING DO LOOP READS ALL THE NINE CODES IN
C      THE SET ONE AT A TIME AND COMPUTES THEIR CORRELATION
C      WITH THE CODE PREVIOUSLY READ. THIS SET OF NINE CODES
C      ALSO INCLUDES THE PREVIOUSLY READ CODE AS A MEMBER
C      AND HENCE ONE OF THE OUTPUTS IS THE AUTOCORRELATION
C      AND THE REST ARE THE CROSSCORRELATIONS.
      DO120 KK=1,9
      DO 60 I=1,128
      G(I)=(0.0,0.0)
60      H(I)=(0.0,0.0)

```

```

C      READ A MEMBER FROM THE SET AND CONVERT THE VALUES
C      TO +1 AND -1.
      READ(5,10)(A(I),I=1,128)
61     FORMAT(5X,64F1.0)
      WRITE(6,61)(A(I),I=1,127)
      WRITE(6,220)
      DO 70 I=44,85
      IF(A(I).GT.0)65,62
62     A(I)=-1
      GO TO 70
65     A(I)=1
70     CONTINUE
      DO 80 I=44,85
      H(I)=CMPLX(A(I),0.0)
80     CONTINUE
C      CALCULATE THE FOURIER TRANSFORM.
      CALLFOURIER(H)
C      MULTIPLY THE FOURIER TRANSFORM OF THE CODES.
      DO 90 I=1,128
90     G(I)=T(I)*H(I)
C      COMPUTE THE FOURIER TRANSFORM OF THE PRODUCT TO OBTAIN
C      AS THE OUTPUT THE CORRELATION BETWEEN THE CODES.
      CALLFOURIER(G)
      DO 120 I=1,128
120    R(K,I)=CABS(G(I))
C      NORMALIZE THE MAGNITUDES OF ALL THE ELEMENTS IN THE
C      OUTPUTS WITH REFERENCE TO THE VALUE OF THE LARGEST
C      ELEMENT IN THE ENTIRE SET.
      XM=0.0
      DO122 I=1,9
      DO122J=1,128
122    XM=MAX1F(B(I,J),XM)
      DO125I=1,9
      DO125J=1,128
125    G(I,J)=B(I,J)*99/XM
C      PLOT EACH OF THE NORMALIZED OUTPUTS TO A WIDTH OF
C      2.56 INCHES.
      DO500K=1,3
      DO400L=1,3
      CALLPLOT(0.0,-2.56,2)
      CALLPLOT(0.0,0.0,2)
      J=(K-1)*3+L
      DO160I=1,128
160    CALLPLOT(B(J,I)/40,-I*0.02,2)
C      PRINT THE NORMALIZED VALUES OF THE CORRELATION OUTPUT.
      WRITE(6,200)(B(J,I),I=1,128)
200    FORMAT(5X,16F4.0)

```

```

WRITE(6,220)
220 FORMAT(//)
400 CALLPLOT(0.0,-3.0,-3)
500 CALLPLOT(3.0,9.0,-3)
CALLPLOT(0.0,0.0,999)
END

```

```

SUBROUTINE FOURIER (B)
C THIS SUBROUTINE CALCULATES THE FOURIER TRANSFORM
C OF AN ARRAY OF 128 ELEMENTS,
C THIS PROGRAM ALSO SHIFTS THE ELEMENTS IN THE
C ARRAY TO TAKE CARE OF THE FFT ALGORITHM WHICH
C ASSUMES THE FIRST ELEMENT AS THE ORIGIN.
DIMENSION M(3),S(32),INV(32),B(128)
TYPE COMPLEXX,B
DATA(M=7,0,0)
IT=0
10 DO 20 I=1,64
X=B(I)
B(I)= B(I+64)
B(I+64)=X
20 CONTINUE
IF(IT.EQ.1)30,22
C CALL FFT ALGORITHM HARM.
22 CALL HARM (B,M,INV,S,1,IFERR)
IT=1
30 TO 10
30 RETURN
END

```



## APPENDIX C

Computer Program to Simulate the Output  
of a Multiplexed Hologram Using Gold Codes  
as Phase Diffusers in the Reference Beam Path.

```

PROGRAM MPXHOLD
C THIS PROGRAM SIMULATES THE OUTPUT OF A SYSTEM
C USING THE GOLD CODES AS DIFFUSERS IN THE
C REFERENCE BEAM PATH TO REPRESENT A SPACE-VARIANT
C PROCESSOR. A TOTAL OF TWO TRANSFER FUNCTIONS
C REPRESENTING THE SPACE-VARIANT SYSTEM ARE MULTIPLEXED
C IN A SINGLE ARRAY. THE PROGRAM ALSO PLOTS THE
C IMPULSE RESPONSES USED IN THE SIMULATION AND THE
C OUTPUT WHEN THEY ARE RECORDED AND PLAYED BACK
C USING THE GOLD CODES WITHOUT ANY MULTIPLEXING.
C IN THIS PROGRAM ONLY THE CENTRAL 42 BITS OF THE
C 128 BIT CODE ARE USED IN THE CALCULATION SO THAT THE
C OUTPUT OF THE SIMULATION WITH THE TOTAL WIDTH
C EQUAL TO THE SUM OF THE WIDTHS OF THE TWO CODES
C AND THE WIDTH OF THE IMPULSE RESPONSE IS LESS THAN
C THE SIZE OF THE OUTPUT ARRAY. FOR THE SAME
C REASON THE IMPULSE RESPONSES ARE ALSO LIMITED
C TO A SIZE OF 42 BITS.
C DIMENSION A(128),G(128),H(128),S(128),R(128),T(128)
C TYPE COMPLEX G,H,T,CMPLX,CONJ ,S
C CALL PLOTS(0,0,1)
C DO 5 I=1,128
5 I(I)=(0.0,0.0)
C DO 100 K=1,2
C DO 7 I=1,128
7 S(I)=0.0
C READ A 128 BIT GOLD CODE. VALUES READ IN
C ARE ZEROS AND TWOS.
C READ(5,10)(A(I),I=1,128)
10 FORMAT(64F1.0)
C CONVERT THE VALUES TO +1 AND -1 TO REPRESENT
C A PHASE MASK WITH 180 DEGREES PHASE DIFFERENCE
C BETWEEN THE ELEMENTS.
C DO 20 I=44,85
C IF(A(I).GT.0) 12,12
12 A(I)=-1
C GO TO 20
15 A(I)=1
20 CONTINUE
C DO 25 I=1,128
C S(I)=(0.0,0.0)
25 H(I)=(0.0,0.0)
C DO 30 I=44,85
C H(I)=CMPLX(A(I),0.0)
30 CONTINUE
C FOURIER TRANSFORM THE ARRAY TO REPRESENT
C THE REFERENCE BEAM ILLUMINATING THE HOLOGRAM.
C CALL FOURIER (H)
C DO 32 I=1,128
32 A(I)=0.0

```

```

C      READ AN IMPULSE RESPONSE OF THE SPACE-VARIANT SYSTEM.
      READ(5,33)(A(J),J=44,85)
33  FORMAT(21F2.0)
      DO35 I=1,128
      G(I)=CMPLX(A(I),0.0)
35  H(I)=ABS(A(I))
C      PLOT AND PRINT THE IMPULSE RESPONSES.
      CALLPLOT(B)
      CALLPLOT(3.0,0.0,-3)
C      COMPUTE THE TRANSFER FUNCTION .
      CALL FOURIER (G)
C      GENERATE THE COMPOSITE TRANSFER FUNCTION ARRAY BY
C      SUMMING THE PRODUCT OF THE FOURIER TRANSFORMS
C      OF EACH OF THE IMPULSE RESPONSES AND THE
C      CORRESPONDING REFERENCE BEAM FUNCTION.
      DO 40 I=1,128
40  T(I)=T(I)+G(I)*CONJG(H(I))
C      SIMULATE THE PLAYBACK OF AN IMPULSE RESPONSE
C      WHEN THE GOLD CODE IS USED IN THE RECORDING
C      AND THE PLAYBACK STEP.
      DO50 I=1,128
50  G(I)=H(I)*CONJG(H(I))*G(I)
      CALL FOURIER (G)
      DO 60 I=1,128
60  R(I)=CABS(G(I))
C      PLOT AND PRINT THE OUTPUT WHEN THE IMPULSE RESPONSES
C      ARE RECORDED AND PLAYED BACK USING THE GOLD CODES.
      CALLPLOT(B)
      CALLPLOT(-3.0,-4.0,-3)
      IF(K.EQ.1)70,100
70  DO80 I=1,128
80  S(I)=H(I)
100  CONTINUE
      CALLPLOT(6.0,8.0,-3)
      DO110 I=1,128
C      SIMULATE THE PLAYBACK OF THE SYSTEM WHEN THE
C      TRANSFER FUNCTIONS ARE ACCESSED (A) INDIVIDUALLY
C      AND (B) SIMULTANEOUSLY FROM THE COMPOSITE ARRAY.
      G(I)=T(I)*S(I)
      T(I)=T(I)+H(I)
110  S(I)=G(I)+T(I)
      CALLFOURIER(G)
      CALLFOURIER(S)
      CALLFOURIER( T )
      DO120 I=1,128
120  R(I)=CABS(G(I))
C      PRINT AND PLOT THE OUTPUT WHEN THE FIRST TRANSFER
C      FUNCTION IS ACCESSED FROM THE COMPOSITE ARRAY.
      CALLPLOT(B)
      CALLPLOT(0.0,-4.0,-3)

```

```

DO130I=1,128
130 B(I)=CABS(T(I))
C PRINT AND PLOT THE OUTPUT WHEN THE SECOND TRANSFER
C FUNCTION IS ACCESSED FROM THE COMPOSITE ARRAY.
CALLPLOT(R)
CALLPLOT(3,0,2,J,-3)
DO140I=1,128
140 H(I)=CABS(S(I))
C PRINT AND PLOT THE OUTPUT WHEN BOTH THE TRANSFER
C FUNCTIONS ARE ACCESSED FROM THE COMPOSITE ARRAY.
CALLPLOT(R)
CALLPLOT(0,0,99,J)
END

```

```

SUBROUTINE FOURIER (B)
C THIS SUBROUTINE CALCULATES THE FOURIER TRANSFORM
C OF AN ARRAY OF 128 ELEMENTS.
C THIS PROGRAM ALSO SHIFTS THE ELEMENTS IN THE
C ARRAY TO TAKE CARE OF THE FFT ALGORITHM WHICH
C ASSUMES THE FIRST ELEMENT AS THE ORIGIN.
DIMENSION M(3),S(32),INV(32),B(128)
TYPE COMPLEXX,R
DATA(M=7,0,0)
IT=0
10 DO 20 I=1,64
X=R(I)
B(I)=B(I+64)
B(I+64)=X
20 CONTINUE
IF(IT.EQ.1)30,22
C CALL FFT ALGORITHM HARM.
22 CALL HARM (B,M,INV,S,1,IFERR)
IT=1
GO TO 10
30 RETURN
END

```

```
      SUBROUTINE PLOTT(B)
C      THIS SUBROUTINE PRINTS AND PLOTS THE MAGNITUDES
C      OF THE OUTPUTS. THE OUTPUTS ARE NORMALIZED WITH
C      REFERENCE TO THE LARGEST ELEMENT IN THE ARRAY.
      DIMENSION B(128)
      XM=0.0
      DO10J=1,128
10    XM=MAX1F(B(J),XM)
      DO20J=1,128
20    B(J)=B(J)+99/XM
      CALLPLOT(0.0,-2.56,2)
      CALLPLOT(0.0,0.0,2)
      DO30I=1,128
30    CALLPLOT(B(I)/4J,-1+0.02,2)
      WRITE(6,40)(B(I),I=1,128)
40    FORMAT(5X,32F3.0)
      WRITE(6,50)
50    FORMAT(////)
      CALLPLOT(0.0,0.0,3)
      RETURN
      END
```

#### APPENDIX D

Computer Program to Evaluate the Correlation Properties  
of the Gold Codes Illuminated by a Spherical Wavefront

```

PROGRAM SPHWAVE
C THIS PROGRAM COMPUTES THE AUTOCORRELATION AND THE
C CROSSCORRELATIONS OF THE GOLD CODES ILLUMINATED BY A
C SPHERICAL WAVEFRONT. THE COMPUTATIONS ARE CARRIED
C OUT FOR DIFFERENT VALUES OF THE CHIRP AS SPECIFIED
C BY THE RADIUS OF CURVATURE OF THE WAVEFRONT AND THE
C WIDTH OF THE MASK. THE OUTPUTS ARE NORMALIZED BY
C FORCING THE AREA UNDER EACH OF THE AUTOCORRELATION
C PEAK FOR DIFFERENT VALUES OF THE CHIRP TO BE EQUAL
C SO THAT THE OUTPUTS MAY BE COMPARED WITH EACH OTHER.
C AN ESTIMATE OF THE NOISE TO SIGNAL RATIO IS ALSO
C MADE BY CALCULATING THE RATIO OF AREA UNDER THE
C CORRELATION CURVES TO THE AREA OF THE AUTOCORRELATION
C PEAK.
C DIMENSION A(128),H(2048),T(2048),B(128),C(128),D(128)
C TYPE COMPLEX H,T,CMPLEX,CONJG,C,D,ARA,ARC
C CALLPLOTS(0,0,1)
C READ THE TWO 128 BIT CODES. CONVERT THE VALUES TO
C +1 AND -1 TO REPRESENT A PHASE MASK WITH 180
C DEGREES PHASE DIFFERENCE.
C READ(5,10)(A(I),I=1,128) ,(B(I),I=1,128)
10 FORMAT(64F1,0)
C DO 20 I=44,85
C IF(A(I).GT,0) 15,12
12 A(I)=-1
C GO TO 20
15 A(I)=1
20 CONTINUE
C DO 26 I=44,85
C IF(B(I).GT,0.0) 25,22
22 B(I)=-1
C GO TO 26
25 B(I)=1
26 CONTINUE
C THE FOLLOWING DO LOOP COMPUTES THE AUTOCORRELATION
C OF (A) WITH ITSELF AND CROSSCORRELATION OF (A) WITH
C (B) FOR DIFFERENT VALUES OF CHIRP.
C DO 500 KK=1,8
C DO 51 I=1,2048
C H(I)=(0.0,0.0)
5 T(I)=(0.0,0.0)
C READ THE RADIUS OF CURVATURE OF THE SPHERICAL
C WAVEFRONT AND THE WIDTH OF THE CODE MASK.
C READ(5,8)R,W
8 FORMAT(2F6,2)
C LOAD THE CODES IN A LARGER ARRAY SO THAT EACH ELEMENT
C IN THE ORIGINAL ARRAY OCCUPIES 16 ELEMENTS IN THE
C NEW ARRAY. THIS IS NECESSARY TO REPRESENT THE PHASE
C VARIATIONS WITHIN EACH ELEMENT WHEN THE CODE
C IS ILLUMINATED BY A SPHERICAL WAVEFRONT.

```

```

DO 30 I=44,85
DO30J=1,16
T((I-1)*16+J)=CMPLX(R(I),0.0)
30 H((I-1)*16+J)=CMPLX(A(I),0.0)
C CALCULATE THE PATH DIFFERENCE AT THE CENTER OF EACH
C ELEMENT RELATIVE TO THE CENTER OF THE ARRAY.
DO35 I=1,1024
S=(SQRT (R**2+((I-0.5)*w/2048)**2)-R)
C COMPUTE THE PHASE DIFFERENCE FOR A WAVELENGTH OF
C 500 NANOMETERS.
D=S*(10**4)/5
L=D
D=(D-L)*2*3.1425
C CHANGE THE VALUES OF THE ELEMENTS IN THE COMPLEX ARRAY
C TO INCLUDE THE EFFECT OF THE PHASE CHANGE DUE TO
C THE CURVATURE OF THE WAVEFRONT.
T(1024+I)=T(1024+I)*CMPLX(COS(D),SIN(D))
T(1024-I)=T(1024-I)*CMPLX(COS(D),SIN(D))
H(1024+I)=H(1024+I)*CMPLX(COS(D),SIN(D))
35 H(1024-I)=H(1024-I)*CMPLX(COS(D),SIN(D))
C COMPUTE THE AUTO AND THE CROSS-CORRELATIONS.
CALL FOURIER (H)
CALLFOURIER(T)
DO 40 I=1,2048
T(I)=T(I)*CONJG(H(I))
40 H(I)=H(I)*CONJG(H(I))
CALLFOURIER(T)
CALL FOURIER (H)
C COMPUTE THE AVERAGE MAGNITUDE OF EVERY 16 ELEMENTS
C AND GENERATE OUTPUT ARRAYS OF 128 ELEMENTS EACH.
DO 120 I=1,128
J=(I-1)*16+1
K=J+14
DO110K=J,M
T(J)=T(J)+T(K+1)
110 H(J)=H(J)+H(K+1)
D(I)=T(J)
120 C(I)=H(J)
C COMPUTE THE MAGNITUDE OF THE PEAK OF AUTO-CORRELATION.
XM=0.0
130 DO135I=1,128
X=CABS(C(I))
135 XM=MAX1F(X,XM)
C COMPUTE THE ALGEBRAIC SUM OF THE ELEMENTS IN THE
C OUTPUT ARRAYS.
ARA=(0.0,0.0,0.0)
ARC=(0.0,0.0,0.0)
140 DO150 I=1,128
ARA=ARA+C(I)
150 ARC=ARC+D(I)
AA=CABS(ARA)

```



```

      AC=CABS(ARC)
C     COMPUTE THE NOISE TO SIGNAL RATIO OF AUTOCORRELATION
C     AND THE CROSSCORRELATION FUNCTIONS USING THE PEAK
C     OF AUTOCORRELATION AS REFERENCE.
      RA=AA/XM-1
      RC=AC/XM
C     NORMALIZE THE VALUES WITH REFERENCE TO THE PEAK OF
C     AUTOCORRELATION, ALSO SCALE THE VALUES ACCORDING TO THE
C     WIDTH OF THE MASKS WITH WIDTH=3.81 AS REFERENCE.
C     THIS ENSURES THAT THE AREA UNDER THE AUTOCORRELATION
C     PEAKS FOR MASKS WITH DIFFERENT WIDTHS ARE ALL EQUAL.
      DO170 I=1,128
      D(I)=D(I)*(99/XM)*(3.81/W)
170   C(I)=C(I)*(99/XM)*(3.81/W)
      WRITE(6,190)R
190   FORMAT(5X,21HRA=AREA OF WAVEFRONT =,F6.2)
      WRITE(6,200)W
200   FORMAT(5X,21HWIDTH OF CODE MASK = ,F6.2)
      WRITE(6,210)XM
210   FORMAT(5X,21HHEIGHT OF AUTOCORRELATION PEAK=,E9.2//)
      WRITE(6,220)AA
220   FORMAT(5X,21HAA=AREA OF AUTOCORN ,E9.2)
      WRITE(6,230)AC
230   FORMAT(5X,21HAC=AREA OF CROSSCORN ,E9.2)
      WRITE(6,240)RA
240   FORMAT(5X,
141HNOISE TO SIGNAL RATIO OF AUTOCORRELATION=,F8.2//)
      WRITE(6,250)RC
250   FORMAT(5X,
151HRATIO OF NOISE OF CROSS CORN TO SIGNAL OF AUTOCORN=,
2F8.2//)
C     PLOT THE AUTO AND THE CROSS-CORRELATIONS. THE WIDTH
C     OF PLOTS ARE SCALED ACCORDING TO THE WIDTH OF EACH
C     MASK. (WIDTH OF PLOTS FOR MASK WITH W=3.81 IS
C     TAKEN AS 2.56 INCHES AND IS USED AS REFERENCE FOR
C     COMPUTING THE PLOT SIZE FOR OTHER MASK WIDTHS.)
      CALLPLOT(0.0,-2.56*W/3.81,2)
      CALLPLOT(0.0,0.0,2)
      DO300I=1,128
      X=CABS(C(I))
300   CALLPLOT(X/100,-I*0.02*W/3.81,2)
      CALLPLOT(0.0,-4.0,-3)
      CALLPLOT(0.0,-2.56*W/3.81,2)
      CALLPLOT(0.0,0.0,2)
      DO400I=1,128
      X=CABS(D(I))
400   CALLPLOT(X/100,-I*0.02*W/3.81,2)
      CALLPLOT(3.00,4.00,-3)
500   CONTINUE
      CALLPLOT(0.0,0.0,999)
      END

```

```
SUBROUTINE FOURIER (B)
  DIMENSION M(3),S(512),INV(512),B(2048)
  TYPE COMPLEXX,B
  DATA(M=11,0,0)
  IT=0
10  DO 20 I=1,1024
     X=B(I)
     B(I)= S(I+1024)
     S(I+1024)=X
20  CONTINUE
     IF(IT.EQ.1)30,22
22  CALL HARM (B,M,INV,S,1,IFERR)
     IT=1
     GO TO 10
30  RETURN
  END
```

## APPENDIX E

Computer Program to Simulate the Output  
of a 1-D Processor Using the Sampled Transfer  
Function Approach for Multiplex Holography

## PROGRAM SPCEIN.V

```

C
C THIS PROGRAM MULTIPLEXES THE TRANSFER FUNCTIONS
C OF FOUR IMPULSE RESPONSES AND GENERATES A
C SINGLE COMPOSITE ARRAY USING THE SAMPLING
C TECHNIQUE IN THE TRANSFER FUNCTION PLANE.
C THE PROGRAM PLOTS THE INPUTS REPRESENTING THE
C IMPULSE RESPONSE AND THEIR RESPECTIVE
C TRANSFER FUNCTIONS BEFORE AND AFTER SAMPLING.
C THE PROGRAM ALSO SIMULATES AND PLOTS THE
C PLAYBACK OF THE IMPULSE RESPONSES WHEN
C THE TRANSFER FUNCTIONS ARE ACCESSED (A) INDIVIDUALLY,
C (B) SIMULTANEOUSLY.
C DIMENSION A(128),B(128),G(128),H(128),T(128),C(128)
C TYPE COMPLEX G,H,T,C,CMPLX,CONJG,X
C CALL PLOTS(0,0,1)
C DO100K=1,4
C READ THE IMPULSE RESPONSE.
C READ(5,10)(A(I),I=1,128)
10 FORMAT(64F1,0)
C DO20I=1,128
20 H(I)=CMPLX(A(I),0,0)
C GENERATE THE TRANSFER FUNCTION USING THE FAST
C FOURIER TRANSFORM ROUTINE.
C CALL FOURIER (H)
C SAMPLE THE TRANSFER FUNCTION AT AN INTERVAL OF FOUR
C ELEMENTS AND LOAD THE SAMPLES IN THE COMPOSITE ARRAY.
C DO30 I=K,128,4
30 T(I)=H(I)
C SCALE THE IMPULSE RESPONSES TO A MAXIMUM
C VALUE OF 99 AND PRINT.
C XM=0.0
C DO 40 I=1,128
C A(I)=ABS(A(I))
40 XM=MAX1F(A(I),XM)
C DO50I=1,128
50 A(I)=A(I)*99/XM
C WRITE(6, 60)(A(I),I=1,128)
60 FORMAT(5X,32F3,0)
C WRITE(6,70)
70 FORMAT(////)
C PLOT THE IMPULSE RESPONSE.
C CALLPLOT(0,0,-2.56,2)
C CALLPLOT(0,0,0.0,2)
C DO30I=1,128
30 CALLPLOT(A(I)/40,-I*0.02,2)
C CALLPLOT(0,0,-4.0,-3)
C PLOT THE MAGNITUDE OF TRANSFER FUNCTION.
C DO45I=1,128
45 B(I)=CABS(H(I))

```

```

      XM=0.0
      DO90I=1,128
90  XM=MAX1F(B(I),XM)
      CALLPLOT(0.0,-2.56,2)
      CALLPLOT(0.0,0.0,2)
      DO95I=1,128
      B(I)=B(I)*2.5/XM
-95  CALLPLOT(B(I),-1*0.02,2)
      CALLPLOT(3.0,4.0,-3)
100  CONTINUE
      CALLPLOT(-12.0,0.0,-3)
      CALLPLOT(0.0,0.0,999)
      CALLPLOTS(0,0,1)
C    SIMULATION OF PLAYBACK.
      DO200K=1,4
      DO110I=1,128
110  G(I)=(0,0,0,0)
C    SAMPLE THE COMPOSITE ARRAY TO RETRIEVE
C    ALL THE SAMPLES BELONGING TO A TRANSFER FUNCTION.
C    PLOT THE MAGNITUDES OF THE SAMPLED
C    TRANSFER FUNCTION.
      DO120I=K,128,4
120  G(I)=T(I)
      DO130I=1,128
130  F(I)=CABS(G(I))
      XM=0.0
      DO140I=1,128
140  XM=MAX1F(F(I),XM)
      CALLPLOT(0.0,-2.56,2)
      CALLPLOT(0.0,0.0,2)
      CALLPLOT(0.0,-K*0.02,2)
      DO150I=K,128,4
      F(I)=B(I)*2.5/XM
      CALLPLOT(B(I),-1*0.02,2)
      CALLPLOT(B(I),-(I+1)*0.02,2)
      CALLPLOT(0.0,-(I+1)*0.02,2)
150  CALLPLOT(0.0,-(I+4)*0.02,2)
      CALLPLOT(0.0,-4.0,-3)
C    FOURIER TRANSFORM THE SAMPLED TRANSFER FUNCTION.
      CALL FOURIER (G)
C    PLOT THE OUTPUT REPRESENTING THE PLAYBACK
C    OF THE SYSTEM WHEN THE TRANSFER FUNCTIONS ARE
C    INDIVIDUALLY ACCESSED.
      DO160I=1,128
160  F(I)=CABS(G(I))
      XM=0.0
      DO170I=1,128
170  XM=MAX1F(F(I),XM)

```

```

DO175I=1,128
175 B(I)=B(I)*99/XM
WRITE(6, 60)(B(I),I=1,128)
WRITE(6,70)
CALLPLOT(0.0,-2.56,2)
CALLPLOT(0.0,0.0,2)
DO180I=1,128
180 CALLPLOT(B(I)/40,-I*0.02,2)
CALLPLOT(3.0,4.0,-3)
200 CONTINUE
CALLPLOT(-12.0,0.0,-3)
CALLPLOT(0.0,999)
CALLPLOTS(0.0,1)
C PLOT THE MAGNITUDE OF THE COMPOSITE TRANSFER FUNCTION
C ARRAY REPRESENTING THE MULTIPLEXED HOLOGRAM.
DO210I=1,128
210 B(I)=CABS(T(I))
XM=0.0
DO220I=1,128
220 XM=MAX1F(B(I),XM)
CALLPLOT(0.0,-2.56,2)
CALLPLOT(0.0,0.0,2)
DO225I=1,128
B(I)=B(I)*2.5/XM
225 CALLPLOT(B(I),-I*0.02,2)
CALLPLOT(0.0,-4.0,-3)
C FOURIER TRANSFORM THE COMPOSITE ARRAY.
CALL FOURIER (T)
C PLOT THE OUTPUT REPRESENTING THE PLAYBACK
C OF THE SYSTEM WHEN ALL THE TRANSFER FUNCTIONS
C ARE SIMULTANEOUSLY ACCESSED.
DO230I=1,128
230 B(I)=CABS(T(I))
XM=0.0
DO240I=1,128
240 XM=MAX1F(B(I),XM)
DO250I=1,128
250 B(I)=B(I)*99/XM
WRITE(6, 60)(B(I),I=1,128)
CALLPLOT(0.0,-2.56,2)
CALLPLOT(0.0,0.0,2)
DO280I=1,128
280 CALLPLOT(B(I)/40,-I*0.02,2)
CALLPLOT(0.0,4.0,-3)
CALL PLOT(0.0,999)
END

```

```

SUBROUTINE FOURIER (B)
C   THIS SUBROUTINE CALCULATES THE FOURIER TRANSFORM
C   OF AN ARRAY OF 128 ELEMENTS.
C   THIS PROGRAM ALSO SHIFTS THE ELEMENTS IN THE
C   ARRAY TO TAKE CARE OF THE FFT ALGORITHM WHICH
C   ASSUMES THE FIRST ELEMENT AS THE ORIGIN.
  DIMENSION M(3),S(32),INV(32) ,B(128)
  TYPE COMPLEXX,B
  DATA(M=7,0,0)
  IT=0
10  DO 20 I=1,64
    X=B(I)
    B(I)= B(I+64)
    B(I+64)=X
20  CONTINUE
    IF(IT.EQ.1)30,22
C   CALL FFT ALGORITHM HARM.
22  CALL HARM (B,M,INV,S,1,IFERR)
    IT=1
    GO TO 10
30  RETURN
    END

```

APPENDIX F

Computer Program to Generate 2-D Composite  
Hologram and the Output of a Processor Using the  
Sampled Transfer Function Approach



```

PROGRAM SAMPLER
C THIS PROGRAM GENERATES AND PLOTS THE MULTIPLEXED
C TRANSFER FUNCTION HOLOGRAM OF FOUR IMPULSE
C RESPONSES USING THE SAMPLING TECHNIQUE IN THE
C FREQUENCY PLANE. THE PROGRAM ALSO SIMULATES AND
C PLOTS THE SIMULTANEOUS PLAYBACK OF ALL THE
C TRANSFER FUNCTIONS.
C DIMENSION A(64,64) ,B(32) ,C(64)
C TYPE COMPLEX A,X,CMPLX ,B
C WRITE (6,5)
5 FORMAT(////)
C PI=3.1415926535
C DO100K=1,2
C DO100L=1,2
C READ THE IMPULSE RESPONSE.
C READ(5,10)((A(I,J),J=1,64),I=1,64)
10 FORMAT(32(C(F1,U,F1,0)))
C
C MULTIPLY THE IMPULSE RESPONSE WITH A CHECKERBOARD
C MASK OF +1 AND -1 VALUES. THIS IS DONE TO SPREAD OUT
C THE TRANSFER FUNCTION MORE EVENLY IN THE FOURIER PLANE.
C (HOWEVER THIS WILL NOT AFFECT THE OUTPUT OBSERVED
C AS MAGNITUDE.)
C
17 DO18 I=1,16
DO18II=1,4
DO18 J=1,16
DO18JJ=1,4
18 A(((I-1)*4+II),((J-1)*4+JJ))=A(((I-1)*4+II),
1((J-1)*4+JJ))*(-1)**(I+J)
C GENERATE THE TRANSFER FUNCTION.
C CALLFOURIER(A)
C CONVERT THE VALUES OF THE TRANSFER FUNCTION INTO
C MAGNITUDE AND ANGLE.
C DO50I=1,64
DO50J=1,64
AM=CABS(A(I,J))
AA=CANG(A(I,J))
IF(AA)20,30,30
20 AA=AA+2*PI
30 AL=AM
A(I,J)=CMPLX(AL,AA)
50 CONTINUE
C SAMPLE THE TRANSFER FUNCTION BY SELECTING EVERY
C ALTERNATE ELEMENTS IN EACH DIMENSION.
C STORE THE SAMPLES ON A TAPE.
DO80I=K,64,2
80 WRITE(3)(A(I,J),J=L,64,2)
100 CONTINUE
REWIND 3

```

```

C      GENERATE SAMPLED COMPOSITE TRANSFER FUNCTION HOLOGRAM.
      DO200K=1,2
      DO200L=1,2
      DO200I=K,64,2
      READ(3)B
      DO200J=1,32
      A(I,((J-1)*2+L))=B(J)
200  CONTINUE
      REWIND3

C
C      THE FOLLOWING DO LOOP GENERATES THE MULTIPLEXED
C      HOLOGRAM PLOT WHEN THE INDEX IS 1 AND SIMULATES
C      THE SIMULTANEOUS PLAYBACK OF ALL THE IMPULSE
C      RESPONSES WHEN INDEX IS 2.
210  DO700L=1,2
C      SCALE THE MAGNITUDES OF THE TRANSFER FUNCTION
C      TO A VALUE OF 15.
      XM=0.0
      DO250I=1,64
      DO250J=1,64
250  XM=MAX1F(REAL(A(I,J)),XM)
      DO300I=1,64
      DO300J=1,64
      AM=(REAL(A(I,J))/XM)*15.0
300  A(I,J)=CMPLX(AM,AIMAG(A(I,J)))
      CALLPLOTS(0,0,1)
C      PLOT THE ORIENTATION MARKER.
      CALLPLOT(-0.5,0.0,2)
      CALLPLOT(0.0,0.0,2)
      CALLPLOT(0.0,-0.5,2)
      CALLPLOT(0.0,0.0,2)
      CALLPLOT(-1.5,0.0,-3)
      DO500I=1,64
      DO500J=1,64

C
C      IF THE PHASE OF THE TRANSFER FUNCTION ELEMENT IS
C      BETWEEN 0 AND 120 DEGREES RESOLVE THE VALUE INTO
C      COMPONENTS ALONG 0 AND 120 DEGREES.
      A1=0
      A2=0
      A3=0
      AM=REAL(A(I,J))
      AA=AIMAG(A(I,J))
      IF(AA.LT,2*PI/3)330,340
330  A1=AM*(COS(AA)+(SIN(AA)/SQRT(3.0)))
      AA=2*PI/3-AA
      A2=AM*(COS(AA)+(SIN(AA)/SQRT(3.0)))
      GOTU370

```

```

C      IF THE PHASE OF THE TRANSFER FUNCTION ELEMENT IS
C      BETWEEN 120 AND 240 DEGREES RESOLVE THE VALUE
C      INTO COMPONENTS ALONG 120 AND 240 DEGREES.
340  IF(AA.LT,4*PI/3)350,360
350  AA=AA-2*PI/3
      A2=AM*(COS(AA)+(SIN(AA)/SQRT(3.0)))
      AA=2*PI/3-AA
      A3=AM*(COS(AA)+(SIN(AA)/SQRT(3.0)))
      GOTU370
C      IF THE PHASE OF THE TRANSFER FUNCTION ELEMENT IS
C      BETWEEN 240 AND 360 DEGREES RESOLVE THE VALUE
C      INTO COMPONENTS ALONG 240 AND 0 DEGREES.
360  AA=AA-4*PI/3
      A3=AM*(COS(AA)+(SIN(AA)/SQRT(3.0)))
      AA=2*PI/3-AA
      A1=AM*(COS(AA)+(SIN(AA)/SQRT(3.0)))
C      QUANTIZE THE MAGNITUDE OF TRANSFER FUNCTION INTO 15
C      STEPS AND PLOT THE RESOLVED COMPONENTS TO A WIDTH OF
C      0.05 INCHES AND THE HEIGHT PROPORTIONAL TO THE
C      MAGNITUDE.
370  IF(A1.LT,1.0)400,380
380  NM=A1
      DO390K=1,NM
      CALLPLOT(-K*0.01,-0.05,2)
390  CALLPLOT(-K*0.01,0.0,2)
400  CALLPLOT(0.0,-0.05,-3)
      IF(A2.LT,1.0)430,410
410  NM=A2
      DO420 K=1,NM
      CALLPLOT(-K*0.01,-0.05,2)
420  CALLPLOT(-K*0.01,0.0,2)
430  CALLPLOT(0.0,-0.05,-3)
      IF(A3.LT,1.0)460,440
440  NM=A3
      DO450K=1,NM
      CALLPLOT(-K*0.01,-0.05,2)
450  CALLPLOT(-K*0.01,0.0,2)
C      MOVE THE PEN TO THE LOCATION OF THE NEXT ELEMENT.
460  CALLPLOT(0.0,-0.05,-3)
500  CONTINUE
C      MOVE THE PEN TO THE BEGINING OF THE NEXT LINE.
      CALLPLOT(-0.15,0.60,-3)
600  CONTINUE
C      RETURN THE PEN TO THE STARTING POSITION AND REMARK
C      THE ORIENTATION MARKER. ( THIS WILL CHECK THE TOTAL
C      CUMULATIVE ERROR IN THE PLOTTER POSITIONAL ACCURACY.)
      CALLPLOT(11.10,0.0,-3)

```

```

CALLPLOT( 0.0,-J.5,2 )
CALLPLOT( 0.0,0.0,2 )
CALLPLOT( -0.5,0.0,2 )
CALLPLOT( 0.0,0.0,2 )
IF(L.EQ,2)695,653
C   CONVERT THE MAGNITUDE AND PHASE OF THE TRANSFER
C   FUNCTION BACK INTO REAL AND IMAGINARY PARTS,
653 DO654I=1,64
    DO654J=1,64
        AM=REAL(A(I,J))
        AA=AIMAG(A(I,J))
        AX=AM*COSF(AA)
        AY=AM*SINF(AA)
654 A(I,J)=CMPLX(AX,AY)
C   FOURIER TRANSFORM THE TRANSFER FUNCTION TO SIMULATE
C   THE OUTPUT OF THE SYSTEM WHEN ALL THE FUNCTIONS ARE
C   SIMULTANEOUSLY PLAYED BACK,
655 CALL FOURIER(A)
C   CONVERT THE OUTPUT INTO MAGNITUDE AND PHASE AND
C   RETURN TO THE PLOT ROUTINE TO PLOT THE OUTPUT.
    DO680 I=1,64
        DO680 J=1,64
            AM=CABS(A(I,J))
            AA=CANG(A(I,J))
            IF(AA)660,680,680
660 AA=AA+2*PI
680 A(I,J)=CMPLX(AM,AA)
695 CALLPLOT(0,0,999)
700 CONTINUE
    END

```

```

C      THIS SUBROUTINE COMPUTES THE FOURIER TRANSFORM
C      OF A 2-D ARRAY OF 64 X 64 ELEMENTS.
C      THE PROGRAM ALSO SHIFTS THE QUADRANTS OF THE ARRAY
C      TO TAKE CARE OF THE FFT ALGORITHM WHICH ASSUMES THE
C      FIRST ELEMENT AS THE ORIGIN.

      DIMENSION A(64,64),INV(16),S(16),M(3)
      TYPE COMPLEX A,X
      DATA(M=6,6,0)
      IT=0
      IFSET=1
10    DO20I=1,32
      DO20J=1,32
      X=A(I,J)
      A(I,J)=A(I+32,J+32)
      A(I+32,J+32)=X
      X=A(I,J+32)
      A(I,J+32)=A(I+32,J)
20    A(I+32,J)=X
      IF(IT.EQ.1)40,30
      CALL THE FAST FOURIER TRANSFORM ALGORITHM HARM.
30    CALL HARM(A,M,INV,S,IFSET,IFERR)
      WRITE(6,35)IFERR
35    FORMAT(5X,6HIFERR=,I3////)
      IT=1
      GOT010
40    RETURN
      END

```

APPENDIX G  
Fabrication of 2-D Phase Masks

A computer program to plot a 2-D amplitude mask of 127 x 127 elements using a 127 bit Gold code given in Table (2-2) has been described [20]. Using a modified version of this program a set of nine plots was prepared on a thick bright white drawing sheet to a size of 3.81" x 3.81" each. A typical enlarged plot is shown in the Fig. (G-1). These nine plots were mounted on a white poster board to form a 3 x 3 array with center to center distance between each plot in either dimension equal to 13 inches. This array of plots was then photo-reduced such that the center to center distance between the plots is equal to 0.3 inches. This dimension was chosen to match a fly's eye lens array with which the masks were to be used. After this reduction the size of each cell in the array is approximately equal to 18 microns. Thus to retain good resolution after photo reduction, high resolution film plates type Kodak 649F was used. The exposure details and the processing times were as follows:

Distance between the camera (fitted with a 50 mm lens) and the plots: 94 inches.

Exposure: 4 secs. (plots illuminated by diffused daylight in the shadow of a building during bright sunlight).

Develop in D11 solution: 12 minutes.

Rinse in Kodak stop bath: 30 seconds.

Rapid fix with hardener: 5 minutes.

Wash in running water: 20 minutes.

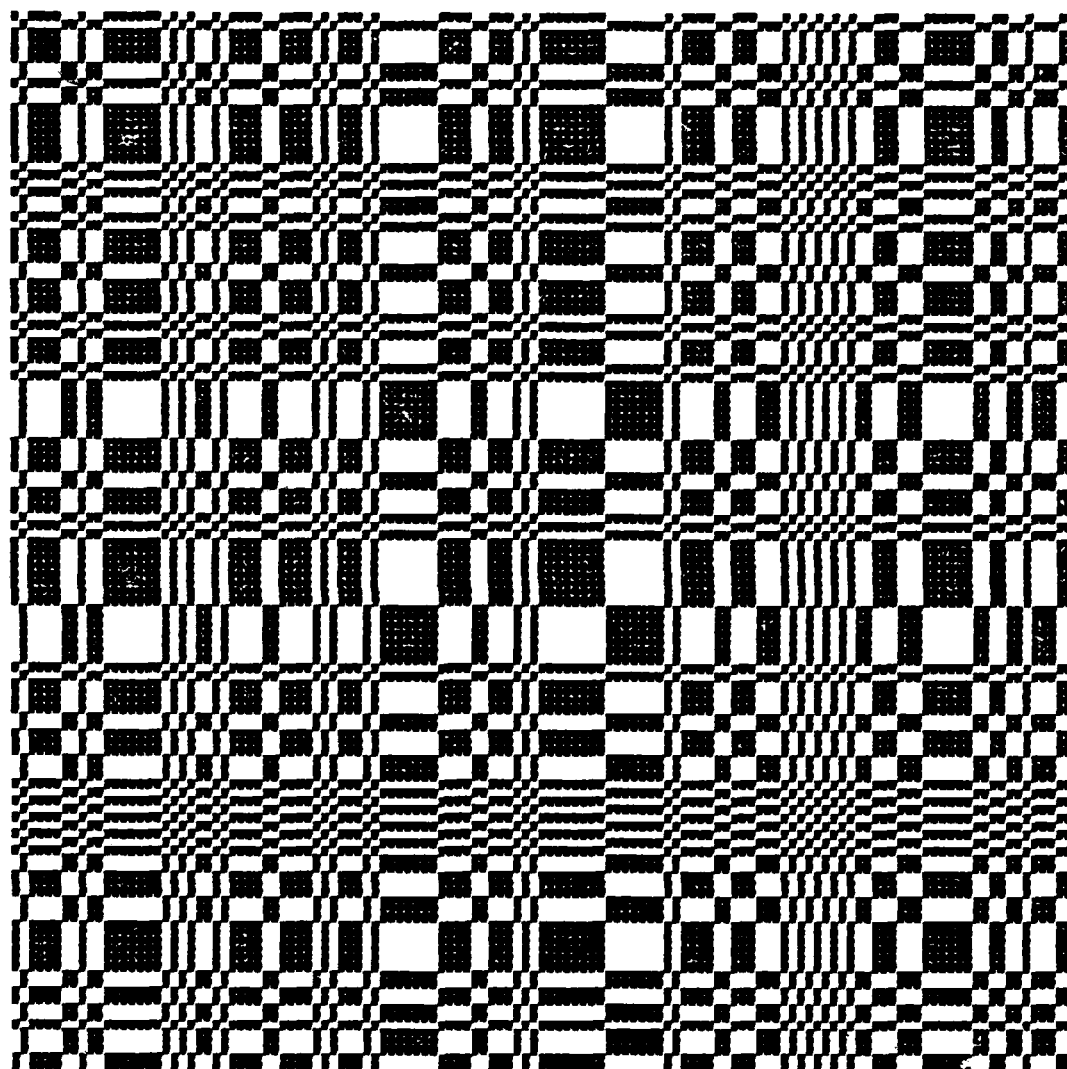


Figure G-1. Typical 127 x 127 element Gold code mask.



A technique to fabricate phase masks from this binary amplitude mask using photo resist solution has been described [21]. It was observed that in this method non uniform thickness of the coating of the photo resist resulted in variations in the phase difference in different regions of the plate. An alternative method is to use the photo sensitive property of gelatin sensitized by a dichromate solution. A number of papers have been published describing the technique of fabricating phase holograms using dichromated gelatin [22-26]. One such method makes use of Kodak 649F plates in the starting step to prepare the sensitized plates [27]. The advantage of using the 649F plates is that the glass base of the film plate is already coated with a uniform layer of gelatin and hence the problem of coating the glass with a uniform gelatin layer is avoided. The detailed processing procedure is given below:

I. Preparation of plates coated with gelatin.

- (1) Fix a 649F plate in rapid fixer with hardener for 15 minutes.
- (2) Wash in running water for 10 minutes.
- (3) Soak in methyl alcohol for 10 minutes with agitation.
- (4) Soak in clean methyl alcohol for 10 minutes with agitation.
- (5) Dry in a vertical position.

At the end of these steps we have a clear glass plate coated with a layer of gelatin on one side.

## II. Sensitization of the plate.

(1) Dissolve 10 gms of purified ammonium dichromate (Baker brand or equivalent) in 200 cc of distilled water. Add 0.5 cc of photoflow solution.

(2) Filter the solution.

(3) Place the glass plate with the gelatin side up in a flat tray and pour the ammonium dichromate solution till the plate is completely covered. Leave it in this position for 5 minutes.

(4) Remove from the solution and place at a small inclination (approximately  $10^\circ$ ) for 3 minutes to let the excess solution to flow down. Clean the edge of the plate with a paper towel.

(5) Place in a light tight box at the same inclination as in step 4 above for 24 hours.

The steps 3, 4 and 5 have to be carried out under safelight illumination using red filter. At the end of these steps we have a sensitized and prehardened plate.

## III. Exposure.

(1) Place the sensitized plate and the amplitude mask such that their emulsion sides are facing each other.

(2) Expose for 12 minutes under a 500 watts

tungsten filament photo lamp placed at 13 inches distance. (Actually several exposures ranging from 4 minutes to 20 minutes are necessary to obtain at least one mask with the desired phase difference.)

#### IV. Development.

(1) Wash in clean running water at 68°F for 10 minutes under safelight illumination using red filter.

(2) Soak with agitation for 2 minutes in a mixture of 50% isopropyl alcohol and 50% water.

(3) Soak with agitation for 10 minutes in 100% isopropyl alcohol.

(4) Pull the plates out of the alcohol at a rate of 1 cm/min., simultaneously blowing hot air directed at the surface for rapid drying.

These steps complete the process and a phase mask is obtained.

The phase mask thus fabricated was checked in a Mach-Zehnder interferometer to check the phase difference between the elements. However in view of the extremely small size of the cells it is difficult to resolve the fringe patterns intersecting each cell. Thus a reference mark of large size was made on the plots and was used as reference to check the phase difference between the exposed and the unexposed parts. However because of the following processing problems, phase masks to the desired accuracy could not be fabricated.

(1) Due to the high resolution required during the fabrication of amplitude masks Kodak 649F plates were used. But these high resolution plates are not of high contrast type. This resulted in non uniform contrast in the amplitude mask due to differences in illumination and hence non uniform exposure of the dichromated gelatin plates.

(2) The sensitivity of the dichromated gelatin plate is a function of the time lag after sensitization. Thus exposure time required was different for each trial depending on this prehardening.

(3) The development process is highly sensitive to the temperature and the Ph of water [24] and it was not possible to control these parameters in the existing set up.

(4) The measurement was based on a large reference mark made on the plot. But due to difference in the contrast of this reference patch with those of the actual cells it could not be confirmed whether all the cells in the mask have the same phase difference.

All these problems require further study before a standard process to obtain repeatable results may be finalized.